COMPENDIUM OF STUDENT PAPERS

**Transportation Scholars Conference
Iowa State University
November 20, 1998**

Analysis of Paratransit Services in Ottumwa, Iowa
John Witmer, Graduate Student in Transportation, Iowa State University

**A Method of Examining Dependence of Crashes on
Demographic and Socioeconomic Data**
Michael Pawlovich, Graduate Student in Civil Engineering, Iowa State University

**An Assessment of Emergency Vehicle Response Pre-Deployment
Using GIS Identification of High-Accident Density Locations**
Bradley Estochen, Graduate Student in Civil Engineering, Iowa State University

Pedestrian Accidents in Lincoln, Nebraska
Patrick Byrd, Graduate Student in Civil Engineering, University of Nebraska-Lincoln

Field Procedures and Guidelines on Using Video Vehicle Detection Systems
Daniel Jessen, Undergraduate in Civil Engineering, University of Nebraska-Lincoln

Methods of Shear Testing and Their Relation to Fiber Composite Dowel Bars
Clifton Melcher, Graduate Student in Civil Engineering, Iowa State University

Sponsor   **Host**

Mid-America
Transportation Center

CTRE

**Center for Transportation
Research and Education**

IOWA STATE UNIVERSITY

Daniel Jessen
Undergraduate Student
Department of Civil Engineering
University of Nebraska-Lincoln

Field Procedures and Guidelines
on using
Video Vehicle Detection Systems

ABSTRACT

Video vehicle detection systems, when properly set-up, may provide a cost-effective alternative to conventional traffic data collection techniques. The main factors influencing the accuracy of the data collected by video detection are the location of the camera, the camera's tilt, and the calibration grid needed to establish a relationship between the video-image and the real-world coordinate system. The camera should be placed as close to the roadway as possible, without bringing attention to itself. Also, the calibration grid needs to be placed out with instrument measuring equipment and high visibility markers to ensure that the camera's field of view can be precisely calibrated. The precision of these tasks will provide the researcher with traffic data that can be used in performing the necessary analyses.

key words: video vehicle detection systems, Autoscope

length of paper: 2,324

INTRODUCTION

In recent years, traffic data collection techniques have became more advanced. New data collection technologies enable researchers to conduct their studies with a higher degree of precession and in more detail. One of the recently developed technologies is video vehicle detection. These systems are applied throughout the United States for providing signal timing at intersections, reducing the amount of travel time delay for motorists. Also, this technology has been effective in the lab for analyzing traffic data. One video detection system that is widely used is the Econolite Autoscope 2003. In this study, the Econolite Autoscope 2003 was used as the video vehicle detection system. This report provides guidance on how to properly setup a study site, and highlights some of the important features of video vehicle detection systems in the lab.

OBJECTIVE

The objective of this report was to provide instructional information on how to prepare a study site so that a video vehicle detection system can accurately collect data. The suggestions made within this report can be adapted for other types of video vehicle detection systems.

FIELD PROCEDURES

Location

The location of the camera is important because it will determine the field of view of the camera, which in turn will influence the quality of the recorded data. The placement of the camera is a function of the surroundings, road type, and the type of traffic data to be collected. In general, the camera should be placed as close to the

roadway as possible. For example, if the merging operation of vehicles at a lane drop is to be studied, the camera should be located close to the beginning of the merge taper, in the closed lane of traffic, if possible, and behind an arrow board or changeable message sign (Figure 1). For intersection studies, the camera should be placed on one of the corners of the intersection depending on which direction of traffic is being studied (Figures 2 & 3). If traffic operation of the entire intersection is being studied, two cameras might be necessary, placed on opposite corners. Also, if the study area is along an interstate or rural highway, with no lane closure present, the best location for a camera is slightly off the shoulder, behind a sign or behind a guardrail (Figure 4). If on- or off-ramp traffic is being studied, the camera should be placed as high on the ramp as possible. Generally, cameras should not be placed in the median unless you are only interested in studying the inside lane of traffic. The reason for this is because the medians of rural 4-lane highways or interstates are usually around 6-12 ft lower than the actual paved surface. This causes a decrease in camera height that could interfere with the data reduction process of the outer lanes of traffic.

Camera Tilt

Another factor that needs to be considered in setting up a camera, is the tilt of the camera. The field of view of the camera is a function of tilt. The required field of view depends on the data types to be collected. For example, smaller fields of view are required for determining speed data than queue length. The tilt of the camera needs to be judged on site after the camera is deployed. Templates provide good estimations of what field of view will correspond to a tilt (Figure 5). Templates with a scale of 1:40 and 1:100 provide the best results. The only thing needed is a drawing of the study site

scaled to one of the templates. Place the template on top of the drawing of the site and adjust it until you achieve the best field of view. On each template there is a number of different trapezoidal field of views. The number corresponding to a trapezoid is the number of feet away from the camera that you could see on the bottom of the monitor screen. As stated earlier, these templates are very effective estimators, but minor adjustments might need to be made in the field.

Limitations

There are a few limitations that need to be considered when designing the location of the camera for a study site. The first limitation is the shadow caused by the sun's movement throughout the day. The majority of the shadows occur during the early morning or late afternoon. The Autoscope has a built in function for the detection of shadows, but it is not effective enough to eliminate all of the false detections caused by shadow interference. Cloudy days are the best times for video recording because there are no shadows. A second limitation may stem from the improper placement of the camera relative to the lane of interest. For example, a semi-trailer may be detected twice, once in both lanes, if the camera is not properly placed. The only way to minimize this problem is to elevate the camera to its maximum height.

Grid Layout

Video vehicle detection systems operate on screen pixels. In order to obtain reliable distances, speeds, and other traffic data from a video, a relationship must be established between the screen-pixel coordinates of the roadway image and the real-world coordinates of the roadway section within the field of view. This process can be done by setting up a calibration grid within the camera's field of view. The markers in the

field of view need to be set up in a grid-like manner. When calibrating the Autoscope, it requires a minimum of five lines, with three lines going crosslane or downlane, with the other two going in the direction not chosen for the set of three lines. Downlane refers to the direction that runs parallel to traffic and crosslane refers to the direction that crosses the traffic path (Figure 6). Therefore, one large rectangular box with two smaller rectangular boxes inside will be created on the pavement. A total of six markers will be placed onto the pavement. The distance between them should be between 10 – 70 feet. As you move away from the camera, the markers and the distances between them, from the perspective of the computer, appear less, as does the size of the markers themselves. The distance between the first and second markers does not need to be the same. Also the last marker, which is farthest from the camera, should be at least twice as thick as the other markers so the calibration lines can be drawn with more accuracy. The distance and speed data collected with the video-detection system are particularly sensitive to the accuracy of the calibration grid. A few feet error could result in a difference of 2-10 mph in speed and 5-15 feet in vehicle length.

The best way to start the layout of the grid is to pick any point on the pavement, out of the lane of traffic. This point now becomes one of the corners of the rectangle grid. At this point, there are a couple of different options that can be taken, depending on the location and volume of traffic present at the site. On roads and at intersections of lower volume, the 3-4-5-triangle rule may be used. A total of four individuals are needed in performing this task, three individuals will place the markers, as the other one watches the traffic. Consider an example where a grid needs to be set out in an intersection at

an urban 4-lane highway. The grid consists of three downlane lines and two crosslane

lines. The distance between the downlane markers is 15 feet and the distance between

the crosslane markers is 20 feet. One individual needs to stand at the point which was

chosen as the corner (should be along the shoulder or sidewalk area) holding "0" and

"60 ft" on the tape. The other individuals will stand holding the tape at "20 ft" and the

other at "45 ft" creating a triangle (Figure 7). The locations of "20 ft" and "45 ft" are

the two spots where the markers need to be placed. Then go to the location of the

marker at "45 ft" and continue the process until all six markers are located. It is

recommended that a lumber crayon is used first to mark the location with an "X" and

the markers can then be placed after the entire grid is located. Also do not assume that

the joints or lane/crosswalk stripping are straight or parallel because it is generally not

the case (see: Figure 8).

Another method of setting out an accurate grid is to use a transit/total station. This

option works best when a grid is being set along a rural interstate or along an urban

street with very high traffic volumes. This procedure only requires two individuals,

100-ft tape, total station/transit, a range pole or Jacob's staff and a prism. For this

example there are three crosslane lines and two downlane lines. The distance between

the crosslane lines is 40 ft and then 50 ft, respectively. The distance between the

downlane lines is 36 ft. Once the first point is chosen in the shoulder of the interstate

(corner of the rectangle), then the distance of 90 ft is then measured with the tape along

the shoulder as straight as possible through "eyeing." The total station is then set up

over the corner point and the total station zeroed on the point that was measured 90 ft

away. Then the instrument operator needs to position the individual with the staff 40 ft

away from the initial point while keeping him lined up with the initial point and the

point 90 ft away. Next, a 90° angle is turned to the other shoulder of the same bound

traffic stream and the instrument operator needs to line up the staff 36 ft away from the

initial point. Then an angle of 48° is turned with a distance of 53.8 ft. Lastly an angle

of 68.2° is turned with a distance of 96.9 ft (Figure 9). This technique takes more time

and equipment, but it is safer and it takes fewer individuals than the first option.

The initial point in both options should be tied out and permanently marked so then it

can be found if additional data needs to be obtained. Also a diagram or sketch of the

grid is necessary with the distances between the markers and the camera height inserted

so the values can be entered into the Autoscope during the calibration process.

Marker Type

There are number of different options for the type of markers which can be used in the

placement of the calibration grid. The two types, which we use for the collection of

data, are white spray paint and Bituthene water proofing membrane. We use mostly the

Bituthene because it lasts much longer than spray paint. Bituthene comes in 3' by 8"

strips. It is similar to temporary lane marking tape that adheres to the warm pavement.

The only limitations in using Bituthene is that the temperature needs to be greater than

45° F and you need to clean the spot where the marker will be laid with a broom

because small pebbles and rocks will cause the marker not to adhere to the pavement.

Also, if placing a grid inside of an intersection, it may be necessary to replace the

markers or repaint them throughout the day.

CONCLUSIONS

Data collection using vehicle video detection systems can save time and money, and enhance the quality of traffic engineering studies. The video tapes provide permanent records of traffic operation which enables the traffic engineer to perform a wide-range of sub-sequent data analyzes. The present study highlighted some of the key elements in setting up the system (eg. camera location, calibration grid setup, etc) that may significantly effect the accuracy and reliability of traffic data collected by the vehicle video detection system.

REFERENCES

1.   *Econolite Autoscope 2003 User's Guide*. Econolite Control Products, Inc, 3360
East La Palma Avenue, Anaheim, California, 1992.

LIST OF FIGURES

FIGURE 1 Camera located behind an arrow board

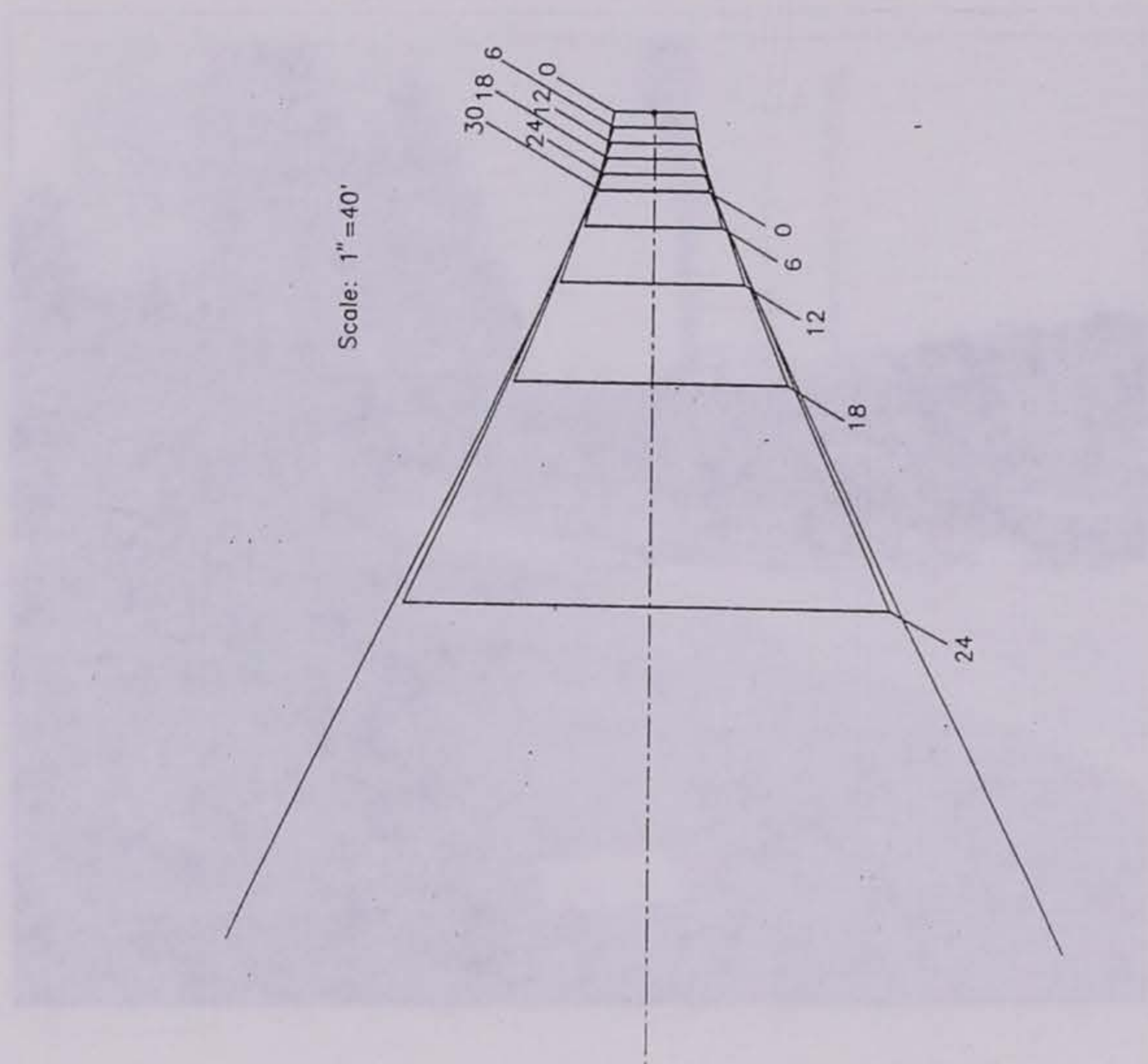**FIGURE 2 Camera monitoring eastbound traffic flow at an intersection**

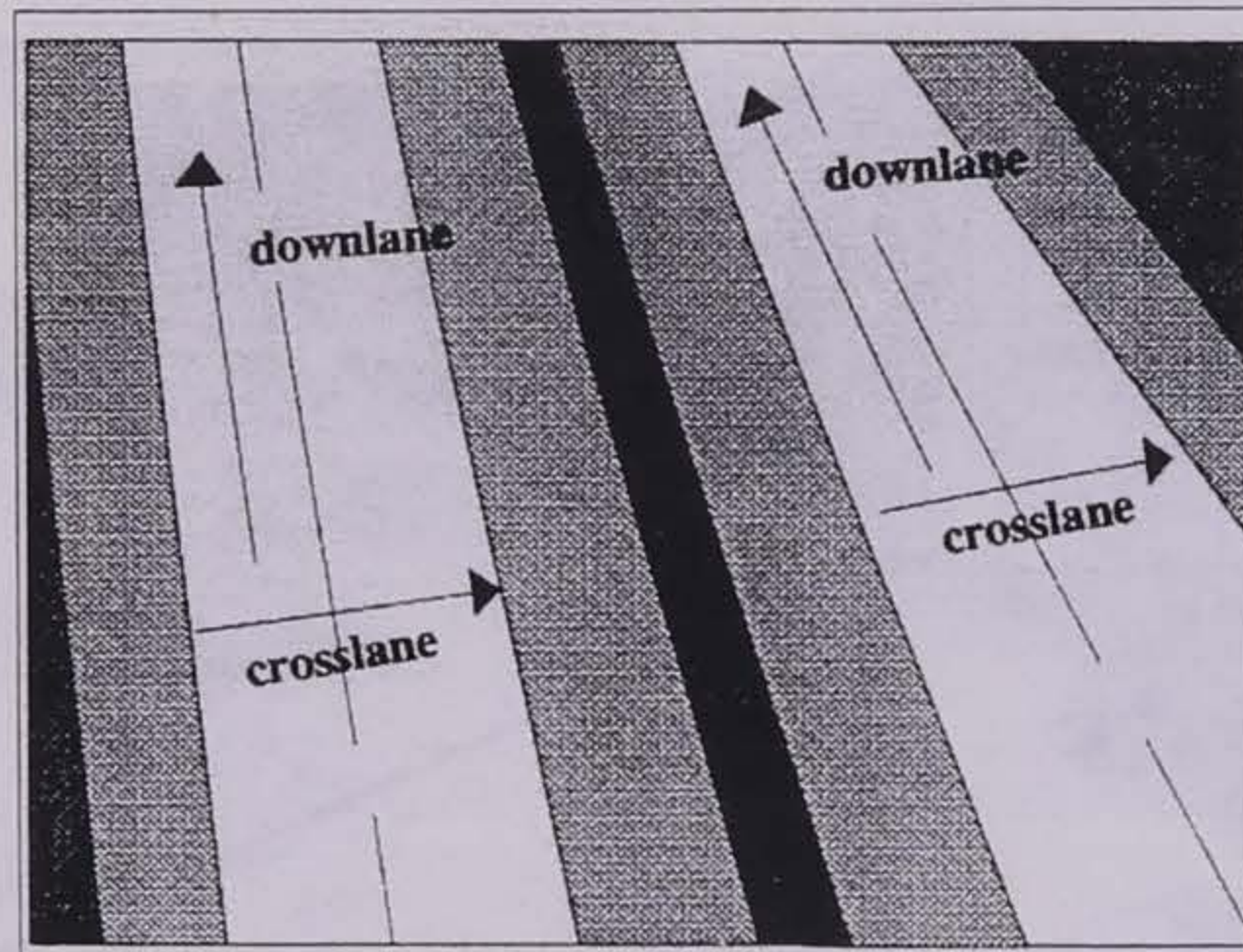**FIGURE 3 Camera located in the northeast corner of an intersection**

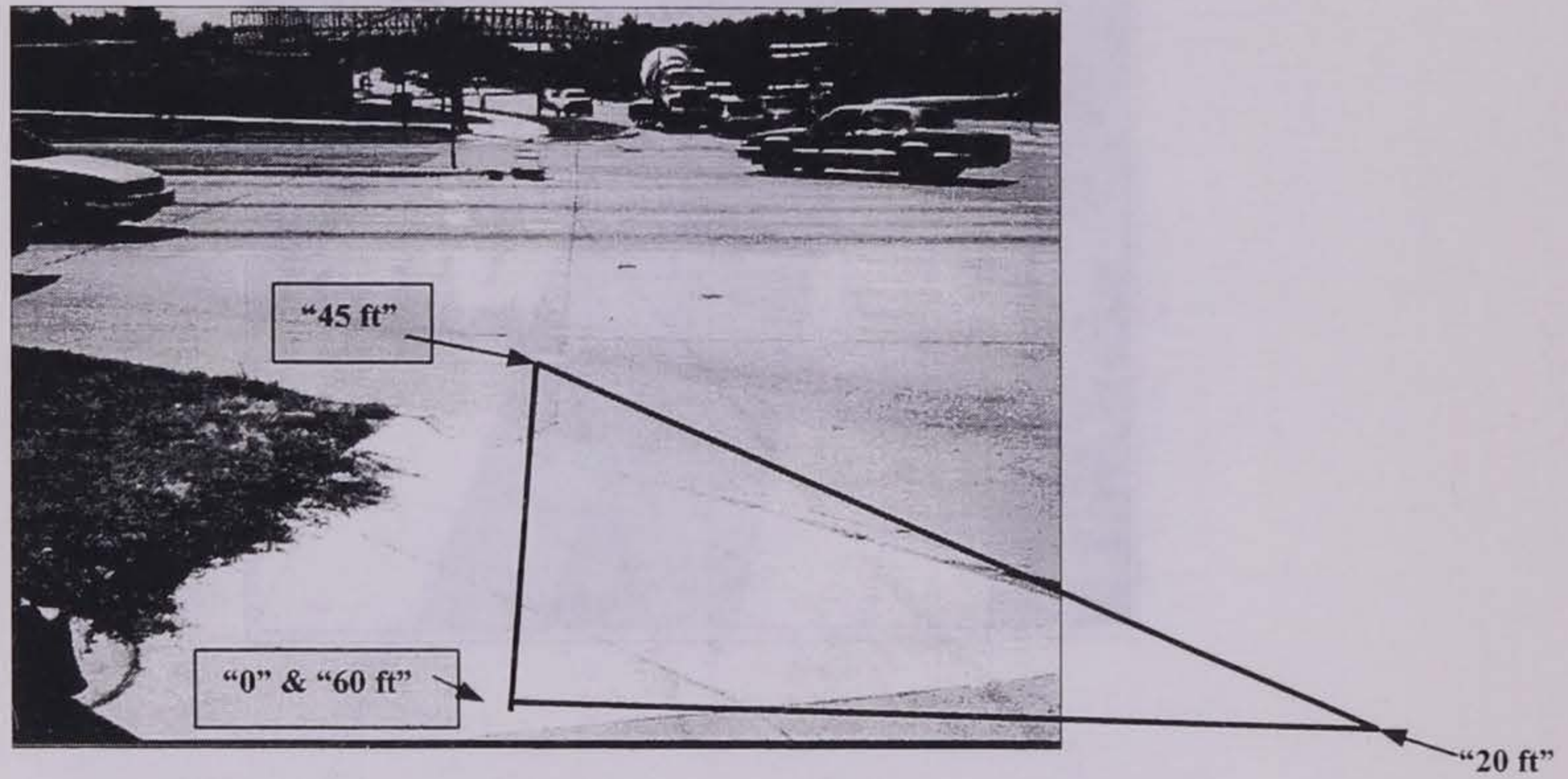**FIGURE 4 Camera located behind a sign and guardrail along Interstate 80**

Scale: 1" = 40'

FIGURE 5 Template used in determining the tilt of the camera

FIGURE 6 Diagram of crosslanes and downlanes

"45 ft"

"0" & "60 ft"

"20 ft"

FIGURE 7 3-4-5-triangle method

FIGURE 8 Grid layout that is not parallel with the joints or crosswalk

markers

50. 0 ft

96. 9 ft

40. 0 ft

53. 8 ft

20.2 °
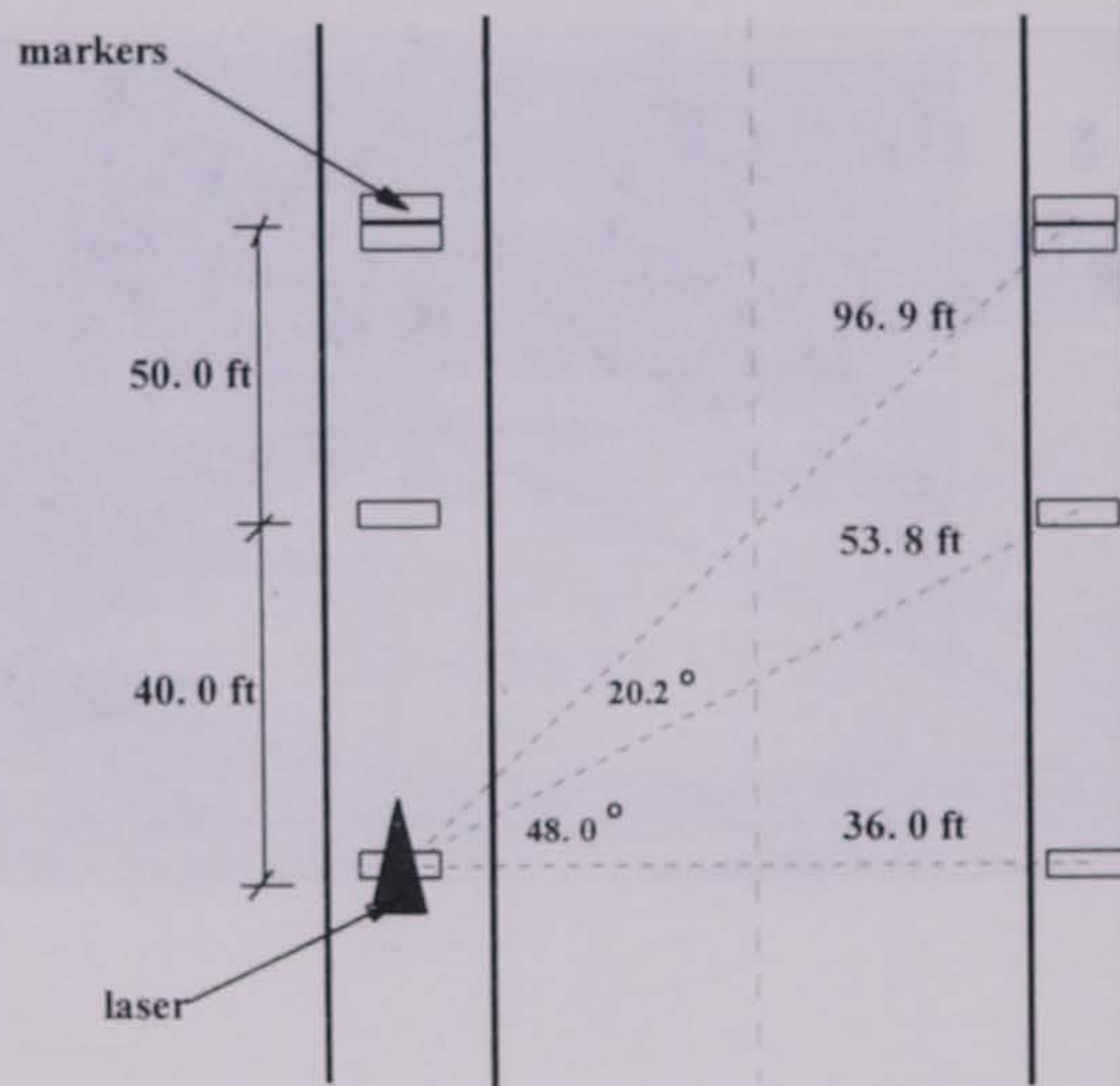
48. 0 °   36. 0 ft

laser

FIGURE 9 Total station method

John Witmer
MS Student - Transportation
Community and Regional Planning
Iowa State University

*Analysis of Paratransit Services
in Ottumwa, Iowa*

Project Objective

The primary goal of this project was to explore the capabilities a geographic information system (GIS) to plan, schedule, and evaluate paratransit bus services in a rural and small town setting. To accomplish this, this project analyzed (1) the performance and (2) potential ridership of three paratransit routes -- Wapello East Tenco, Wapello South Tenco, and Wapello West Tenco -- in Wapello County, Iowa using Environmental Systems Research Institute's (ESRI) ArcView GIS program and Network Analyst extension. ArcView and Network Analyst allow for computer assisted route planning, scheduling, and analysis in a GIS environment.

Background

The Ten-Fifteen Regional Transit Agency in Ottumwa operates all paratransit services in Iowa Department of Transportation (DOT) Region 15. This is a 10-county area centered around Ottumwa, which is centrally located in Wapello County (population 35,687) (Figure 1). Each county may have numerous paratransit routes. Routes generally serve a specific purpose, such as transporting dialysis patients to medical facilities, meals to senior citizens (meals on wheels), pre-school children to Head Start programs, and disabled individuals to sheltered employment workshops. All routes are available to the general public on a "call-in" basis. Ten-Fifteen is also the umbrella agency responsible for the Ottumwa Transit Authority's (OTA) fixed-route bus system serving the city of Ottumwa.

The Wapello Tenco routes are serviced by three vans that transport mentally handicapped individuals from their homes to sheltered job workshops at Tenco Industries in Ottumwa. Vans leave the OTA bus garage at varying times in the morning, but must arrive at Tenco Industries between 8:15 to 8:30 am. The passenger list varies from day-to-day, primarily due to a high number of call-in riders. During the month of February, call-in riders represented 49 percent of all riders. Regular subscription ridership is fairly stable, with most clients traveling three or five days per week.

2

Due to the experience of its staff and low number of employees (five administrative and maintenance personnel), Ten-Fifteen's costs of providing paratransit services are relatively low. For example, Ten-Fifteen's cost per passenger trip in 1996 was $3.50. In the latest year for which national statistics are available, the National Transit Database reports that the average operating expense per passenger trip for demand response service in areas between 50,00 and 200,000 in population was $8.67.

Ten-Fifteen manages, operates, and schedules all transit services based on the experience of its staff. Computers are used to a limited extent, primarily to track expenditures and formulate budgets. This suggests that computer assisted route planning and scheduling could improve performance and reduce operating costs.

Study Design and Tasks

In summary, the design of the study is to:

(1) Use the Network Analyst to help plan and design the three Wapello workshop routes to minimize operating costs. Routes will be designed to minimize distance traveled and/or time traveled..

(2) Compare route design against actual performance data to assess both the effectiveness of the network analysis and the performance of the workshop routes.

(3) Evaluate potential "call-in" ridership using socioeconomic/demographic data. Overlay routes and/or service area maps with thematic maps by Census block of socioeconomic characteristics. Socioeconomic data will focus on those individuals thought most likely to benefit from paratransit services on a call-in

basis (transit-dependent individuals). This includes numbers of mobility-disabled persons, elderly persons, and households with no automobiles.

Data Preparation – Major Tasks

1. <u>Geocode/Address Match: Client List by Route, and Origin and Destination sites</u>. This involves using addresses to locate (geocode) client homes, the route origin, and the route destination on a road network.

First, a database (in spreadsheet format) of all workshop route clients was obtained from OTA. From this worksheet, separate spreadsheet files were created for each of the 3 routes. Another file was created containing the origin and destination points: the OTA bus garage and Tenco Industries. These files were then converted to a DBase format that could be read by ArcView. The following table shows the client list by route.

Wapello County Workshop Route Client List

PASSENGER	STREET	CITY	COUNTY	ROUTE
Wap East Tenco				
Passenger 1	800 Block Hackberry Rd.	Ottumwa	Wapello	Wap East Tenco
Passenger 2	9700 Block Old Agency Rd.	Ottumwa	Wapello	Wap East Tenco
Passenger 3	R.R. 6	Ottumwa	Wapello	Wap East Tenco
Passenger 4	200 Block Paris St.	Ottumwa	Wapello	Wap East Tenco
Passenger 5	10800 Block Bladensburg Rd.	Ottumwa	Wapello	Wap East Tenco
Passenger 6	500 Block Green St.	Ottumwa	Wapello	Wap East Tenco
Passenger 7	11600 Block Rabbit Run Rd	Ottumwa	Wapello	Wap East Tenco
Passenger 8	State Route 23	Ottumwa	Wapello	Wap East Tenco
Wap South Tenco				
Passenger 1	200 Block Poplar St.	Bloomfield	Davis	Wap South Tenco
Passenger 2	Rt. #4	Ottumwa	Wapello	Wap South Tenco
Passenger 3	1400 Block Mowrey St.	Ottumwa	Wapello	Wap South Tenco
Passenger 4	9500 Block 170th Ave.	Ottumwa	Wapello	Wap South Tenco
Passenger 5	Asbury Circle	Ottumwa	Wapello	Wap South Tenco
Passenger 6	100 Block Marianna Ave.	Ottumwa	Wapello	Wap South Tenco
Passenger 7	500 Block S. Ward	Ottumwa	Wapello	Wap South Tenco
Passenger 8	700 Block Ellis Ave.	Ottumwa	Wapello	Wap South Tenco
Passenger 9	RFD #1	Blakesburg	Wapello	Wap South Tenco
Passenger 10	200 Block S. Moore St.	Ottumwa	Wapello	Wap South Tenco
Passenger 11	15000 Block Blackhawk Road	Ottumwa	Wapello	Wap South Tenco
Passenger 12	Hwy 34	Ottumwa	Wapello	Wap South Tenco
Wap West Tenco				
Passenger 1	1000 Block Hackberry Rd.	Ottumwa	Private	Wap West Tenco
Passenger 2	500 Block 4th St.	Eddyville	Wapello	Wap West Tenco
Passenger 3	300 Block Clarence Rd.	Ottumwa	Wapello	Wap West Tenco
Passenger 4	400 Block N. Fifth St.	Ottumwa	Wapello	Wap West Tenco
Passenger 5	300 Block Market St.	Eddyville	Wapello	Wap West Tenco
Passenger 6	400 Block N. Clay	Ottumwa	Wapello	Wap West Tenco
Passenger 7	500 Block W. Wapello	Ottumwa	Wapello	Wap West Tenco
Passenger 8	W. Maple	Ottumwa	Wapello	Wap West Tenco
Passenger 9	1000 Block N. Elm	Ottumwa	Wapello	Wap West Tenco

Second, the four files were address matched using ArcView's Street Map extension. Street Map, which covers the entire U.S., contains a complete road network with address ranges. For the address matching process, match criteria were set relatively low in order to obtain a high match rate. All matched locations were individually checked to ensure accuracy. Reasons for address matching failure included: non-matchable addresses such as rural routes, post office boxes and trailer courts; missing address ranges in the Street Map program; addresses located outside of the address range; and missing roads or towns in the Street Map program. The location of one client was found using a search on the Internet. For all clients that could not be

matched (approximately 9). a road map of the area was sent to OTA, which then hand-marked the location of each client on the map.

Figure 2 shows the results of the address matching.

2. <u>Compile Road Network and Database</u>. To allow calculation of travel times, a geocoded road network based on Iowa Department of Transportation (DOT) data was obtained from the Center for Transportation Research and Education (CTRE) at Iowa State University. These data contained, among many other attributes, speed limits by road segment. This data was used to estimate travel times.

The following is a summary of the procedures required to compile the DOT road database in ArcView. First, the three road databases were combined using MapInfo's append feature (ArcView lacked an append capability). The DOT database was comprised of three separate MapInfo files, one each for primary, secondary, and municipal roads; Network Analyst was unable to recognize a road network consisting of three separate layers/databases. Second, MapInfo was used to spatially connect the three road networks of the combined road database. This involved adding "nodes" where networks crossed over one another, and connecting the end of one network (for example, a municipal road) to another network (a secondary or primary road). This was a time-consuming task and not completely accurate. Third, the database was converted to ArcView using MapInfo's Universal Translator. Finally, a new data field was added to the database to allow for travel time calculations. For each record (or road segment), a field named "hours" was calculated by dividing distance by speed limit.

Due to the time required to assemble the DOT road network, it was used only for the service area analysis. An attempt was made to design Wapello South based on travel time using the DOT road network. However, since the DOT road network was not fully connected (that is, primary to secondary to municipal roads), Network Analyst

was unable to reach all destinations. Therefore, Street Map was used to design the bus routes based on distance.

3. <u>Compile Socioeconomic Data for Ridership Analysis</u>. This task involved exporting the necessary demographic data from the Census to ArcView for thematic mapping. A new product from Geolytics, Inc. made this a relatively pain-free task.

Route Design and Performance Analysis

Figures 3 through 5 show the route design for the three Wapello Tenco bus routes. The routes were designed to minimize distance traveled. Figure 6 shows all three routes overlayed onto one map. This indicates the extent of the combined service area and shows how the three routes relate to one another.

Wapello East Tenco

Figure 3 shows the route for Wapello East Tenco. It begins by picking up the first customer to the east of the city, doubles back and crosses over the Des Moines River to pick up the next three customers on the south side of the city, then crosses back over the river to pick up the remaining customers on the north side of the city.

The minimum distance required to pick up each of the eight clients, take them to the employment workshop at Tenco Industries, then return to the OTA bus garage is 25.44 miles. This is the shortest of the three routes, primarily because all clients are within or near the City of Ottumwa.

Wapello West Tenco

Figure 4 shows the route for Wapello West Tenco. At 38.73 miles, Wapello West is longer than Wapello East due to the two clients located in the town of Eddyville in the

northwest corner of the county. Note that three clients are picked-up before heading out to Eddyville. In terms of customer service, it may be better to pick up the Eddyville clients first.

Wapello South Tenco

Figure 5 shows the route for Wapello South Tenco. At 56.97 miles, Wapello South is the longest route due to the customer located in Bloomfield in Davis County. In terms of customer service, the OTA would be advised to run this route in reverse order from that shown in Figure 5 so that all passengers do not ride to Bloomfield and back. In addition, if this route were designed based on travel time, it would likely traverse over to U.S. 63 on the southbound journey to Bloomfield rather than winding through the secondary county roads.

Limitations of Network Analyst

The capabilities of Network Analyst are limited by a lack of flexibility in ordering stops (pick-ups). Network Analyst can find the most efficient pick-up order and return to the origin, or allow manual ordering of all pick-ups. It does not allow for combinations of the two, which is required for the three Workshop routes. Thus, experimentation was required to arrive at a shortest path. This involved running the analysis at least twice: first finding the most efficient order excluding Tenco and returning to OTA, and second adding Tenco as the second to last stop and using the pickup order determined in step one. This limits the usefulness of Network Analyst in designing paratransit bus routes.

Another feature that would make the Network Analyst more useful would be an ability to calculate the most efficient pickup of all passengers and routes simultaneously. With such a capability, all three Workshop routes could be optimized as a whole.

Finally, the results of the three Wapello routes show that human interpretation is still necessary to derive meaningful results.

Performance Analysis

This section compares the three routes designed by the network analysis to actual OTA performance data. The following tables compare actual ridership and miles traveled versus the shortest path estimated by the network analysis (which uses the client base for passengers).

The table below shows a high rate of "call-in" ridership. For the most recent month available, February, actual ridership was significantly higher than the client base on all three routes. Actual ridership on Wapello West was almost 3 times the client base, Wapello South 1.7 times the client base, and Wapello East 1.3 times the client base. This unexpected finding makes comparison to route miles calculated by the network analysis difficult. However, it does raise interesting questions regarding the reasons for the high rate of call-in ridership. This will be addressed in the socioeconomic analysis.

Wapello Workshop Routes
Network Analysis versus Actual Operating Statistics

Passengers

	Actual Feb. Average	Client Base for NW Analysis	Difference	Percent Difference
Wapello East Tenco	10.6	8	(2.6)	76%
Wapello West Tenco	26.3	9	(17.3)	34%
Wapello South Tenco a/	20.0	12	(8.0)	60%
Total	56.8	29	(27.8)	51%

Distance

	Actual Feb. Avg. Miles	NW Analysis (Clients Only)	Difference	Percent Difference
Wapello East Tenco	58	51	(7.5)	87%
Wapello West Tenco	113	77	(35.3)	69%
Wapello South Tenco a/	83	114	30.9	137%
Total	254	242	(11.9)	95%

Operating Time

	Actual Feb. Avg. Hours
Wapello East Tenco	4.0
Wapello West Tenco	5.7
Wapello South Tenco a/	3.7
Total	13.5

a/ Bloomfield customer not riding in February.

Some comparison of route miles can be made for Wapello East on days in which the actual number of riders was the same as the number in the client base (8). As shown in the following table, on the five most recent days in which this occurred, the average miles traveled was 55. The shortest path analysis for the client base is 51 miles (2 trips, morning and afternoon), or a 7% reduction in miles traveled on average.

Wapello East Tenco
Comparison of Network Analysis To
Recent Operating Statistics with 8 Passengers

	Passengers	Miles	NW Analysis (2 trips)	Percent Reduction	Hours
January 6	8	61	na	17%	4
January 21	8	55	na	7%	4
March 10	8	57	na	11%	4
March 18	8	53	na	4%	4
March 20	8	49	na	-4%	4
Average/Total	8	55	51	7%	4

Socioeconomic Analysis of Potential Call-in Ridership

This section evaluates potential call-in ridership on the Wapello Workshop routes. Specifically, how many persons might Ten-Fifteen expect to serve on a call-in (demand response) basis, and where do these persons live? How do the three routes align with the location of potential riders, and does this help explain the high rate of call-in ridership on Wapello West?

It is assumed that those persons most likely to use the Wapello Workshop routes are transit-dependent individuals, such as mobility disabled persons, the elderly, and persons living in households that do not own an automobile.

Service Area Analysis

To assess potential ridership, the first technique involves estimating numbers of transit-dependent persons living within the service area. The service area is based on one-way travel time from the OTA bus garage.

Figure 7 shows service areas based on a travel time of 10, 20, and 30 minutes from OTA. Figure 8 shows Census blocks in Wapello County overlaid onto the service areas. These maps suggest that most potential riders live within 10 minutes of the OTA garage (and Tenco Industries), that virtually all of Wapello County is within a 20 minute ride, and that the towns of Eddyville and Bloomfield are within a 30 minute ride.

The following chart summarizes the socioeconomic statistics derived from this analysis. It shows: (1) numbers of transit-dependent persons living in Census blocks centered within Wapello County, (2) numbers of transit-dependent persons living in all of Wapello County, and (3) numbers of persons in the second column compared to the numbers of persons served on average during the month of February. Elderly persons consist of the largest single group of potential riders.

Wapello County Demographics
Potential Paratransit Ridership

	Persons w/in 10 Min. of OTA	Persons in Wapello Cnty	Versus Average Feb. Ridership
Population	27,175	35,687	0.2%
Elderly	5,172	6,351	0.9%
Households with No Vehicles	1,207	1,345	4.2%
Mobility Disabled	1,249	1,507	3.8%
16 to 64 years of age	402	513	11.1%
over 65	847	994	5.7%

Route Overlay with Census Block Statistics

During the month of February, the client base accounted for only 51 percent of all Workshop route riders in Wapello County. Out of a total of 57 riders, 29 were regular clients and 28 were call-ins. Most of the call-ins (17 persons, or 62 percent of all call-ins) traveled on Wapello West, almost tripling Wapello West ridership. Call-ins increased ridership on Wapello South by 1.7 times the client base, and Wapello East by 1.3 times the client base.

The high rate of call-in ridership, particularly on Wapello West, raises questions about the origin of these passengers. Do these routes travel through areas where residents have a greater need for public transit?

Figures 9 through 13 show all three routes overlaid onto thematic maps of transit-dependent populations by Census block in Wapello County. The following insights result from observation of these maps.

- Elderly Persons (Figure 9). Elderly persons reside all along the Wapello West route to Eddyville, but are most heavily concentrated in areas surrounding Ottumwa and in the southwest and southeast corners of the county.

- Mobility Disabled Persons (Figures 10 – 12). Two blocks of having large numbers of mobility-disabled persons are located directly north of Ottumwa. Other notable blocks are within Ottumwa and the block in southeast corner (includes town of Eldon). Breaking these statistics down by age indicates that, on the trip to Eddyville, Wapello West runs adjacent to a block with a large number of working-age mobility-disabled persons (Figure 10). Similarly, Wapello South runs through a block with a large number of working-age mobility disabled on the south side of Ottumwa. The largest group of mobility-disabled elderly are concentrated just north of Ottumwa.

❑ <u>No Auto Households (Figure 13)</u>. Most households with no automobile appear to be located in or near Ottumwa, with the exception of the blocks in the northwest, southwest, and southeast corners. These blocks contain the towns of Eddyville, Blakesburg, and Eldon, respectively. The households in Ottumwa may be served by any of the three routes. Interestingly, the single block with the highest number of elderly persons is not in the highest tier of households with no automobile – that is, other factors, such as income, are related to auto ownership.

Conclusions and Recommendations

The findings from the previous sections are summarized as follows:

Route Design

❑ The Network Analyst was used to calculate a "shortest path" for the three Workshop routes. This involved designing routes that minimized the distance required to pick up all clients, take them to Tenco Industries, and return to the OTA bus garage. Routes were not designed to minimize travel time because a properly connected road network containing attribute data (such as speed limits) was not available.

❑ The capabilities of Network Analyst were limited by a lack of flexibility in ordering stops. Arriving at a shortest path required experimentation.

❑ Obtaining practical results requires human interpretation, such as whether or not to pick up passengers on outbound trips.

❑ Although not a necessity, Network Analyst would be more useful for paratransit service planning if it could calculate multiple routes simultaneously.

14

Performance Analysis

- Comparison of the client base to actual ridership showed a high rate of "call-in" ridership. The client base represented only 51 percent of total ridership in February.

- Due to the high rate of call-in ridership, comparison of the shortest path derived from the network analysis to actual vehicle miles traveled was possible only for Wapello East on selected days. On the five most recent days in which the number of riders equaled the number in the client base, the shortest path calculated by the Network Analyst was 7 percent shorter on average than actual vehicle miles traveled. However, since the client base may not represent actual riders on those days, more definitive conclusions are not possible.

Socioeconomic Analysis

- Analysis of service areas indicates that most potential call-in riders live within 10 minutes of the OTA bus garage. Potential call-in riders are defined as persons who are transit dependent, and include the elderly, mobility disabled, and households having no automobile.

- Overlays of the three Workshop routes with thematic maps of transit-dependent riders by Census block suggests that the high rate of call-in ridership is related to the numbers of transit-dependent persons along each route. For example, on the trip to Eddyville, Wapello West runs adjacent to a block with a large number of working-age mobility disabled persons.

In conclusion, the Network Analyst does not offer the flexibility and range of features that a transit agency would need to design paratransit routes. However, this project does indicate several potential benefits of a well-designed system, as well as some of the requirements for that system. Since Ten-Fifteen's passenger/client list changes daily, they would likely find that a well-designed GIS/scheduling system produced savings in

15

vehicle operating costs and reduced the amount of staff time devoted to scheduling. Basic system requirements include a road network that allows route design based on travel time, flexible and easy to use scheduling software, and the ability to quickly and easily geocode passenger locations. Such a system could be an indispensable tool for planning paratransit operations.

The socioeconomic analysis shows that the ability to combine route design with other spatial information allows for analysis of current operations and can help in planning new routes and changes to existing routes.

References

ARC Transit and Ride Solution. "Operational Strategies for Rural Transportation," U.S. Department of Transportation, Technology Sharing Program, March 1996.

Burkhard, Jon E., Hamby, Beth, and McGavock, Adam T. "Users' Manual for Assessing Service-Delivery Systems for Rural Passenger Transportation." Transit Cooperative Research Program, Report 6, National Academy Press, 1995.

Kihl, Mary, Crum, Micheal, and Shinn, Duanne. "Choosing Smart Technologies, A Guide for Busy Rural Paratransit Operators," Iowa State University, September 1, 1996.

Koffman, D, and Lewis, D. "Forecasting Demand for Paratransit Required by the Americans with Disabilities Act," Transportation Research Board, Transportation Research Record 1571, 1997.

Lave, Roy E., Teal, Roger and Piras, Patricia. "A Handbook for Acquiring Demand-Responsive Transit Software," Transit Cooperative Research Program, Report 18, National Academy Press, 1996.

SG Associates, Inc. "Workbook for Estimating Demand for Rural Passenger Transportation," Transit Cooperative Research Program, Report 3, National Academy Press, 1995.

U.S. Department of Transportation, Federal Transit Administration. "Advanced Transportation Systems: The State of the Art, Update '98," January 1998.

Figure 1

Iowa Counties by Population Density

DOT Region 15

WAPELLO

0   50   100

Miles

N
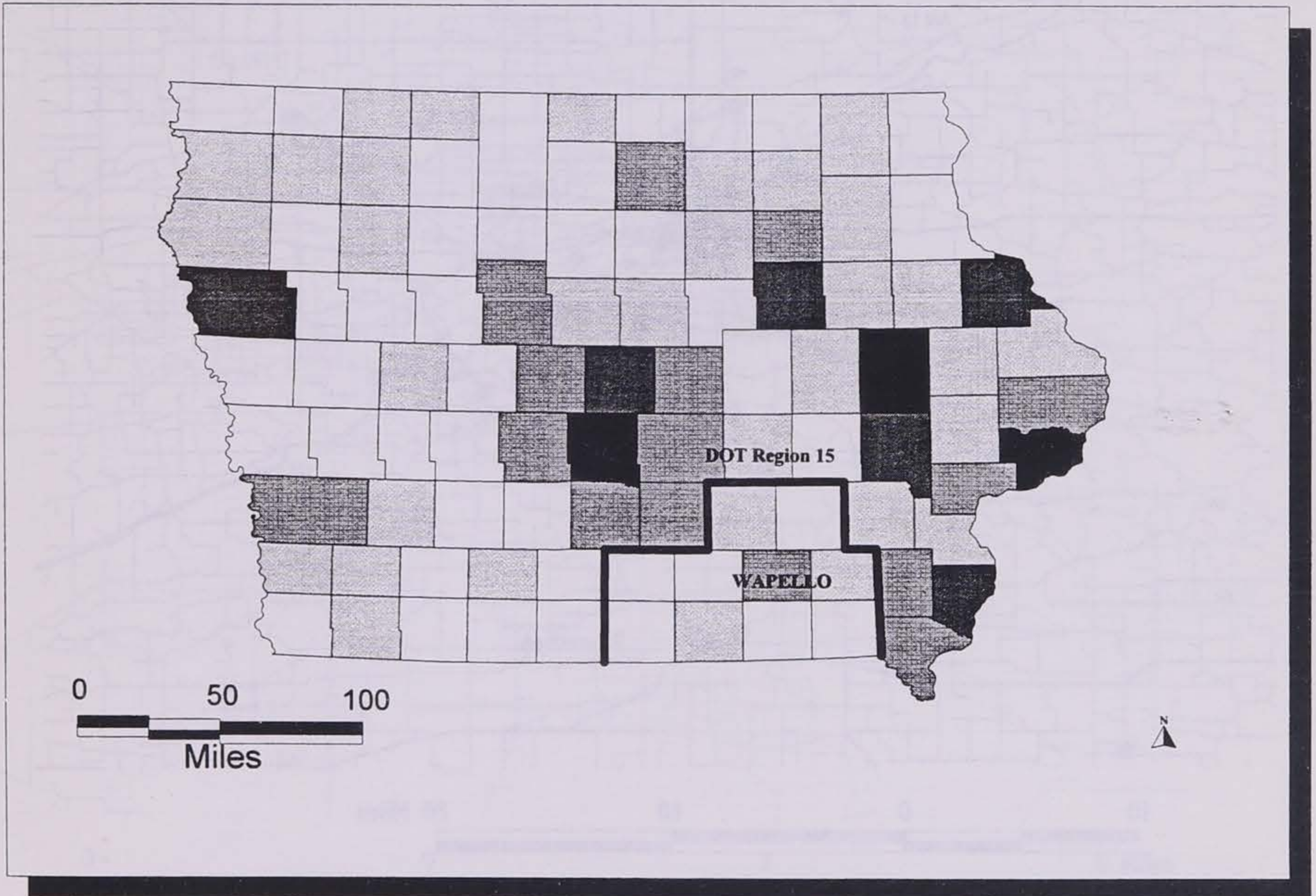
Persons per Square Mile
by category

■	228 to 540	(3)
■	97 to 228	(6)
▨	43 to 97	(15)
□	26 to 43	(33)
□	10 to 26	(42)

Figure 2

Clients by Route
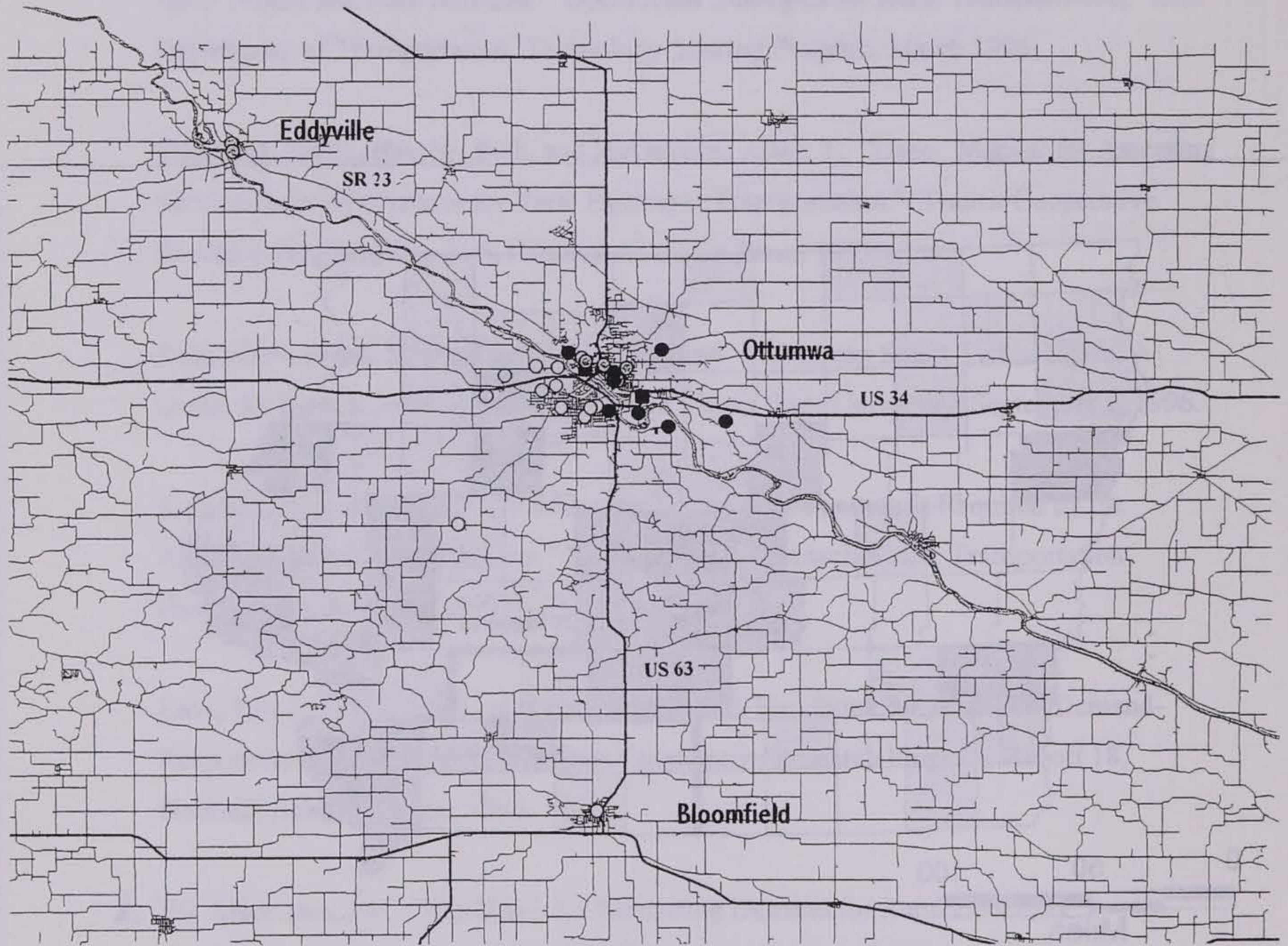
- • Wap East
- ⊗ Wap West
- ○ Wap South
- ▪ OTA-Tenco
- /\/ Primary road
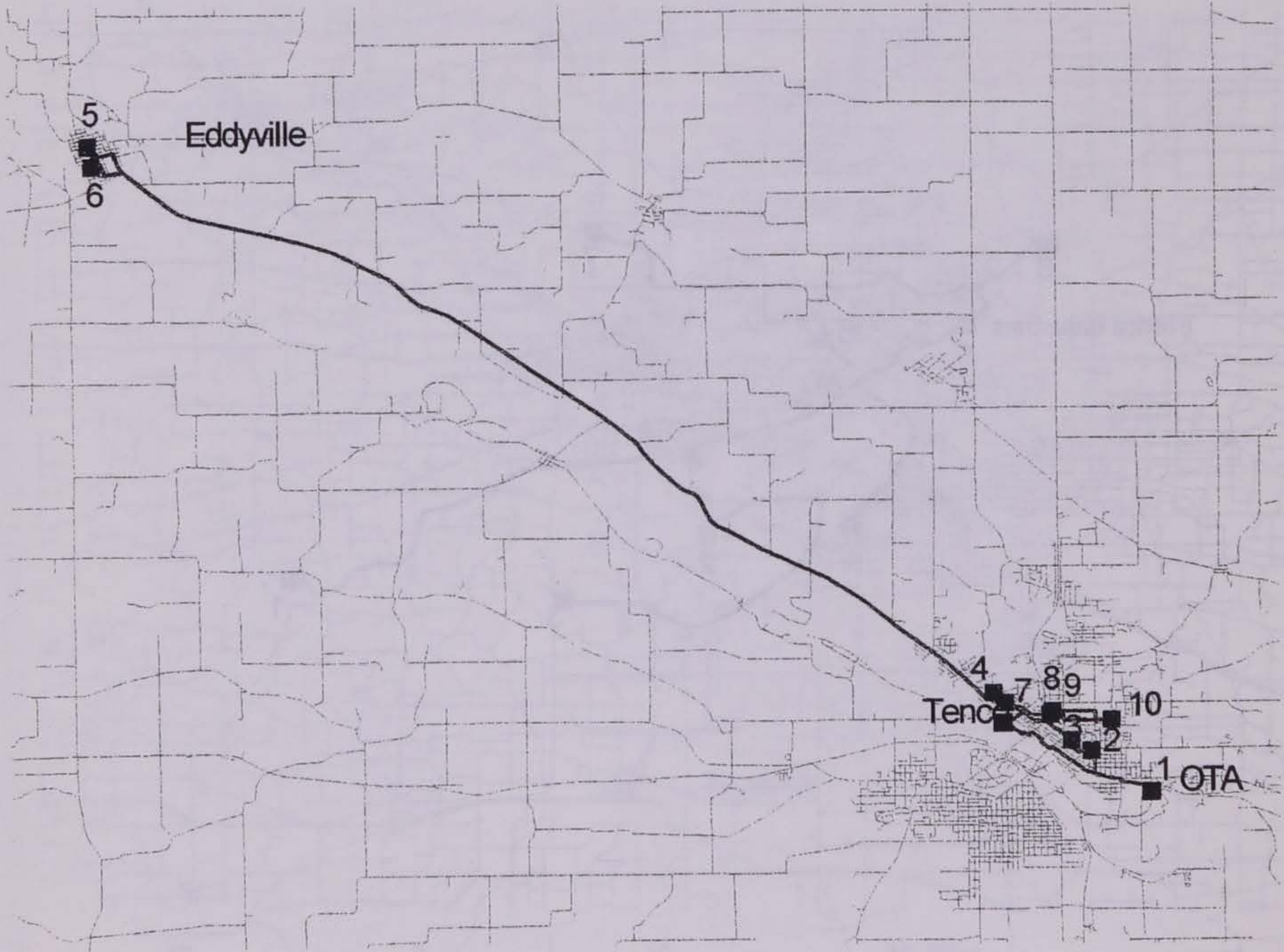- /\/ Secondary and Municipal Roads

Figure 3
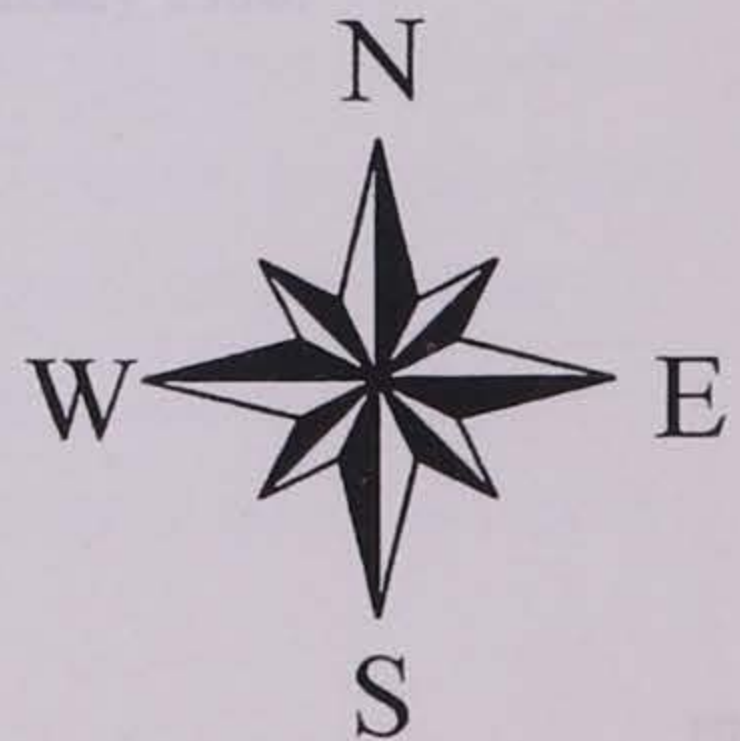
Wapello East - Shortest Path
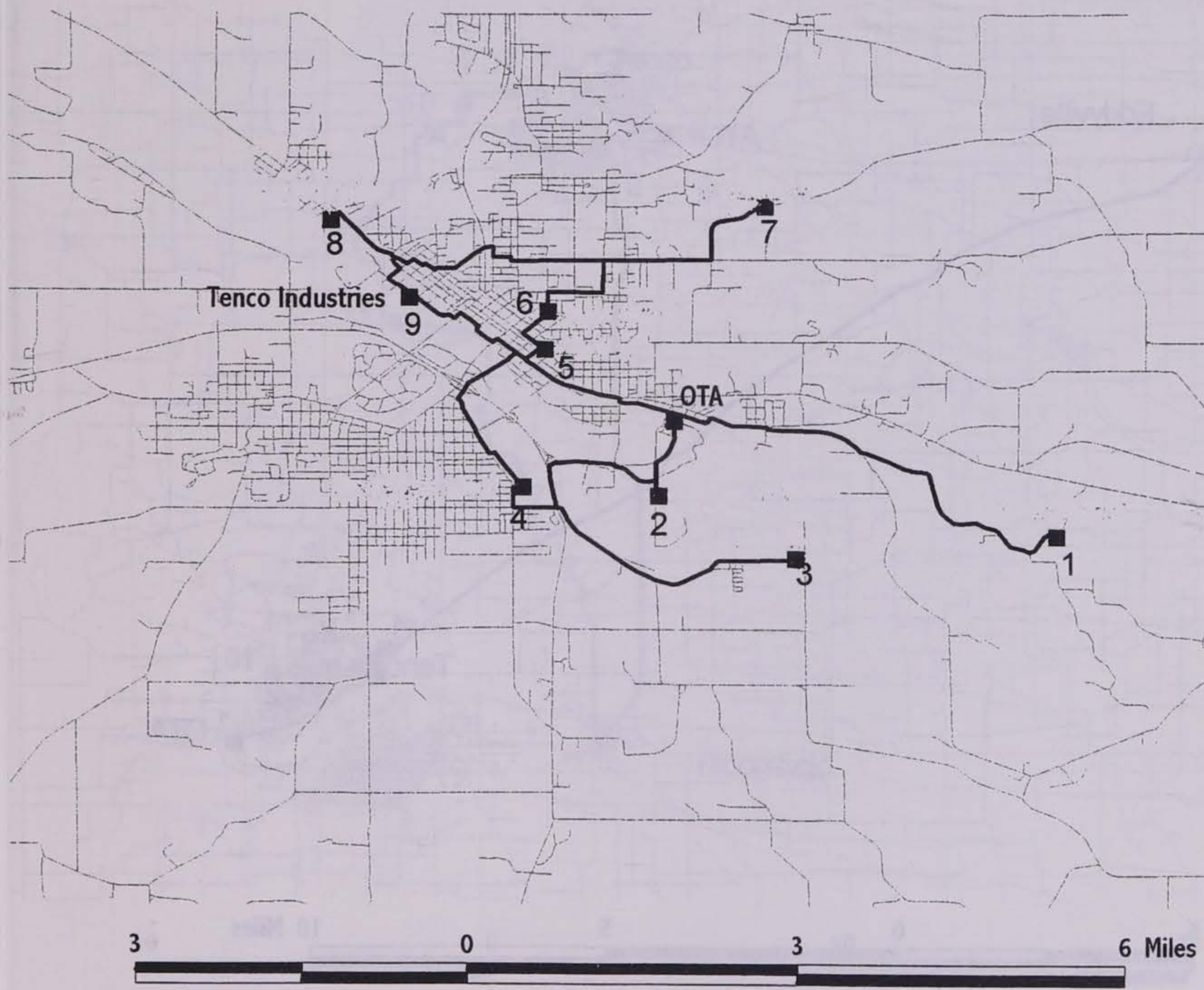
Return to OTA - 25.44 miles
To Tenco - 23.04 miles

Route based on shortest path
Road Network
■ Stop/Clients
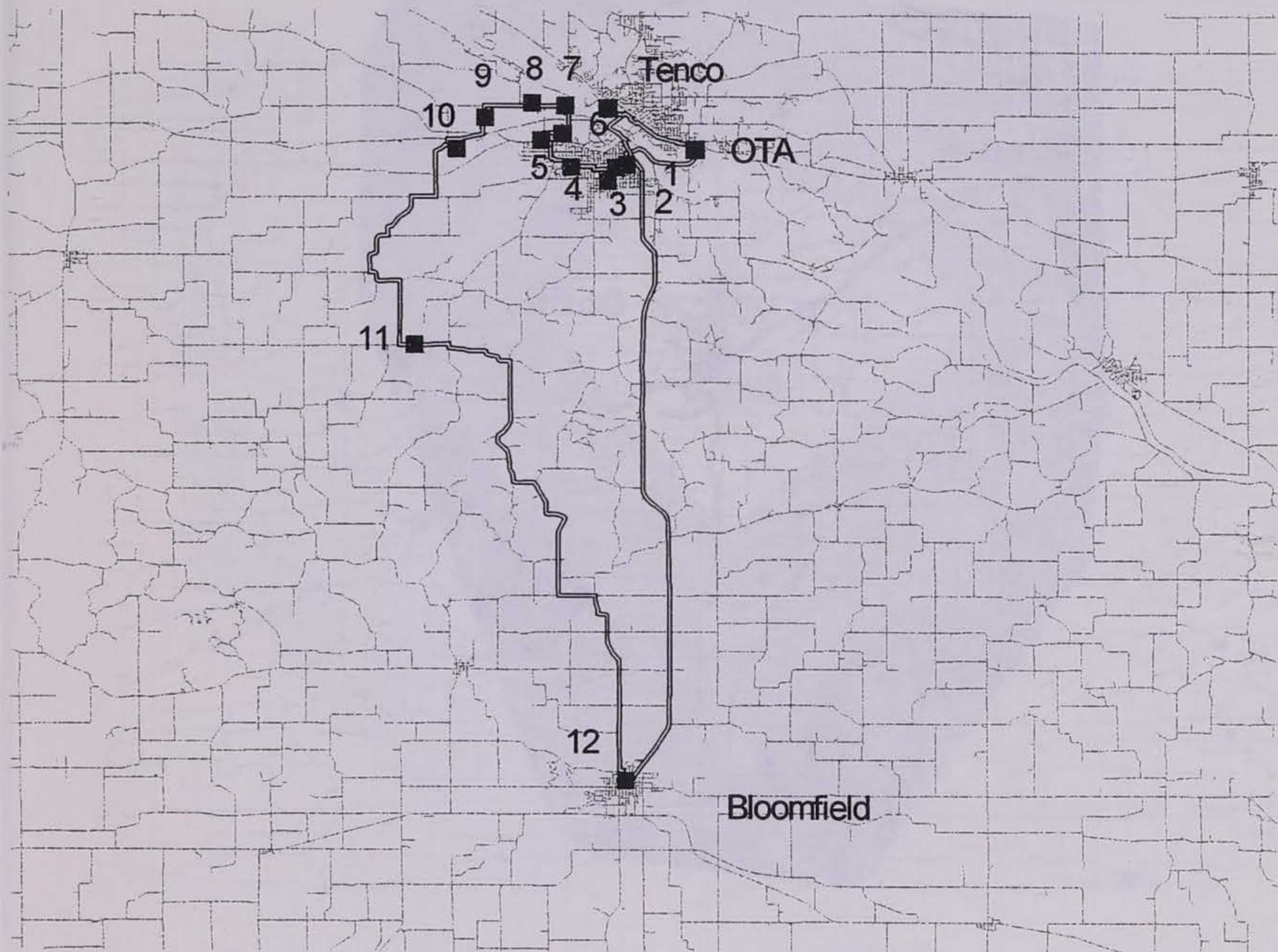■ Orgin-Destination (OTA-Tenco)

Figure 4

Wapello West - Shortest Path

Return to OTA - 38.73 miles
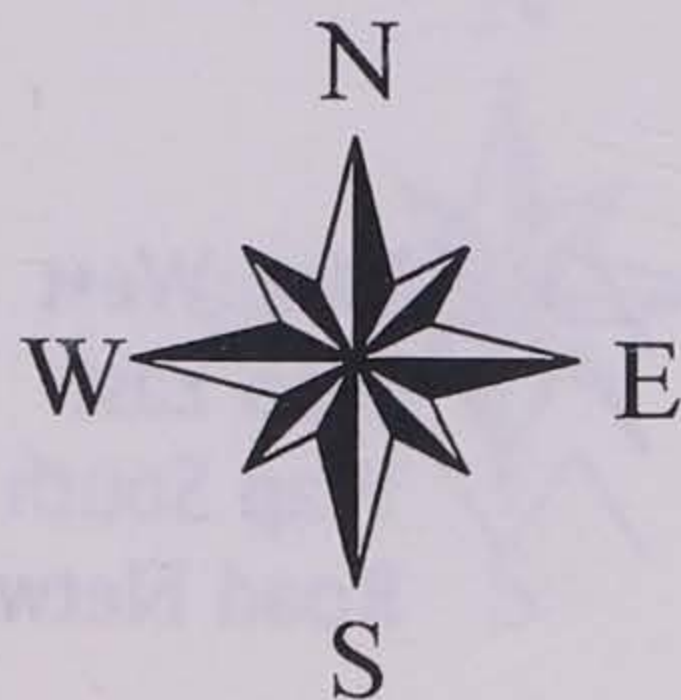To Tenco - 36.33 miles

N
W — E
S
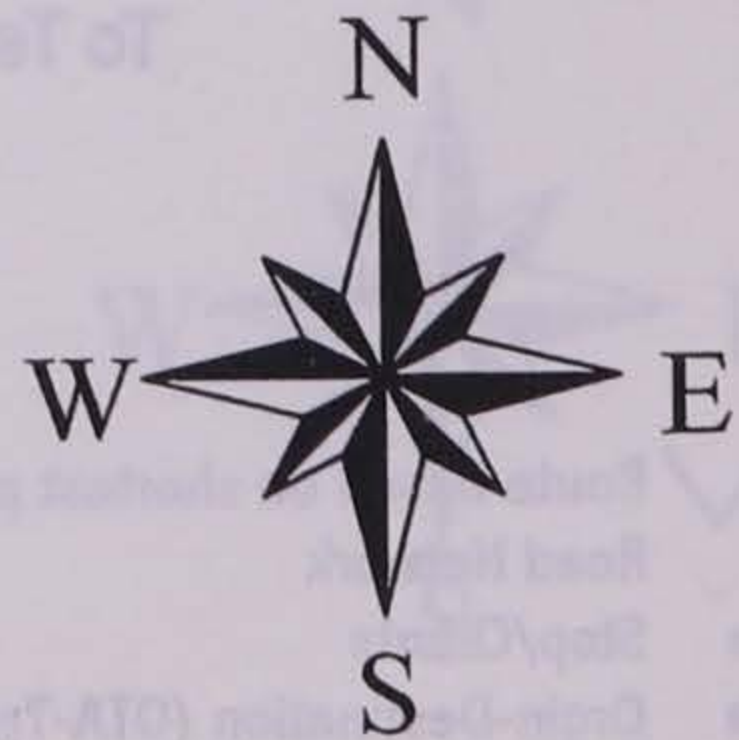
Route based on shortest path
Road Network
Stops/Clients
Origin-Destination (OTA-Tenco)

Figure 5

Wapello South - Shortest Path

10   0   10   20 Miles
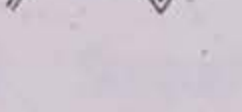
Return to OTA - 56.97 miles
To Tenco - 54.57 miles

Route based on shortest path

Road Network

■   Origin-Destination (OTA-Tenco)

■   Stops/Clients

Figure 6

Workshop Routes

Eddyville

Ottumwa

Bloomfield

10   0   10   20 Miles
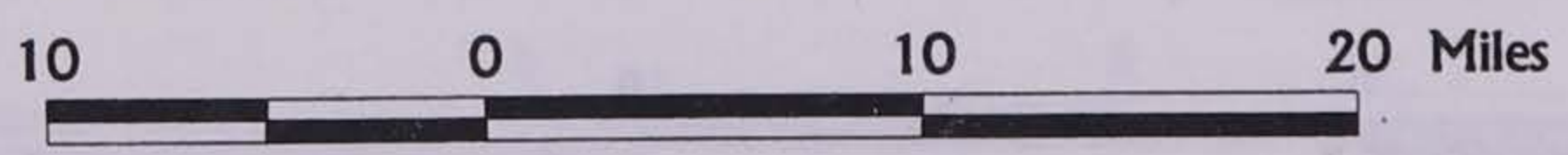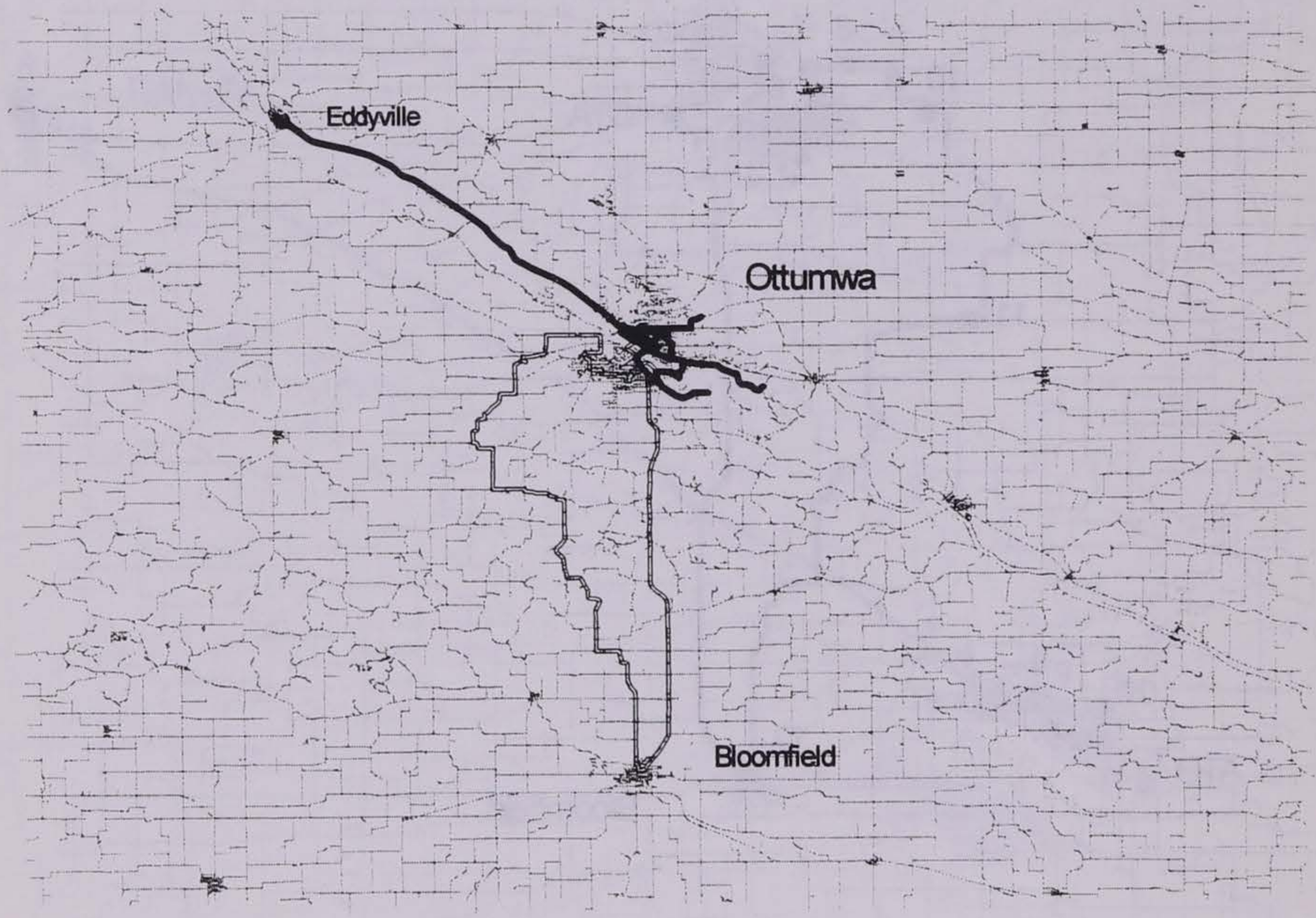
Wap West
Wap East
Wap South
Road Network

N
W   E
S

Figure 7
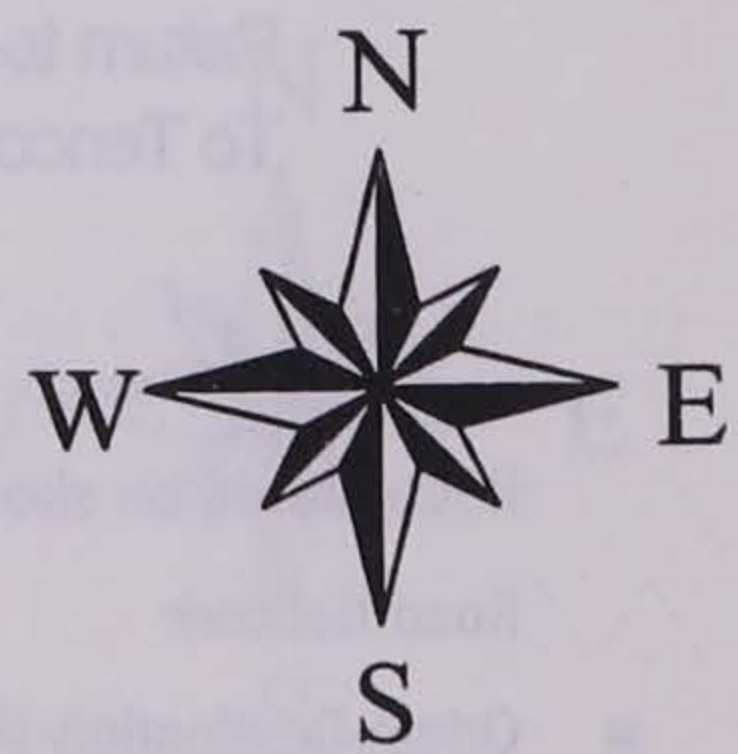
Service Area - Travel Time

10, 20, and 30 minutes from OTA

7   0   7   14   Miles

Road Network - DOT Database

☐ 10 minutes
▨ 20 minutes
■ 30 minutes

N
W   E
S
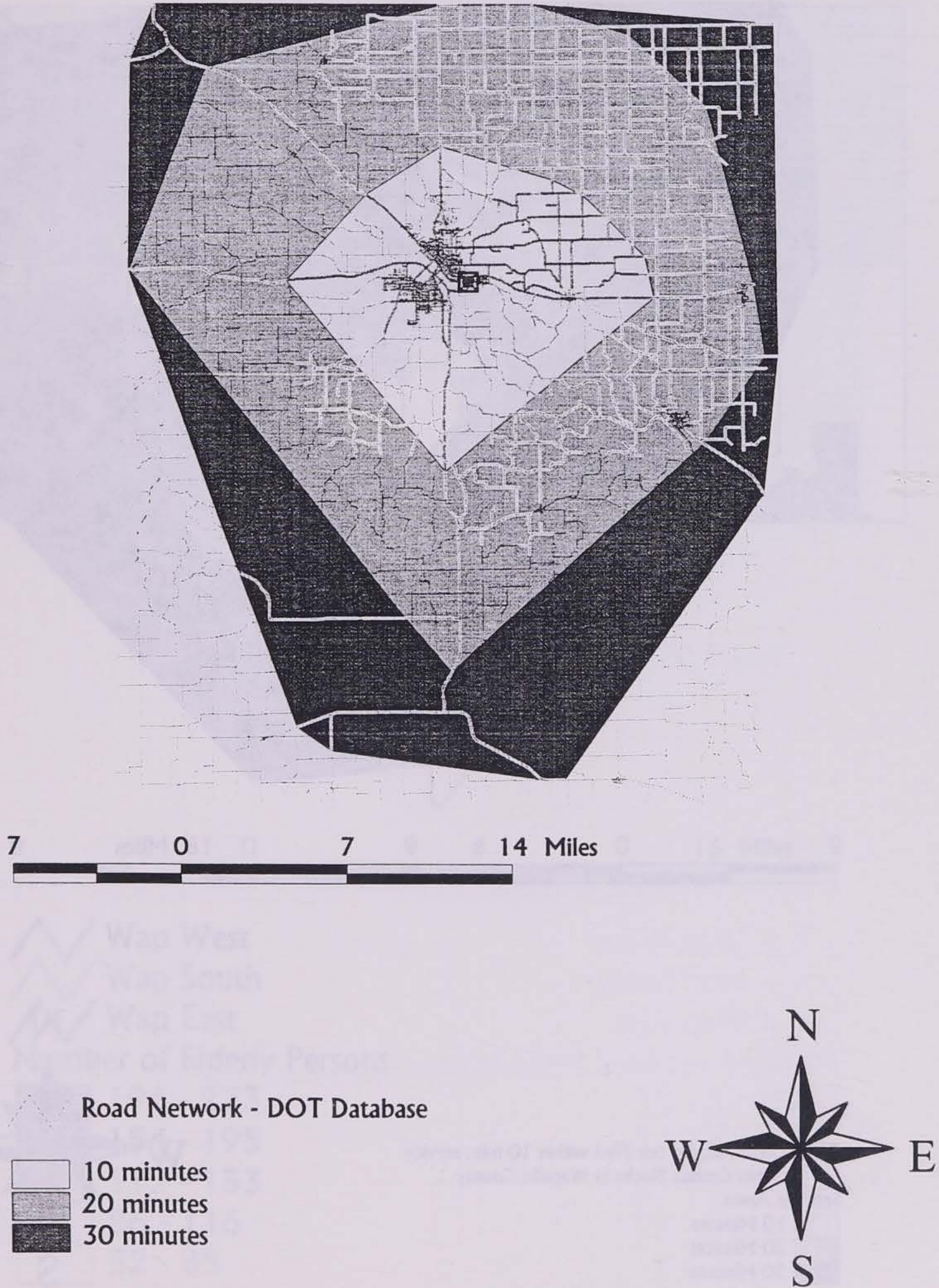
Service Area by Census Blocks in Wapello County

9   0   9   18 Miles
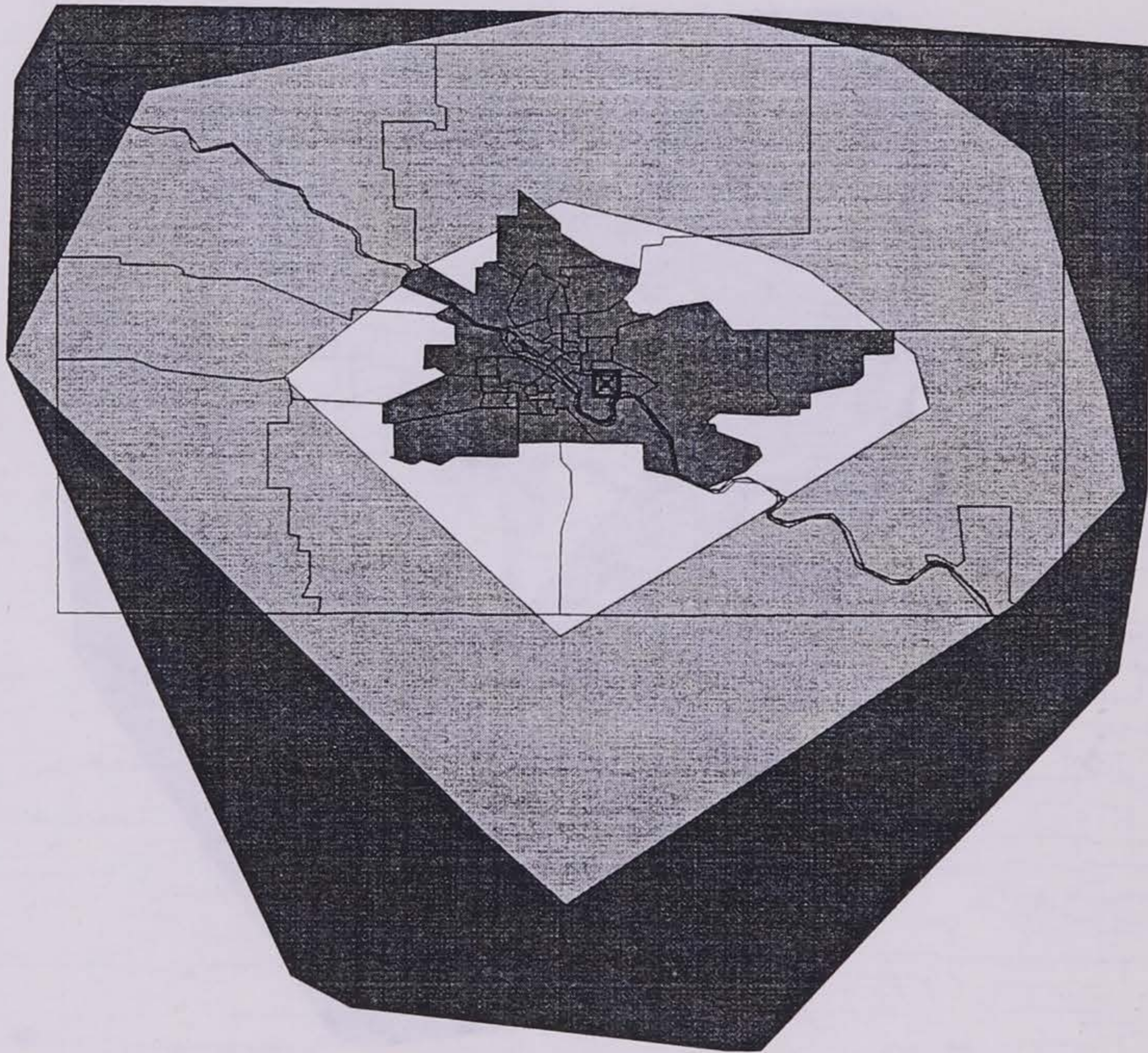
Census Blocks centered within 10 min. service
Other Census Blocks in Wapello County
Services Areas
10 Minutes
20 Minutes
30 Minutes

N
W E
S
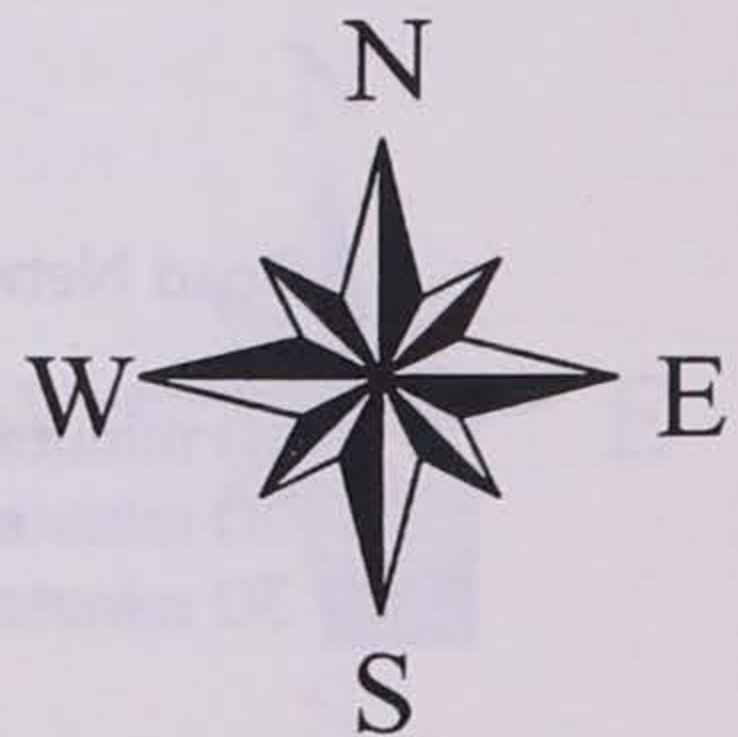
Elderly Persons

Wapello County by Census Block, 1990

8   0   8   16 Miles

ᐱ Wap West
ᐱ Wap South
ᐱ Wap East

Number of Elderly Persons

- ■ 196 - 273
- ■ 154 - 195
- ▨ 117 - 153
- ▢ 86 - 116
- □ 52 - 85

N
W E
S
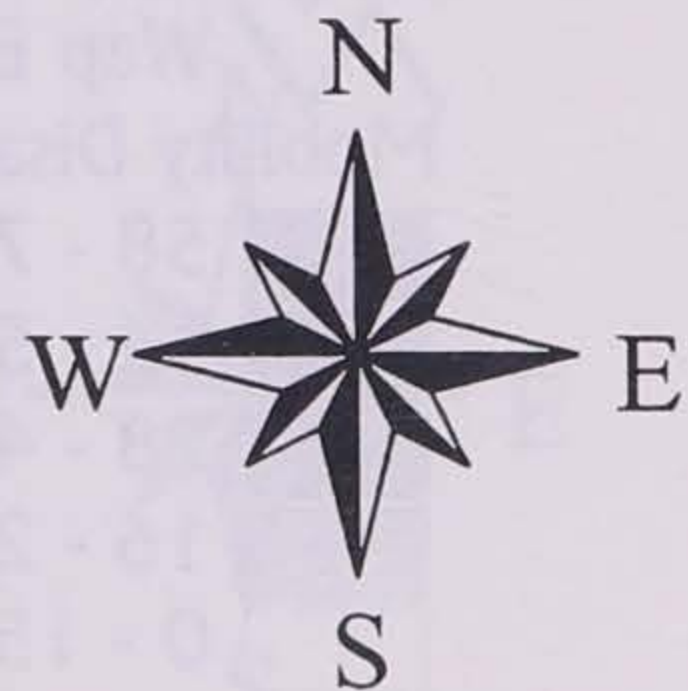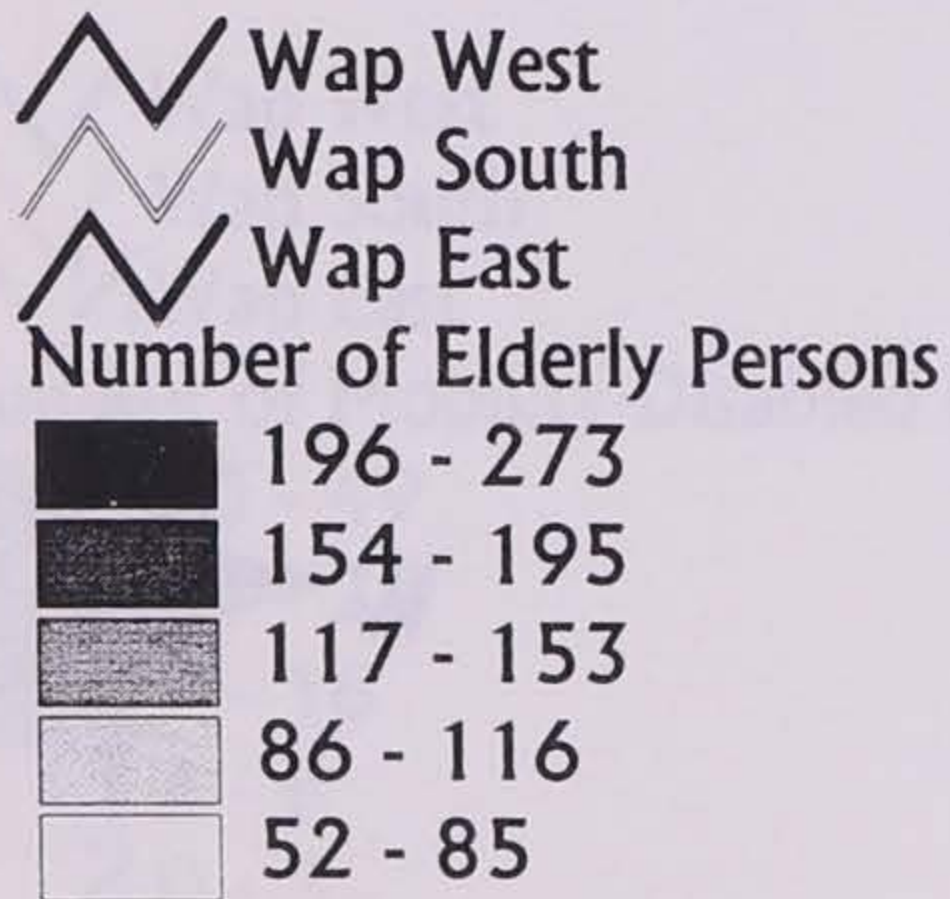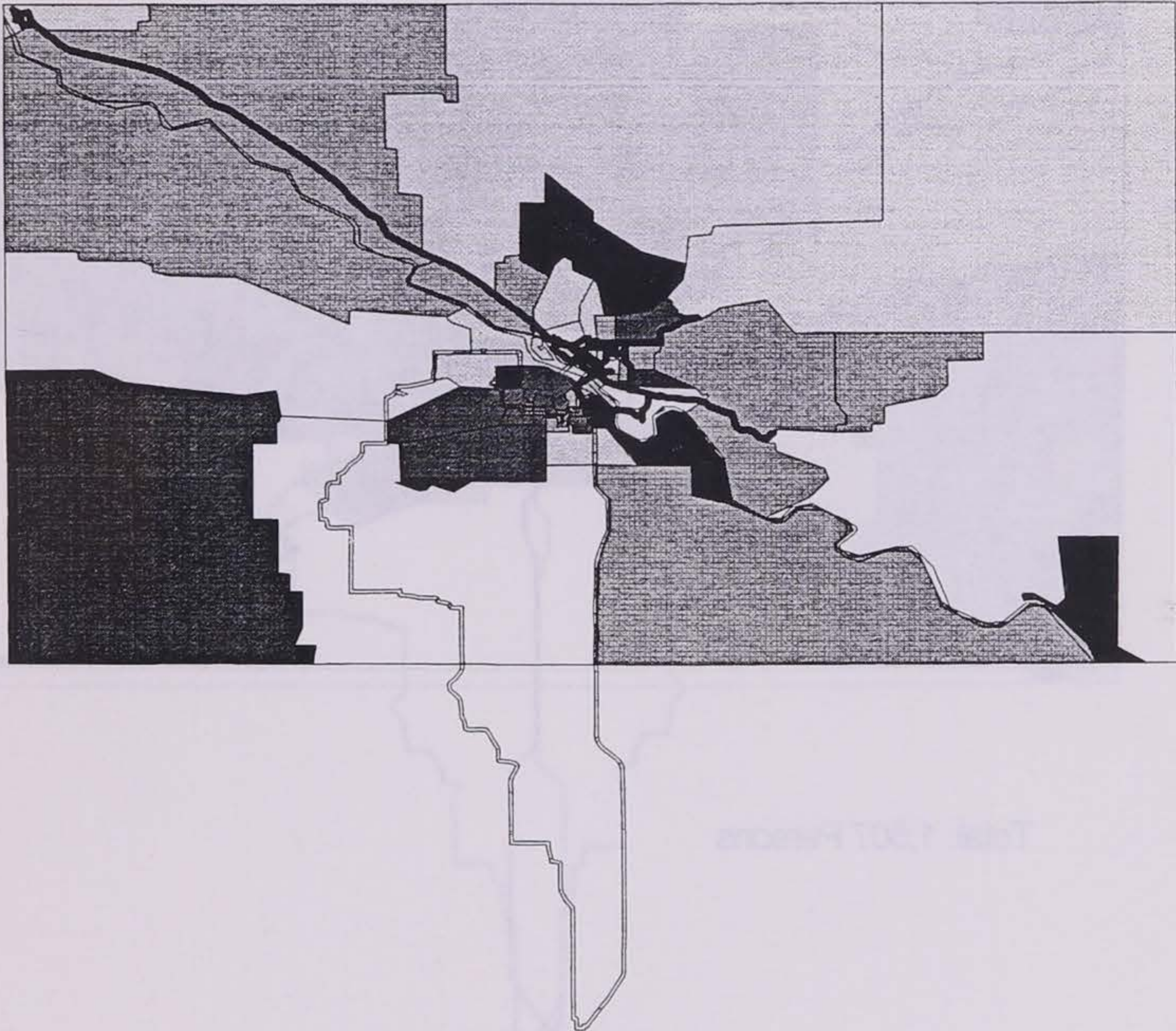
Total Mobility Disabled

Wapello County by Census Block, 1990

Total: 1,507 Persons

0.1   0   0.1   0.2   Miles

Wap West
Wap South
Wap East

Mobility Disabled Persons

58 - 76
44 - 57
28 - 43
16 - 27
0 - 15

N W E S

Figure 11
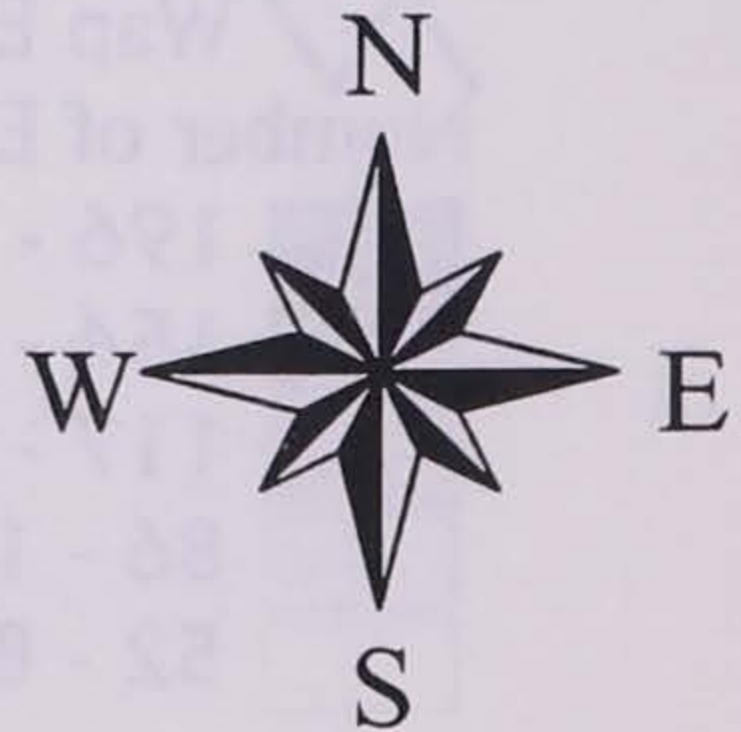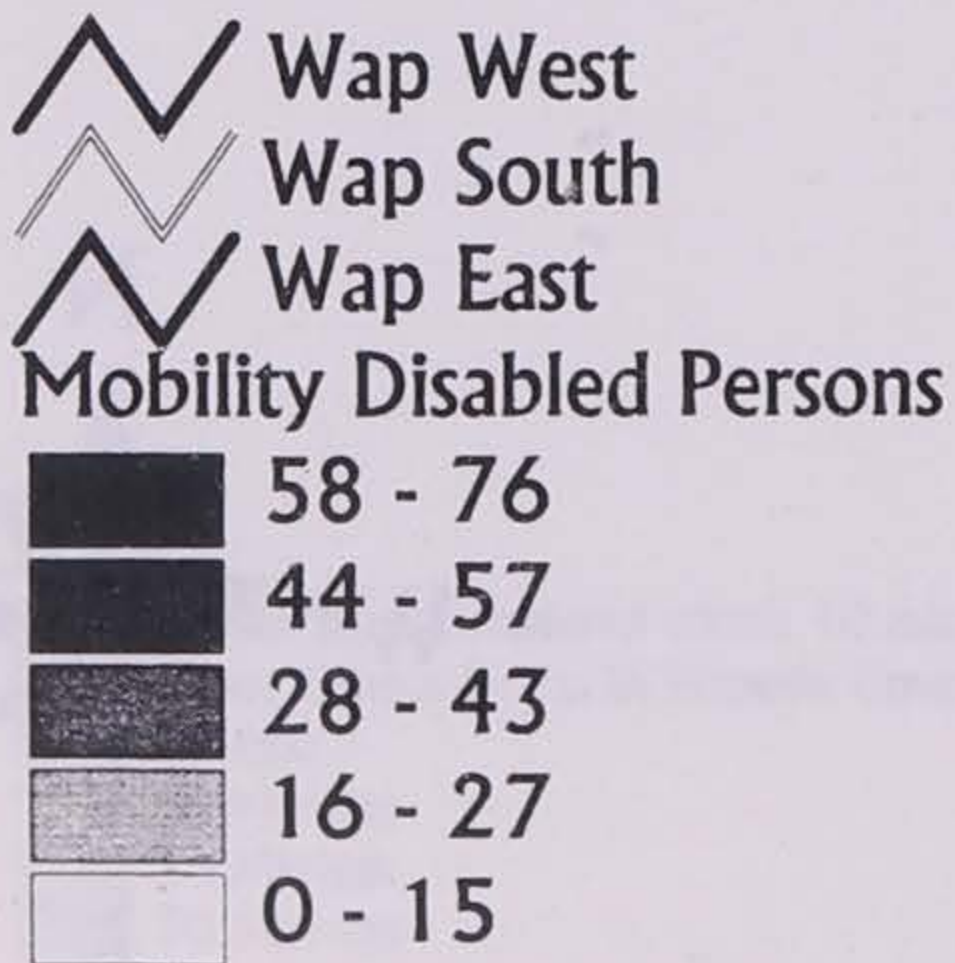
Mobility Disabled, 16 - 64 Years Old

Wapello County by Census Block, 1990

8   0   8   16 Miles

⋀ Wap West
⋀ Wap South
⋀ Wap East
Number of Mobility-Disabled Persons

- 30 - 49
- 17 - 29
- 9 - 16
- 4 - 8
- 0 - 3

N
W E
S
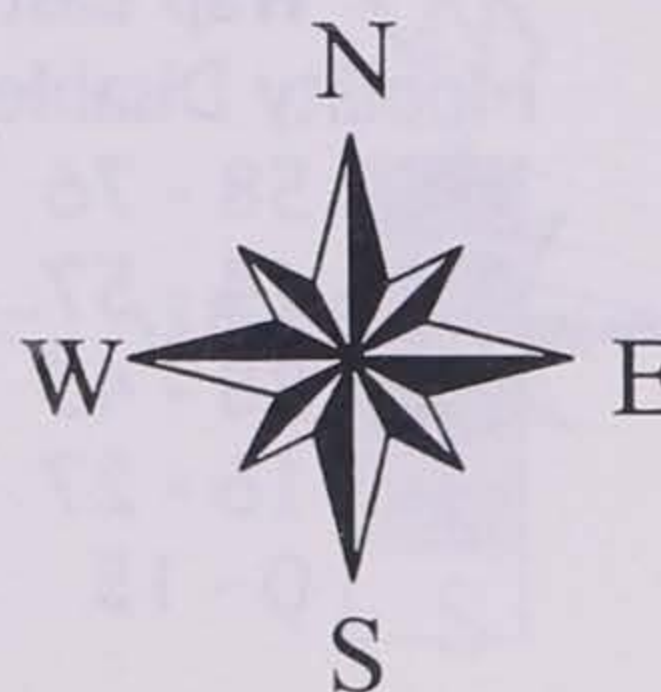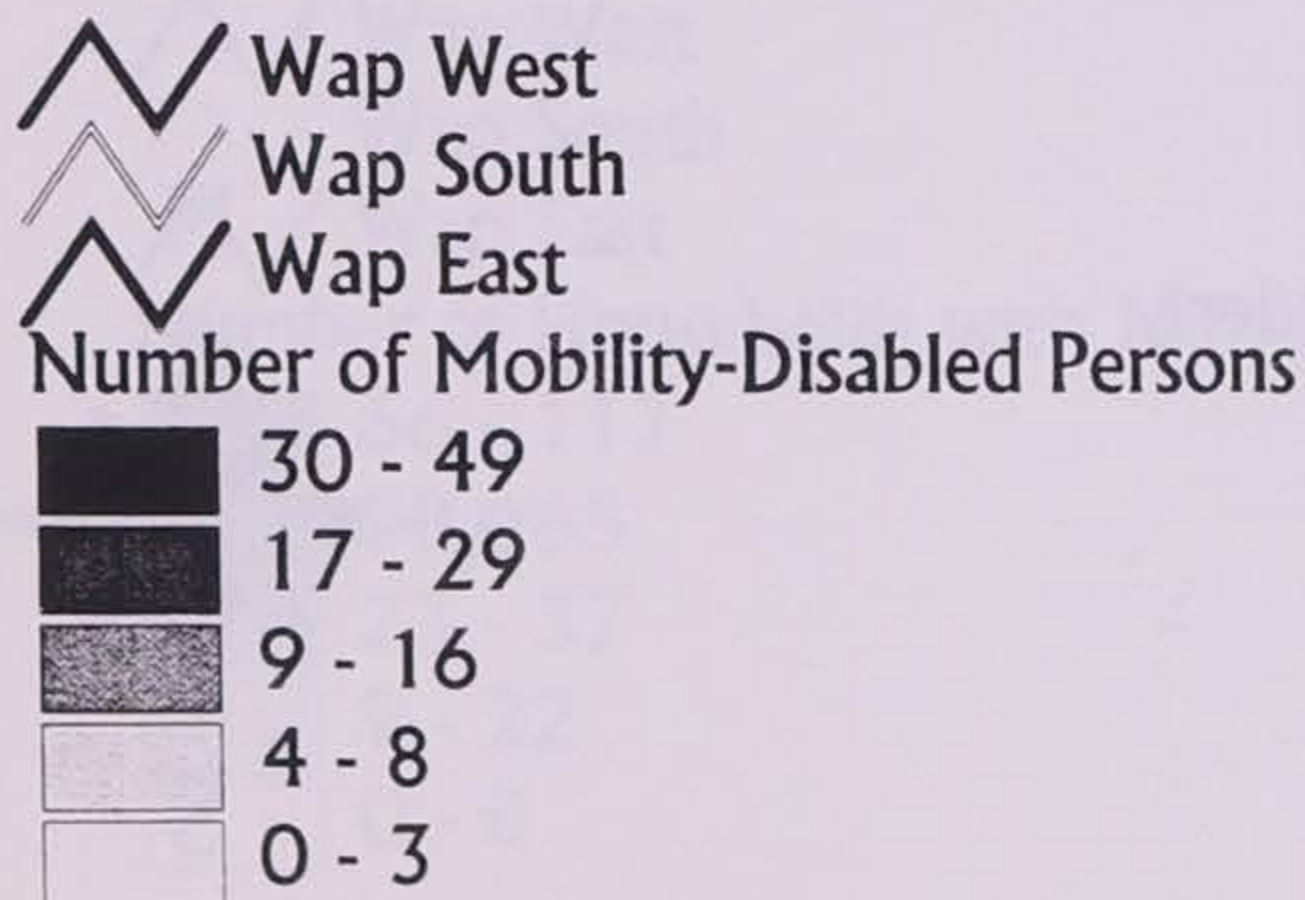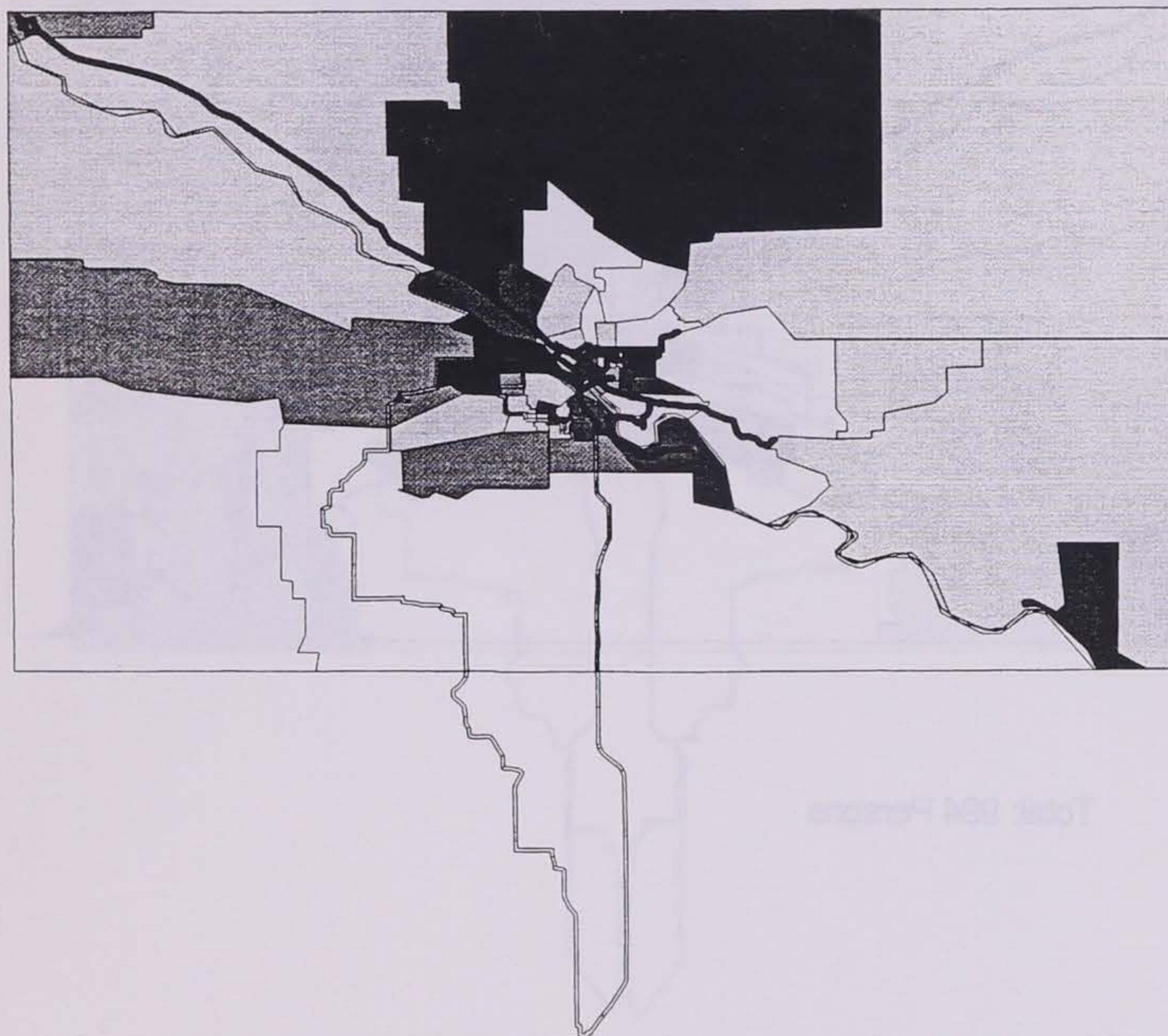
Mobility Disabled & Elderly

Wapello County by Census Block, 1990

Total: 994 Persons

| 0.1 | 0 | 0.1 | 0.2 Miles |

Legend

/\/ Wap West
/\/ Wap South
/\/ Wap East

Mobility Disabled and Elderly

- 58 - 76
- 44 - 57
- 28 - 43
- 16 - 27
- 0 - 15

N
W   E
S

Figure 13
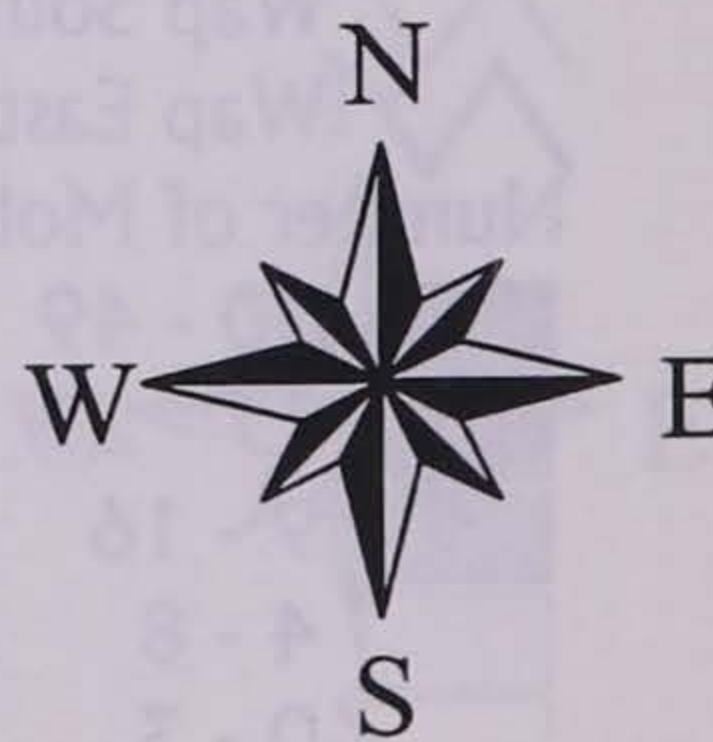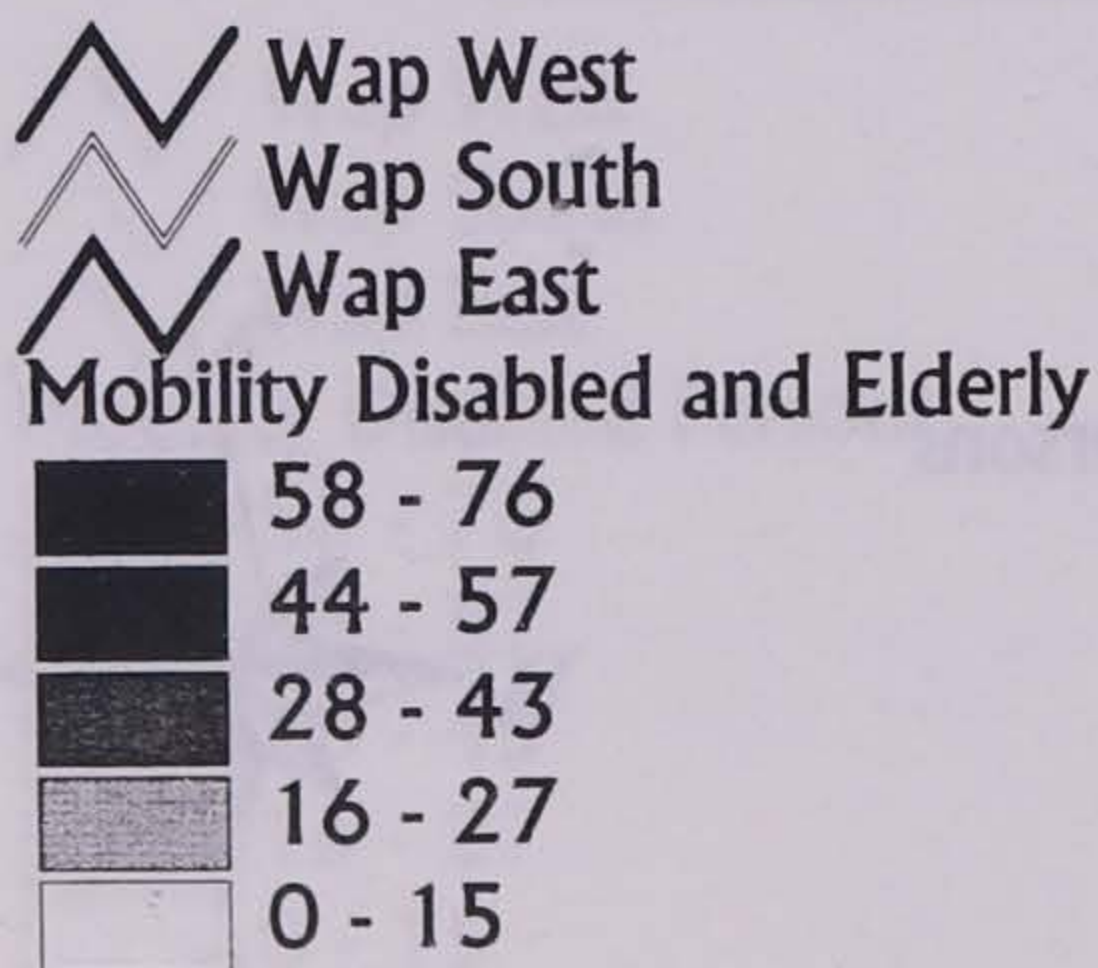
No Auto Households

Wapello County by Census Block, 1990

8   0   8   16 Miles

Wap West
Wap South
Wap East

Number of Households with No Auto

- 66 - 117
- 38 - 65
- 23 - 37
- 9 - 22
- 0 - 8

N
W E
S
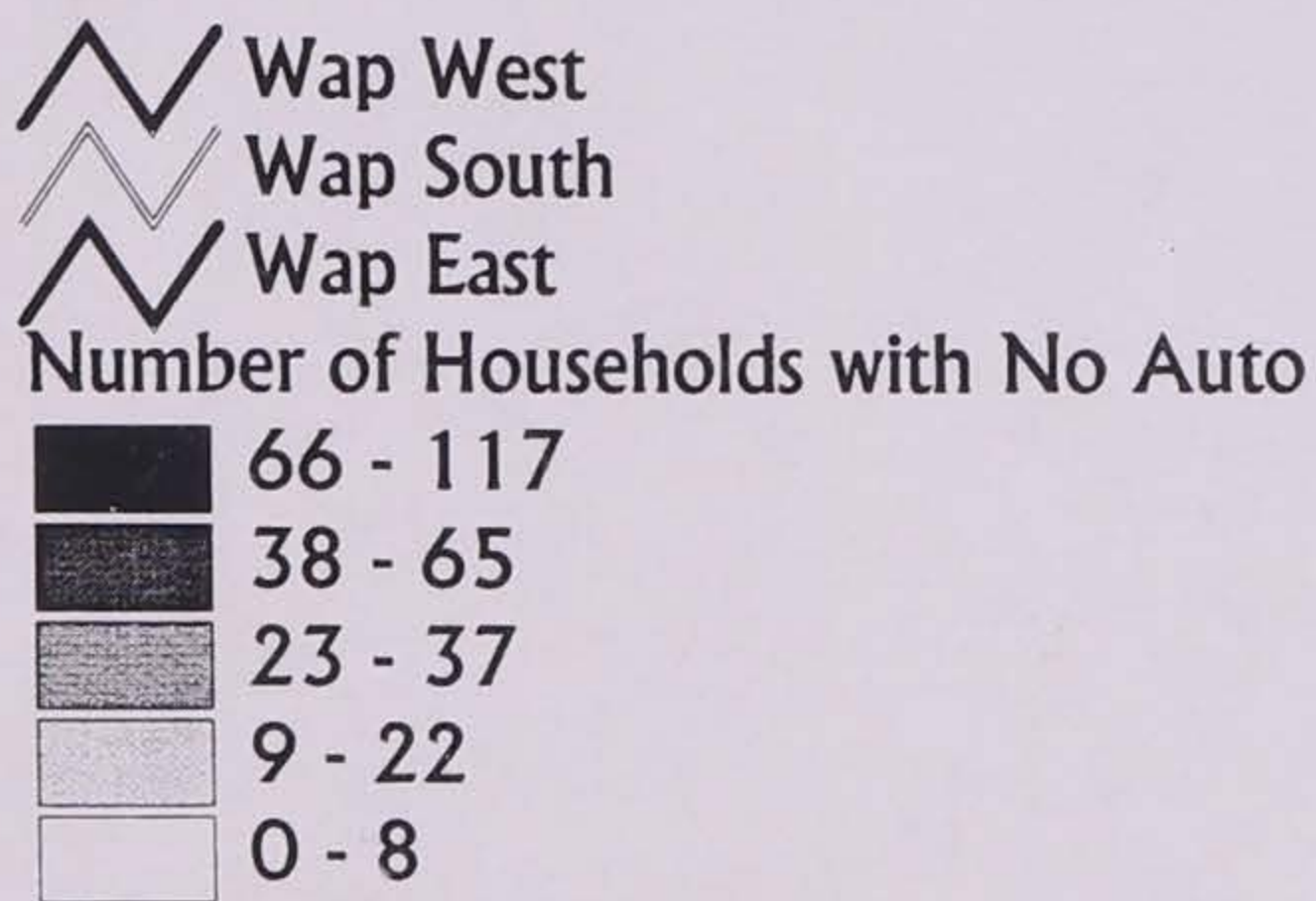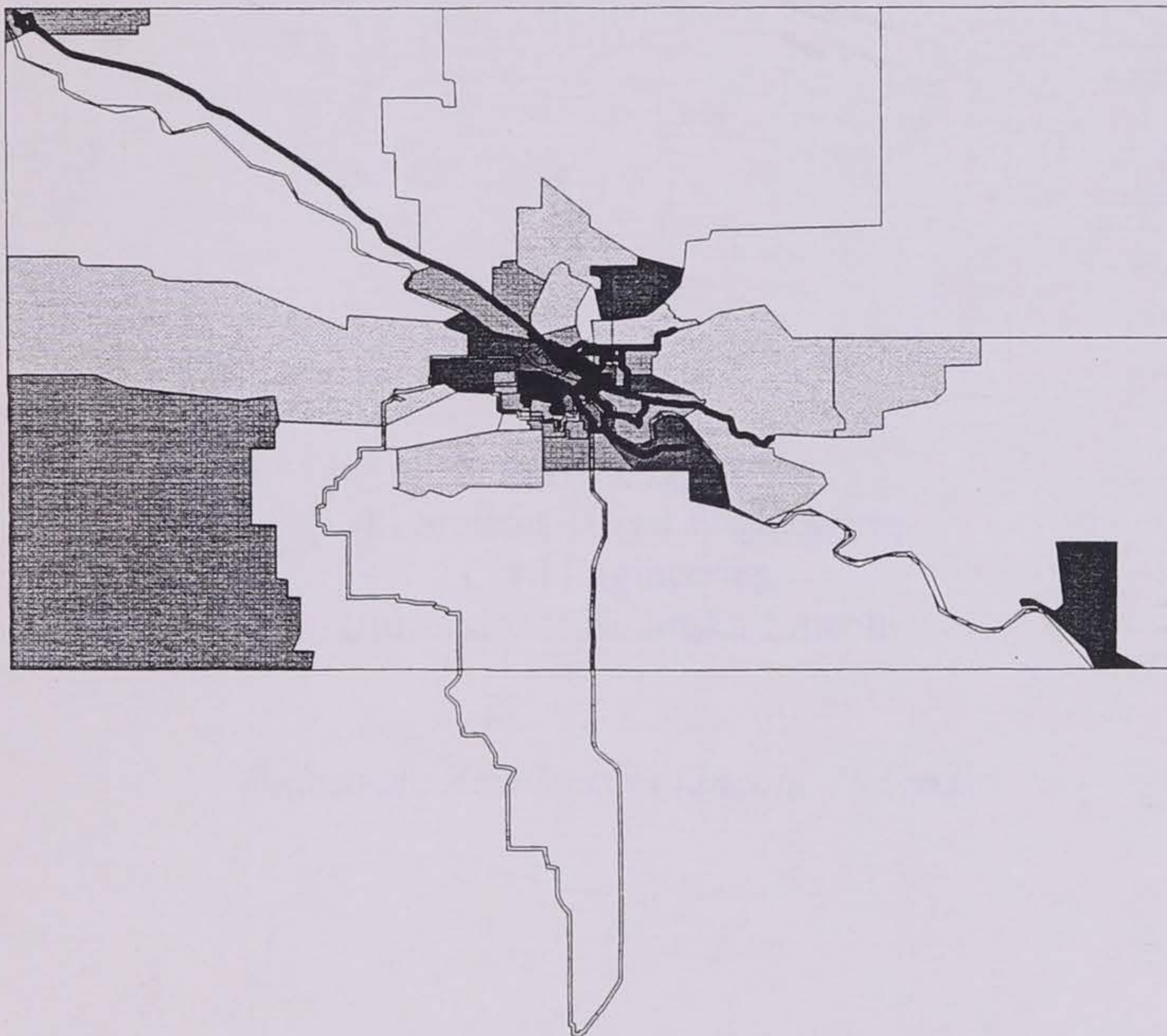
Patrick Byrd
MS Student - Civil Engineering
Civil Engineering
University of Nebraska-Lincoln

Pedestrian Accidents in Lincoln, Nebraska

ABSTRACT

In the United States, accident studies are performed continuously and exhaustively to provide for roadway safety. However, comparatively, less attention is given to pedestrian accidents than to vehicle accidents. Possible causes and solutions should be investigated to reduce pedestrian-auto crashes. The pedestrian accident history, spanning from 1995 to 1997, of Lincoln, Nebraska was analyzed. This was comprised of 320 pedestrian-vehicle accident reports filed by the Lincoln Police Department. An analysis of the data shows that a large percentage of drivers involved in accidents was under the age of twenty-one. This was also true for the pedestrians involved as well. A fact that suggests a lack of experience factor for the drivers as well as the pedestrians. A large amount of pedestrian accidents are due to unauthorized crossings i.e. (darting into the street between blocks). In these situations, it is not enough to simply be following the proper driving laws. One must expect the unexpected when operating a motor vehicle. Many younger drivers and pedestrians, due to their lack of experience and maturity, are not ready for unexpected obstacles when they occur. This is where increased education and driving restrictions can be valuable. Other pedestrian accidents also occurred at larger volume roadways with speed limits between 25mph and 35 mph. These pedestrian accidents can be reduced by enforcing problem area speed limits, increasing warning signs, modifying intersections to make pedestrian crossing safer i.e. (median islands), restricting traffic movements and rerouting traffic around pedestrian areas. This initial study will give further studies of pedestrian accidents specific areas to concentrate more statistically intensive analyses on.

Key Words: pedestrian accidents, classification of pedestrian accidents

BACKGROUND

On average, a pedestrian is killed in a traffic crash every 93 minutes (1). This adds up to approximately 5,600 pedestrian deaths in a year in the United States. Although overall numbers of pedestrian deaths and accidents have steadily decreased in the passed 15 years, there is still a constant problem in urban areas. This is not surprising due to the fact that heavy urban volumes of vehicles are mixed with a large volume of pedestrians. Thus pedestrian-vehicle accidents are more likely to occur.

To reduce these urban area risks for pedestrians, countermeasures need to be formulated to prevent pedestrian injury from vehicles (4). As many studies in the passed have found, the problem with the development of these countermeasures is the lack of descriptive data (2). Police accident reports are good descriptors of the time, persons involved, and location of the accident, however they do not classify the cause of the accident. The NHTSA has developed a pedestrian accident typology that is being used by many researchers and cities (2 – 4). By classifying the type of pedestrian accident, one can discern what happened that led up to the accident in question. An example of a pedestrian accident type would be "pedestrian mid-block dash". This classification has also been applied to bicycle accidents as well (5).

In this research, an abbreviated form of the above typology is used by the city of Lincoln to classify over 300 pedestrian accidents that occurred between 1995 and 1997. The city of Lincoln, Nebraska is a community of about 300,000 people and is comprised of a major university population from the University Nebraska-Lincoln. This results in a large pedestrian and bike-pedaling volume that is mixed with the normal vehicular traffic.

The goal of this research is to isolate possible causes of pedestrian accidents due to

location, and demographics and develop countermeasures for such causes.

ACCIDENT DATA

The data source for pedestrian accidents was strictly from filed accident reports provided

by the city of Lincoln. These accident reports spanned a three-year period between 1995

and 1997, and included over 300 pedestrian accidents. The data provided were hard

copies of the original Police Accident Reports (P.A.R.'s). From these documents, a data

set was created that encoded the time, day, month, driver demography, pedestrian

demography, location, and the types of accident occurring. It is important to note here

that data from accident report depends on the accounts of witnesses and the reporting

officer. Therefore the accounts are as creditable as the witnesses and police officers

involved in the accident.

The following pedestrian accident typology was used for this study and was supplied

by the city of Lincoln.

1) Straight at intersection
2) Left turn at intersection
3) Right turn at intersection
4) Others in Intersection
5) Crossing behind parked car
6) Walking in roadway
7) Mid-block crossing
8) Not in roadway
9) Working or playing in roadway
10) Unauthorized crossing
11) Others in roadway

ANALYSIS OF DATA

Number of Accidents

According to the P.A.R.'s from 1995 to 1997, there were 320 pedestrian-vehicle accidents. Five of those were fatal, and over 2/3 were minor injuries. Using this data set, the frequency of accidents were accounted by certain characteristics of the accident i.e. (age of driver, speed limit, injury severity e.t.c.) Also select variables were cross tabulated to investigate dependence of variables using a chi-squared test.

Accident Characteristics

Almost 50% of the reported accidents occurred in volumes of 6000 to 18000 ADT. These areas would be considered collectors and minor arterial streets.

Well over 75% of the pedestrian accidents occurred at roadways with speed limits of either 25 mph or 35 mph. These facts are shown in Figure 1. Also they occurred primarily at two-way streets as opposed to one way streets. These characteristics are most likely frequent due to the fact that most of the streets in Lincoln fall under these two categories.

Accident Time

The accidents were distributed quite evenly over the year. There was no seasonal pattern observed of pedestrian accidents except for a large amount observed during the months of August to October. This may be due to the fact that weather in the mid-west is more temperate and less wet during the fall months and thus encourages more bicycle and pedestrian traffic. However, evidence of this is not strong enough to draw strong conclusions.

Figure 2 indicates the accident histograms for day of the week and time of day. Its not

surprising that Friday demonstrated the highest pedestrian-vehicle accident frequency.

This is accounted for by the impatient behavior of drivers preparing for the weekend in

conflict with equally impatient pedestrians. Sunday exhibited the fewest accidents with

at least a 60% decrease in accident frequency when compared to the other days of the

week. The other days of the week were constant and generally had frequencies 30% less

than Friday.

Almost 40% of the accidents occurred in the p.m. peak period starting at 4:00 until 6:00.

The rest of the day hours were evenly distributed and not surprisingly the night hours saw

the lowest frequency of accidents. This suggests more volume dependence than a

visibility one.

Driver Characteristics .

Figure 3 shows that the majority of drivers involved in pedestrian accidents were under

the age of 25 years old. Middle age adults were much less frequent and older (over 65)

were very few. The low amount of senior citizens involved in accidents has a lot to do

with the fact that older people drive less than younger. The split between male and

female drivers involved in pedestrian accidents was about 60% and 40% respectively.

Since drinking and driving is a focus concern in this country, the drivers' and

pedestrians' conditions will be discussed. Because of the small sample size not many

conclusions can be drawn, however the following facts can be reported. There were 9

confirmed pedestrian accidents in which the driver and/or the pedestrian were under the

influence of alcohol. It is of interest to note here that 5 out of the 9 accidents occurred

either as an unauthorized crossing or pedestrian was already in the roadway mid-block.

The reduction in reaction time and visual capabilities seems to put those pedestrians that make unauthorized crossings or are already in the roadway more at risk. However, due to the small sample size more data collection would need to be taken specifically collection of strictly alcohol-related accidents.

Pedestrian Characteristics

As the pedestrian age distribution shows (Figure 4), children 20 years and younger showed a much higher frequency than all other age groups. As the age increased the frequency appeared to reduce steadily. The number of males struck by vehicles was about even with the amount of females, with a difference of only 3 accidents over a three-year period.

The severity of injury was divided into 4 categories, and are shown below:

Injury 1-Fatality

Injury 2-Needed a hospital stay and follow up medical attention

Injury 3-Was treated at a hospital but quickly released

Injury 4-Minor injury did not need medical attention

As was mentioned previously, there were 5 pedestrian fatalities that occurred between 1995 and 1997. Injury type 3 occurred most frequently, with a frequency of half the total pedestrian accidents.

From the witness accounts found in the P.A.R.s, it was ascertained whether the pedestrian was walking alone or with a group of pedestrians. In most of the accidents (76%), the pedestrian was alone.

Accident Types

In Figure 5, the accident data is broken down into 11 types and the corresponding percent

frequencies are shown. The most frequent accident type is the unauthorized crossing at

mid-block. Most of these types of accidents are a result of the pedestrian dashing into

the path of oncoming traffic without looking. Other frequencies that were noticeably

higher were those accidents that occurred in the crosswalk comprising of left turn, right

turn and straight-ahead pedestrian-vehicle accidents. This is not surprising since a larger

volume of pedestrians will be crossing at a designated crosswalk, and therefore, a greater

likelihood that an accident would occur at such a location. The other accident types were

much less frequent as shown.

CROSS TABULATIONS

A select amount of variables, mostly involving accident type, were then cross tabulated

with one another. The variables that were crossed were chosen based on their importance

to the cause and effect of pedestrian accidents. The following section discusses the

findings of those cross tabulations that exhibited a good χ^2 value and a p-value of around

.05, and thus dependence on the other. Within those cross-tabulations, those categories

whose frequencies were either under or over represented beyond expected were

commented on.

Due to the lack of field data, many of these chi-squared tests are subject to question

due to the many variables exhibiting frequencies under the chi-squared requirement of 5.

When possible, these problems were rectified by combining categories. Though this

action was performed these cross-tabulations should be looked at in more depth before

drawing a solid goodness-of-fit conclusion.

Accident Type × Driver Age

Table 1 shows the relationship between accident type and driver age, and shows that the younger age group (15-20) accounts for almost 1/3 of the pedestrian accidents a the intersection. This, at first, doesn't seem surprising however this is a large number due to the relatively smaller population of the younger driving population compared to the other two categories. The same can be said for those accidents involving unauthorized crossings. The middle age adult category (21-64) accounts for 70% of those accidents, but this is not surprising due to their larger numbers in the population. The younger drivers though a smaller group still account for 25% of these accidents.

Accident Type × Injury Severity

In Table 2, the 11 accident types are crossed with the 4 injury severity categories previously discussed. What is most noticeable is less severe accidents are over represented in the accidents that occur in the intersection. This could be from the fact that pedestrian accidents at intersections occur at slower speeds and drivers are more pedestrian aware at such locations. Unauthorized crossings and within roadway accidents showed more severe injuries having a larger share of the total. In fact 3 out of the 5 fatalities occurred on unauthorized crossings, 1 occurred crossing behind parked vehicles and 1 within the roadway. Also out of 50 accidents with a type 2 injury, 34% occurred with unauthorized crossings. This is equal to the sum of all accidents occurring within the intersection (Accident types 1, 2, & 3). This again demonstrates that vehicles are driving faster at mid-block and are less cognizant of pedestrians. This in turn leads to more severe injuries at these locations.

Accident Type × Traffic Volume

Most of the accident types across the board, occur between 6,000 and 18,000 ADT, as shown in Table 3, however unauthorized crossings has a much more uniform distribution across all volumes compared to the other types. Whereas straight, left turn, and right turn accidents in intersections resulted in the range of 0 to 12,000 ADT. This makes sense because most of the higher volume areas are major arterial streets, state highways and interstate where less pedestrian traffic can be found. Also its not surprising to see more unauthorized crossing accidents at higher volume locations because generally these types of facilities are not equipped for pedestrian traffic i.e. crosswalks. Also a pedestrian crossing at these high volume areas pose as an unexpected surprise for motorist because of the fact that it is not recognized as a pedestrian area.

Accident Type × Speed Limit

Table 4 displays the accident types and their frequencies within certain speed limits. The majority of all the accidents as stated before occur within 25 to 35 mph. This is not surprising when the distribution of roads in Lincoln are looked at. Lincoln like most municipalities has far more miles of roadway that fall into the 25mph to 35 mph categories.

It is interesting to note that there are surprisingly more unauthorized crossing accidents then expected for those roads with a 35 mph speed limit. This might suggest that there is a certain speed threshold for automobiles trying to avert a pedestrian in the road, and those threshold changes with the change in vehicle and pedestrian traffic volume.

Conclusions

After analyzing the results there are four types of accidents that need to be concentrated on, the left turn, right turn, and through accidents that occur at the intersection, and the unauthorized crossings. It was noted that younger driver accounted for more than their share of these accidents. One obvious solution is to increase education and restriction. This is already being implemented in the state of Nebraska. . Legislation is being looked at by state government that creates a probationary operator's license for those children aged 16 to 18 years. This law essentially states that if a driver within this age group receives some sort of citation or is at fault for an accident, they are required more drivers education at their expense, and their probationary period is extended. To sum it up, youths must show that they are safe drivers to continue the privilege of driving.

It is important to continue in this direction for younger drivers and even take it a step further and require more initial education. This will not only reduce suspect drivers from the road, but will increase the awareness of safety as well. Hopefully, it will create not only a driver that follows the rules of the road but uses defensive driving techniques. It might also help to have some education dedicated to anger control to get young people on the right track.

It was also evident in the conclusions that accidents most frequently occurred at roads with a 25mph or 35 mph speed limit. This might be an indication of problem with vehicles exceeding the speed limit at these sorts of roadways. Not surprisingly, many of the problem area for pedestrians in Lincoln, Nebraska are those area where a constant heavy pedestrian volume comes in conflict with vehicular traffic. This situation will arise

at locations like the downtown business district, in and around the university campus and

other school areas. Its obviously important to have the appropriate speed limit for these

sections, however a city can lower the limit only so much before impeding traffic. What

can be done, especially in a community with a university population, is the separation of

vehicular and pedestrian traffic. Of course the optimum situation would call for the

complete separation of the two, but this is not realistic. This is also currently being

looked at in the city of Lincoln, by rerouting much of the current vehicular university

through traffic around the campus. In areas like the central business district, the vehicle-

pedestrian conflicts can be reduced by implementing controls like right-turn-on-red

restriction. Also installing left-turn arrows when possible can not only be beneficial for

vehicular traffic but also for pedestrians crossing at intersections. The same can be said

for median installment. Medians are not only a good tool for channeling vehicular traffic,

but also for pedestrian traffic to have a safe haven when crossing busy intersections.

Ultimately all of these countermeasures would do one thing, reduce the number of

pedestrian-vehicle conflict.

Finally, another countermeasure is enforcement. By increasing enforcement at

problem areas, especially in those high volume pedestrian areas, will ultimately reduce

these accidents as well. Enforcement does not have to focus on vehicles only. With the

increased enforcement of jay walking and pedestrian crossing laws in pedestrian sections,

unauthorized crossing accidents will be reduced. This is not always popular among

citizens, however the long-term benefit counters the inconvenience.

Due to the small data set solid conclusions are difficult to detect. It would be

beneficial in the future expand the data collection to years prior to 1995, or possibly

extend the study to include pedestrian accidents that occur in the state of Nebraska. Extra data could be gathered from area hospitals as other similar studies have done in the passed (2). This might improve the results and produce more reliable results. Introduction of new variables would be beneficial as well. More specifically, it would help to have a variable citing the person at fault for the accident. Also a more clear location variable would help in isolating problem intersections and streets. The current study is just the first step in formulating causes and countermeasures of pedestrian accidents and further study is recommended.

DISCLAIMER

The views expressed in this paper are solely of the authors' and do not necessarily reflect the views and policy of the city of Lincoln.

REFERENCES

1. Traffic Safety Facts 1993. NHSTA, U.S. Department of Transportation, 1993

2. Stutts, Jane C. Hunter, William W. and Pein, Wayne E. (1995) Pedestrian-Vehicle Crash Types: An Update. Transportation Research Record 1538, 68-74.

3. NHSTA, U.S. Department of Transportation, (1983) Computer and Manual Accident Typing for Pedestrian Accidents. Washington D.C.

4. NHSTA, U.S. Department of Transportation (1977) Causative Factors and Countermeasures for Rural and Suburban Pedestrian Accidents: Accident Data Collection and Analysis. Washington D.C.

5. Hunter, William W. Pein, Wayne E. and Stutts, Jane C. (1994) Bicycle-Motor Vehicle Crash Types: The Early 1990's. Transportation Research Record 1502, 65-74.
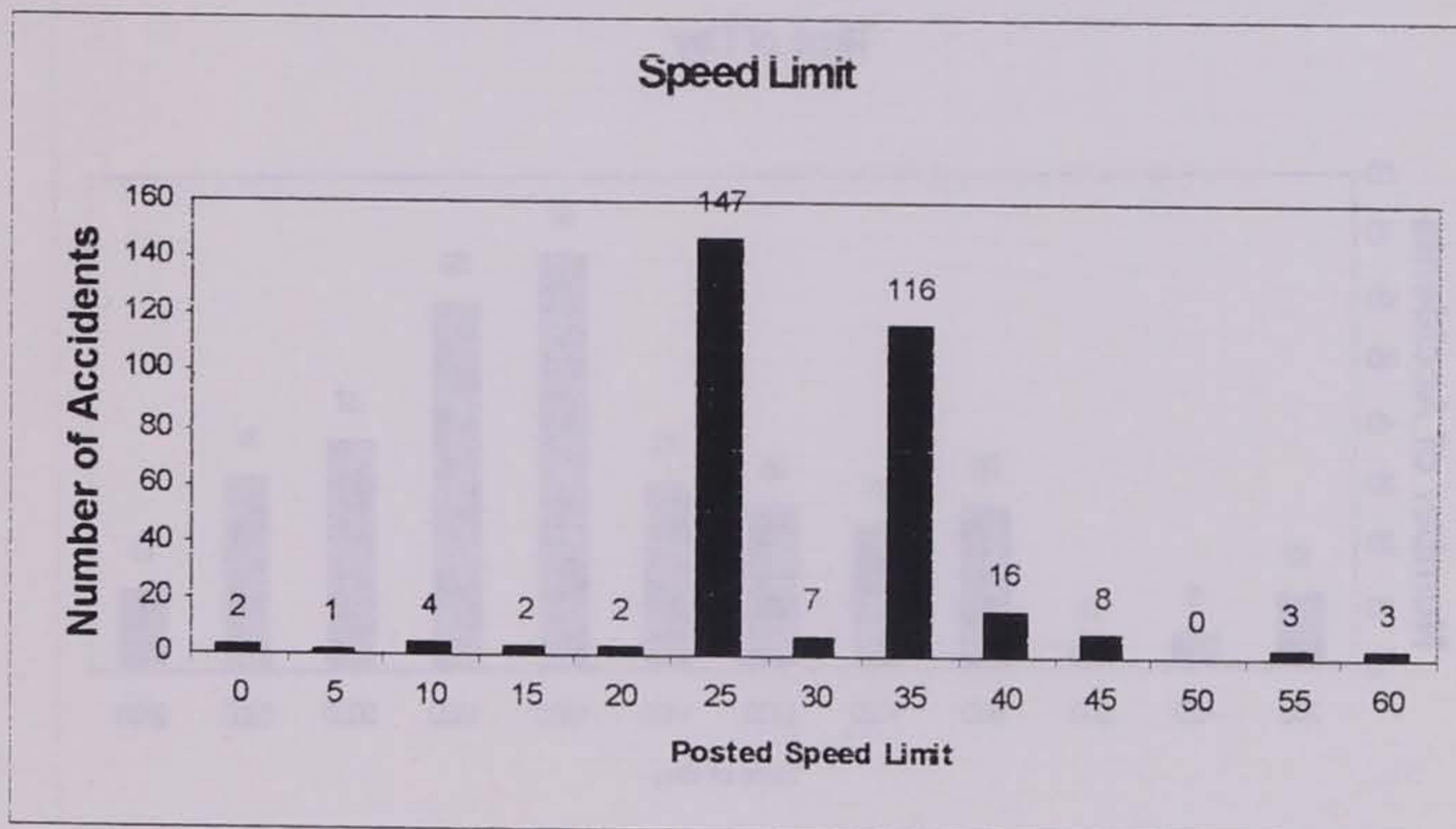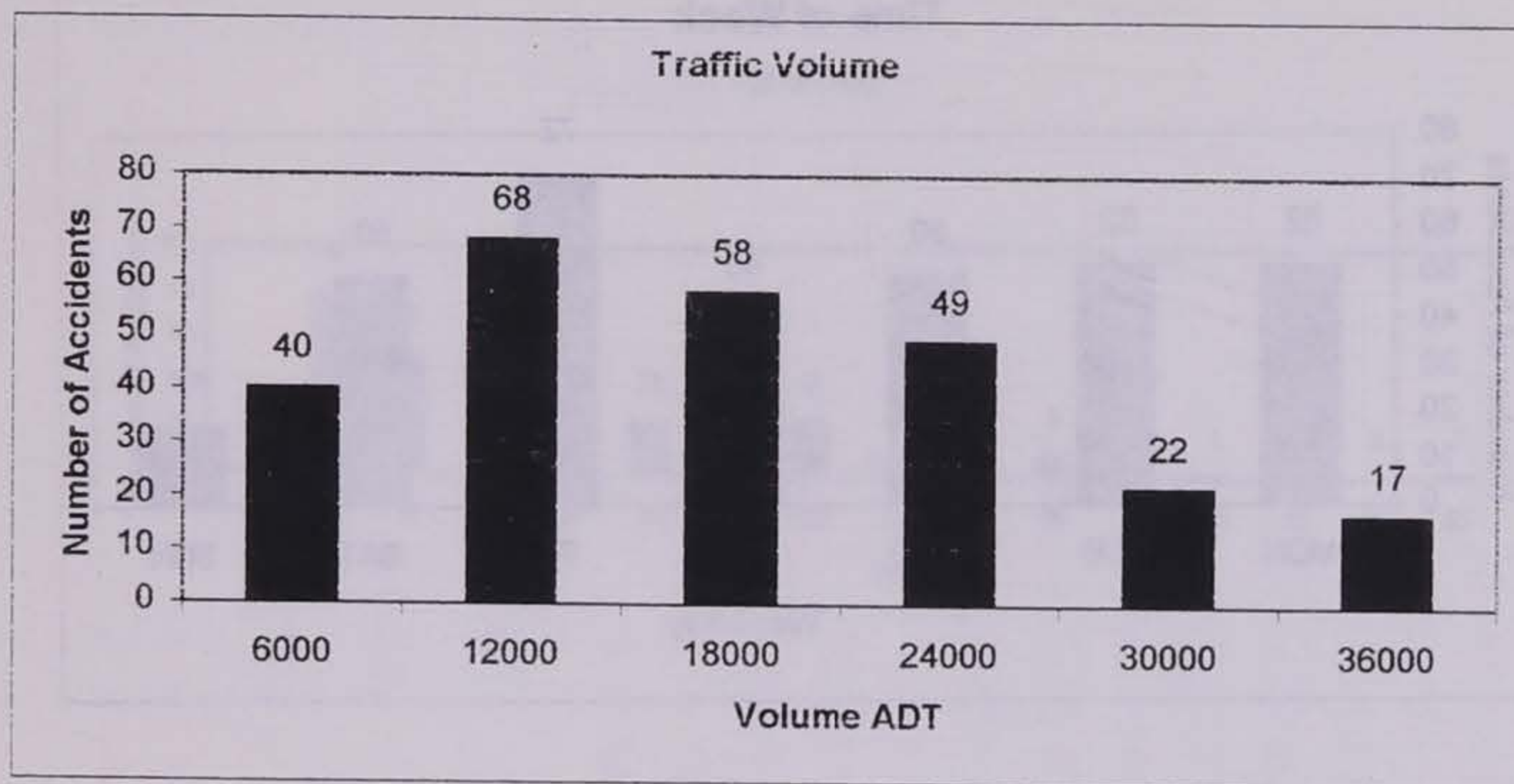
Figure 1 Accident Characteristics

Time of Week

Time of Day
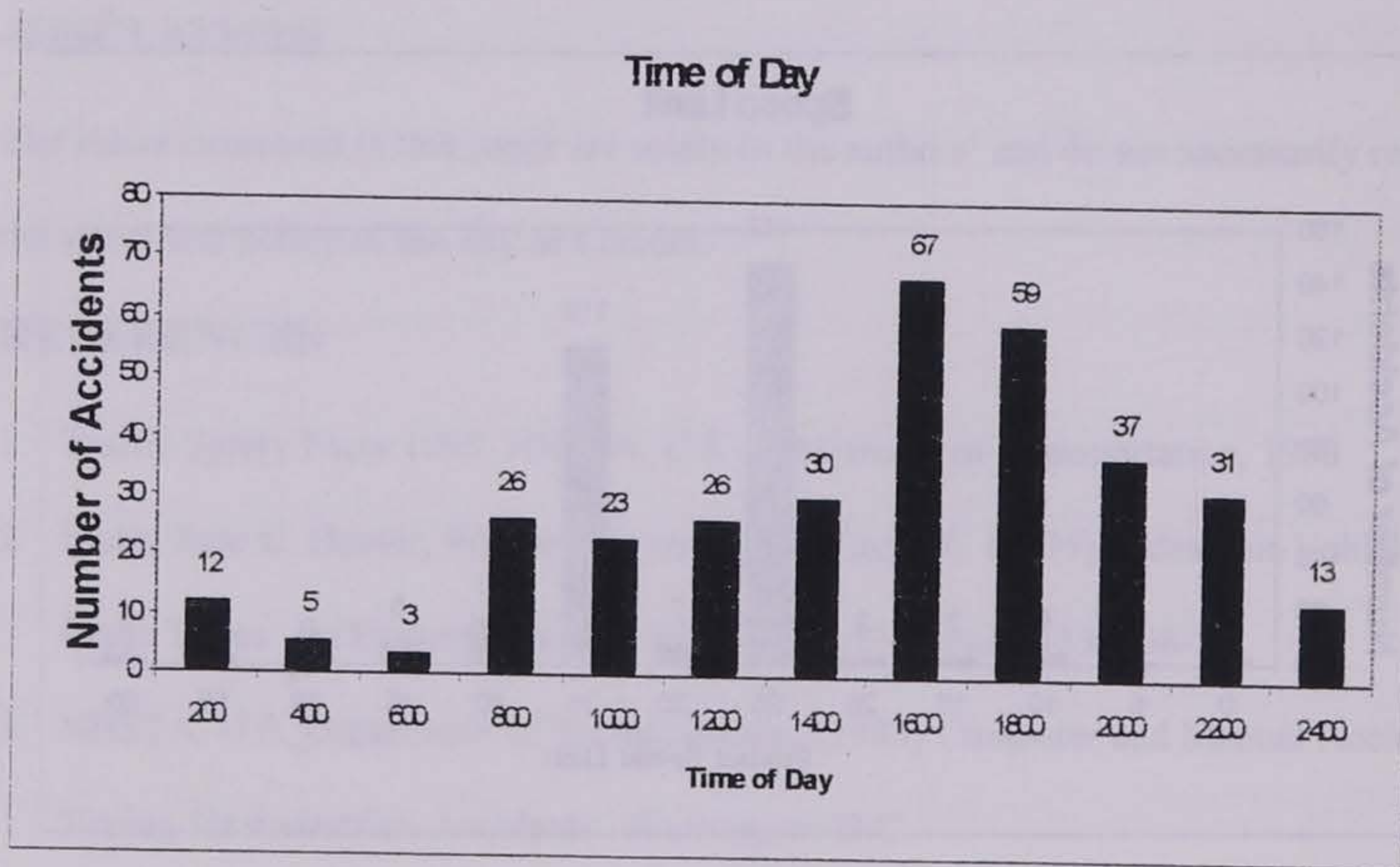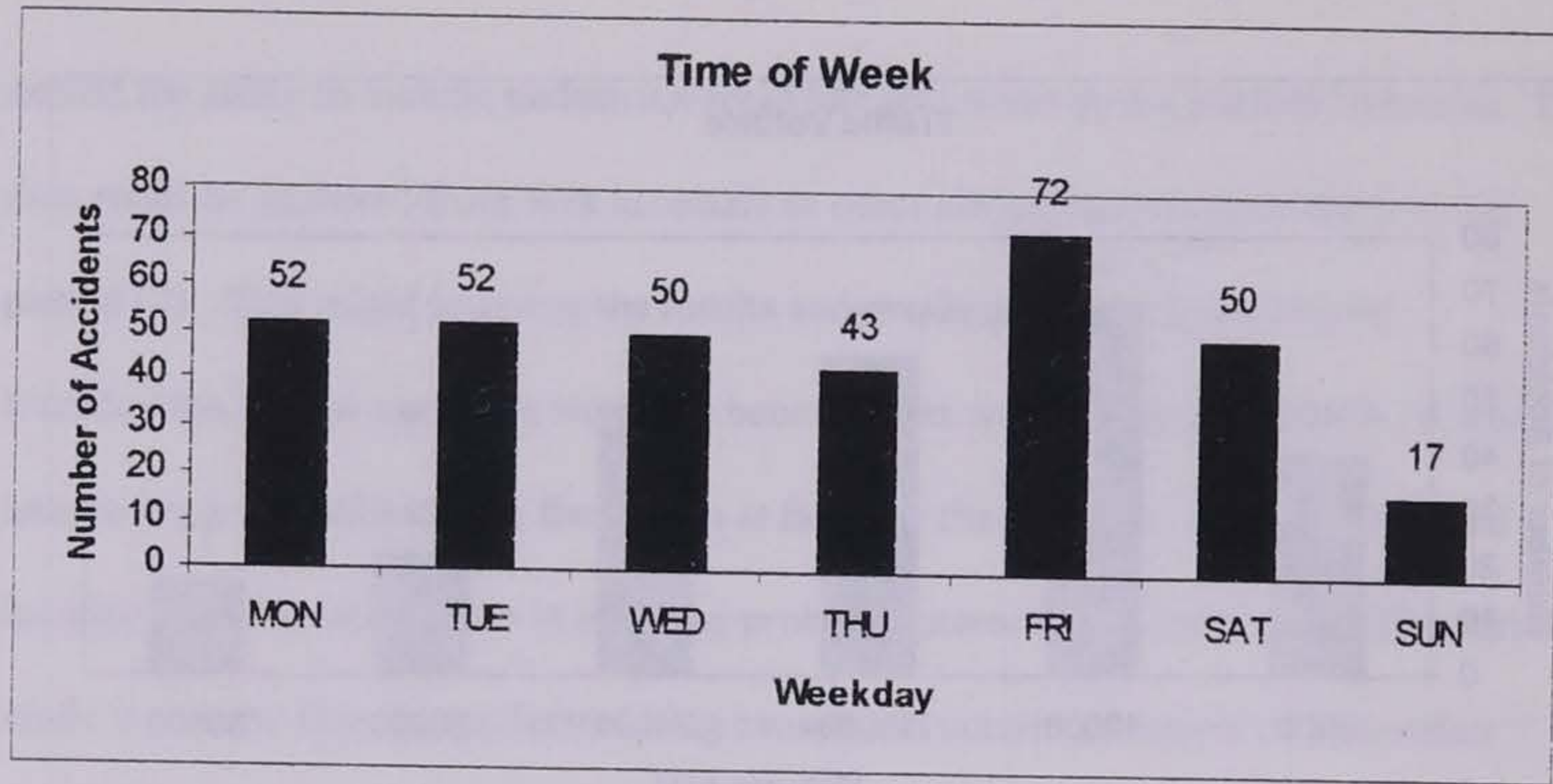
Figure 2 Accident Time
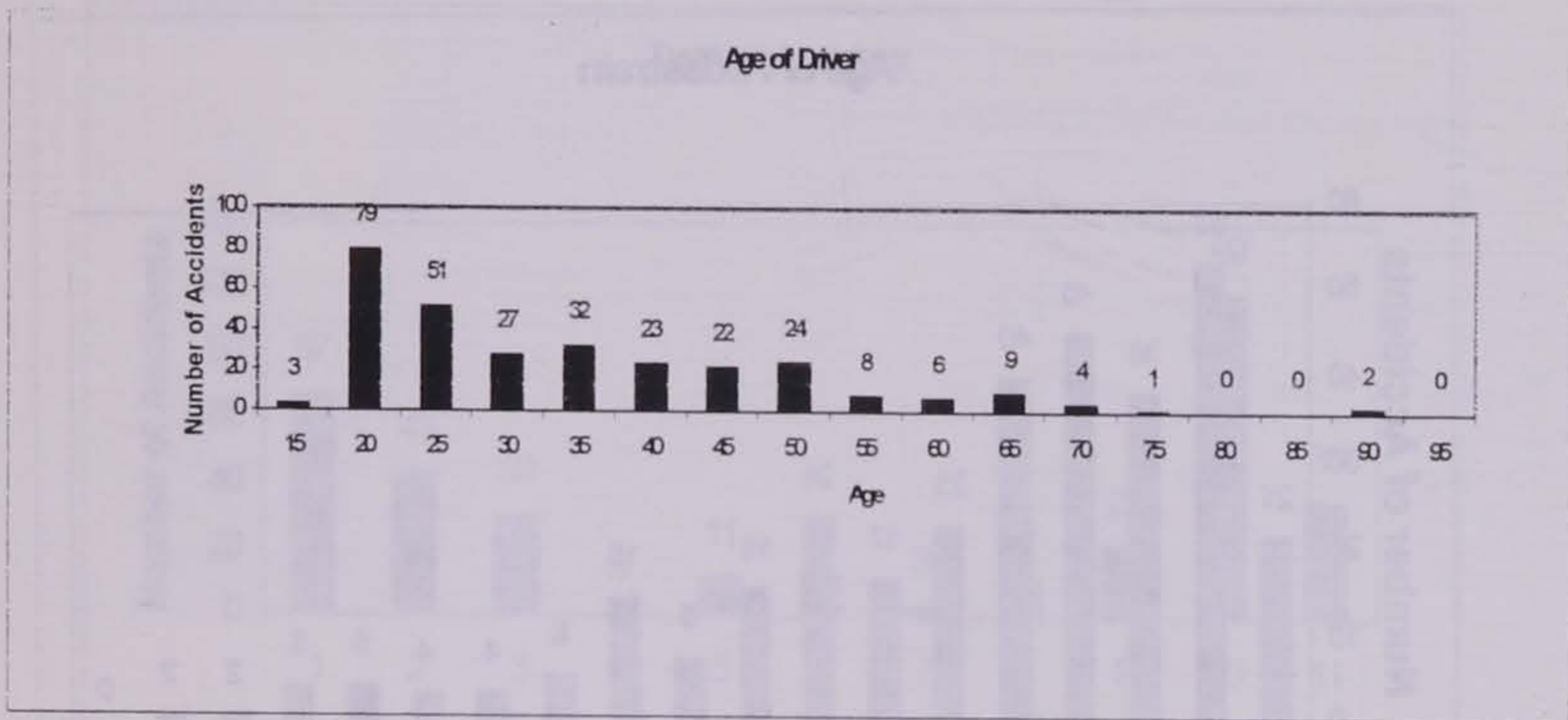
Figure 3 Driver Characteristics

Age of Pedestrain
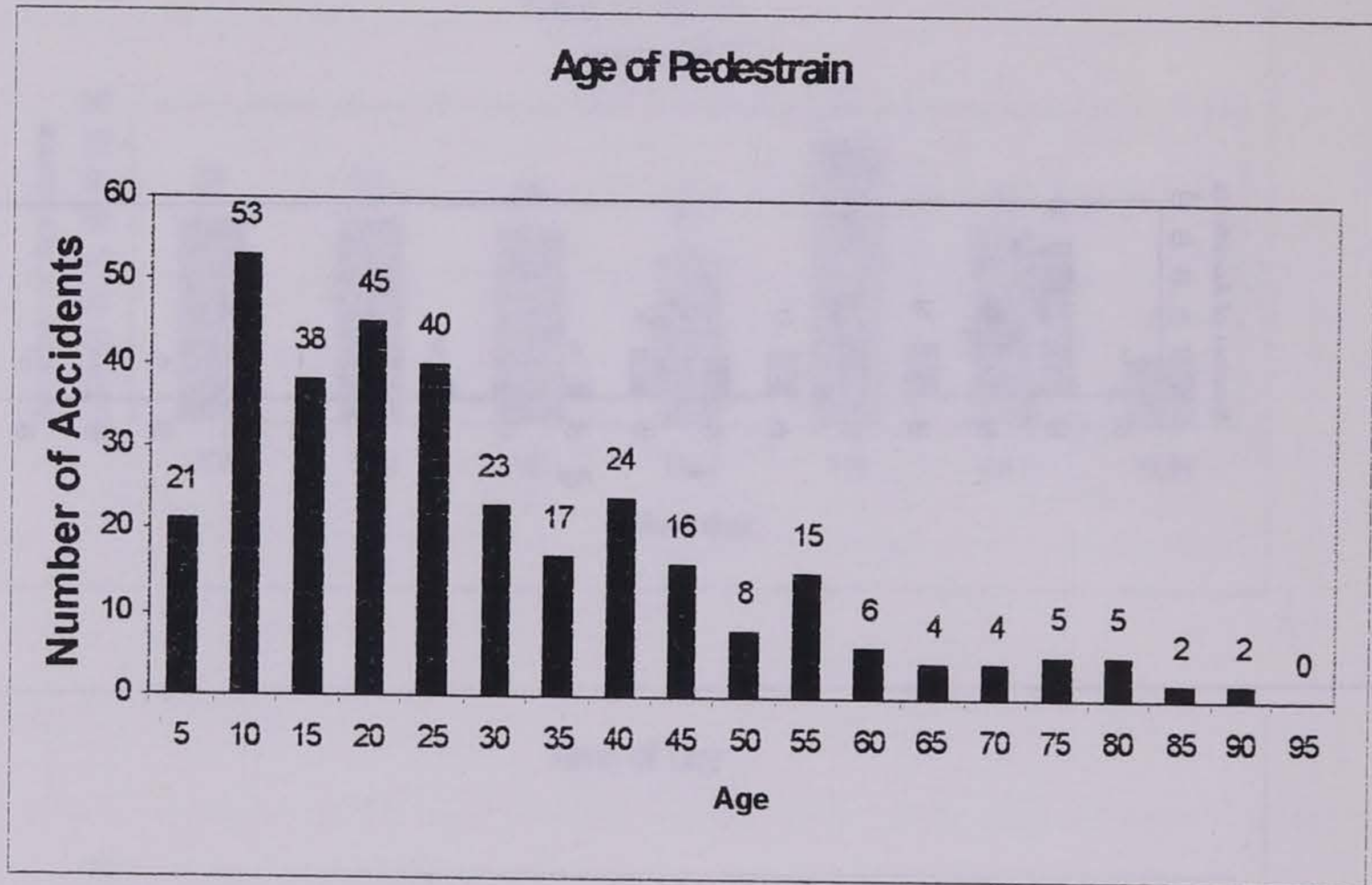
Figure 4 Pedestrian Characteristics

Type of Accident
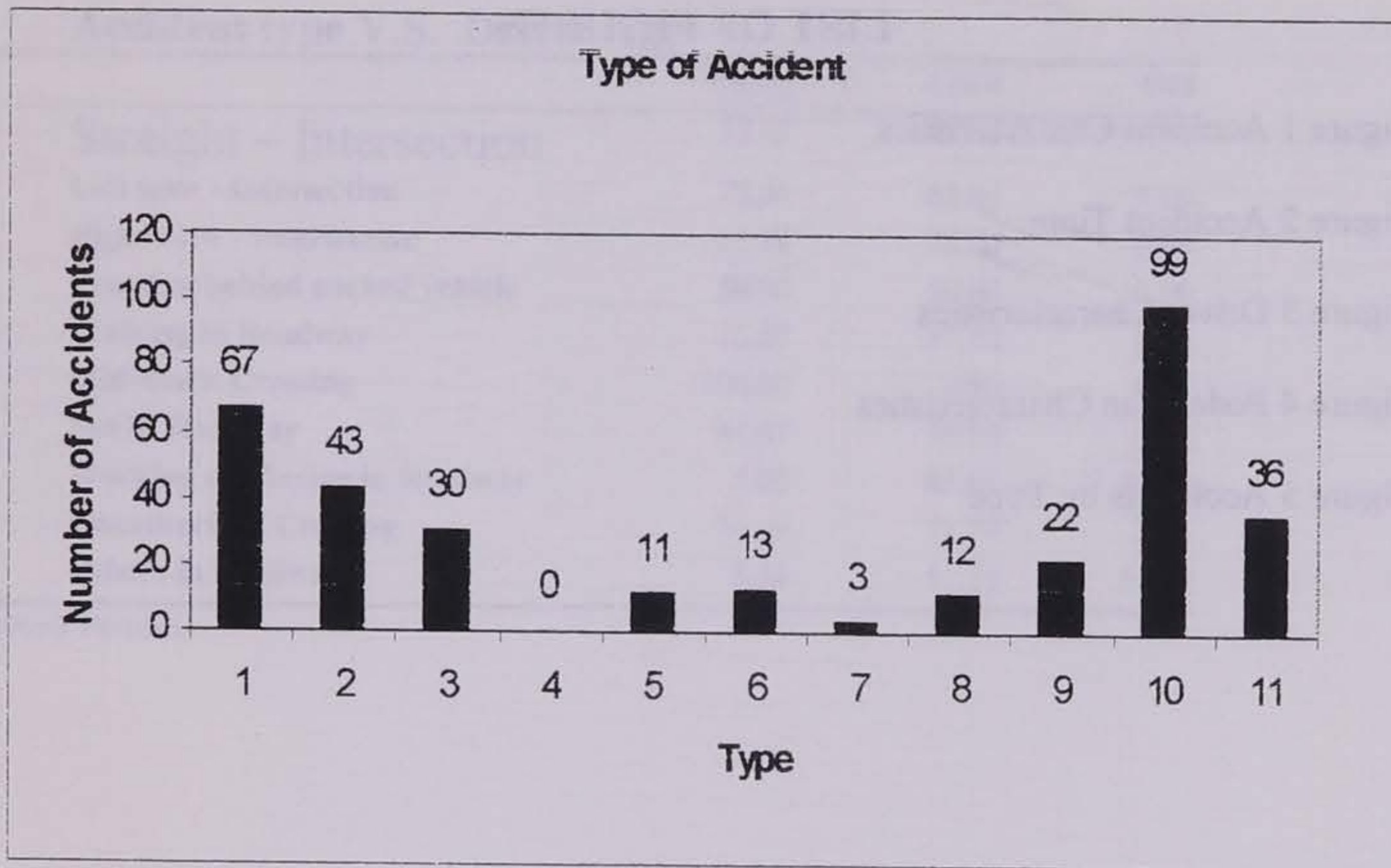
Figure 5 Accidents by Type

LIST OF FIGURES
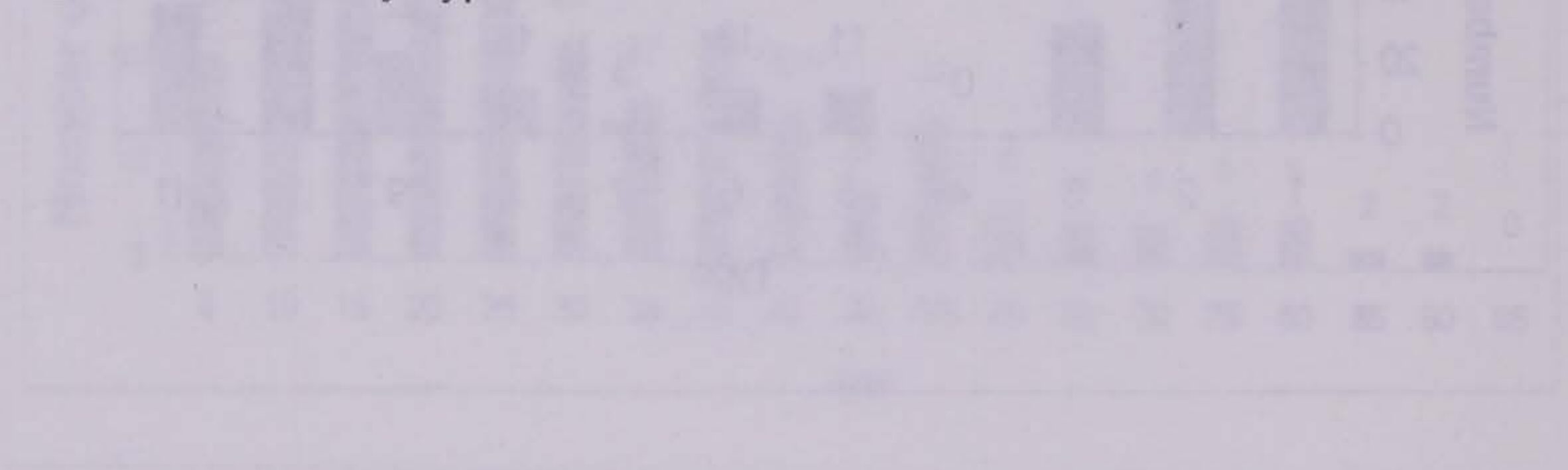
Accident type V.S. Driver Age*

	Young	Adult	Old
Straight – Intersection	33.33	62.75	3.92
Left turn - Intersection	35.14	64.86	0.00
Right turn - Intersection	21.74	78.26	0.00
Crossing behind parked vehicle	50.00	50.00	0.00
Walking in Roadway	16.67	83.33	0.00
Mid-Block Crossing	100.00	0.00	0.00
Not in Roadway	41.67	58.33	0.00
Working or Playing in Roadway	5.00	85.00	10.00
Unauthorized Crossing	26.09	71.74	2.17
Others in Roadway	8.54	11.39	14.29

*Row Percents

Table 1 Accident Type V.S. Drivers age

Accident Type V.S. Injury Severity*

	1	2	3	4
Straight - Intersection	0.00	18.46	58.46	23.08
Left turn – Intersection	0.00	9.30	51.16	39.53
Right turn – Intersection	0.00	3.57	32.14	64.29
Crossing behind parked vehicle	9.09	9.09	45.45	36.36
Walking in Roadway	0.00	30.77	30.77	38.46
Mid-Block Crossing	0.00	66.67	33.33	0.00
Not in Roadway	0.00	10.00	30.00	60.00
Working or Playing in Roadway	0.00	13.64	59.09	27.27
Unauthorized Crossing	3.09	17.53	57.73	21.65
Others in Roadway	2.78	10.00	44.44	38.89

*Row Percents

Table 2 Accident Type V.S. Injury Severity

Accident Type V.S. Traffic Volume*

Average Daily Traffic (vehicles/day)	<6000	6000-12000	12000-18000	18000-24000	24000-30000	>30000
Straight - Intersection	20.00	28.33	23.33	18.33	5.00	5.00
Left turn – Intersection	16.28	25.58	16.28	11.63	11.63	4.65
Right turn – Intersection	12.00	24.00	32.00	16.00	4.00	12.00
Crossing behind parked vehicle	0.00	0.00	100.00	0.00	0.00	0.00
Walking in Roadway	28.57	0.00	28.57	0.00	0.00	42.86
Mid-Block Crossing	0.00	33.33	66.67	0.00	0.00	0.00
Not in Roadway	0.00	0.00	25.00	50.00	0.00	25.00
Working or Playing in Roadway	0.00	30.77	0.00	23.08	38.46	7.69
Unauthorized Crossing	15.38	28.21	19.23	21.79	7.69	7.69
Others in Roadway	18.18	22.73	13.64	27.27	13.64	4.55

*Row Percents

Table 3 Accident Type V.S. Traffic Volume

Accident Type V.S. Road Type*

	<25mph	25-35	35-45	>45
Straight - Intersection	1.54	44.62	53.85	0.00
Left turn – Intersection	0.00	66.67	33.33	0.00
Right turn – Intersection	3.45	41.38	55.17	0.00
Crossing behind parked vehicle	9.09	81.82	9.09	0.00
Walking in Roadway	9.09	54.55	36.36	0.00
Mid-Block Crossing	0.00	66.67	33.33	0.00
Not in Roadway	30.00	50.00	20.00	0.00
Working or Playing in Roadway	10.00	40.00	35.00	15.00
Unauthorized Crossing	0.00	46.24	53.76	0.00
Others in Roadway	6.06	51.52	33.33	9.09

*Row Percents

Table 4 Accident Type V.S. Road Type

LIST OF TABLES

Michael Pawlovich
PhD Student - Transportation Engineering
Civil and Construction Engineering
Iowa State University

A Method of Examining
Dependence of Crashes on
Demographic and Socioeconomic Data

ABSTRACT

Many agencies use traffic crash data to identify problems, establish goals and performance measures, measure progress of specific programs, and support development and evaluation of highway and vehicle safety countermeasures. Traditionally, efforts have considered only crash data and roadway network attributes and have not taken adjacent demographics, socioeconomics, land use, and other non-roadway variables into consideration.

The evaluation of non-roadway variables may support two related types of safety management efforts: identification of additional causal factors for roadway crashes and identification of empirical relationships between crashes and non-roadway factors. The second may provide better estimates of the impact of future changes in land use, demographics, and socioeconomics.

Recent efforts use Geographic Information Systems (GIS) or non-spatial relational databases to combine crash and other data to assess correlation and causation. The variety of data available, both within the traditional approach and with the addition of demographic, socioeconomic, and land use data, creates a complex analytical environment. The complexity of these analyses warrants development of a typology to structure an assessment of the best approach in a given situation. This paper presents a concept typology to organize the use of GIS, along with statistical techniques, to explore the relationship between crash incidence and underlying demographic, socioeconomic, and land use data.

INTRODUCTION

Many agencies use traffic crash data to identify problems, establish goals and performance measures, measure progress of specific programs, and support development and evaluation of highway and vehicle safety countermeasures. Traditionally, efforts have considered only crash data and roadway network attributes and have not taken adjacent demographics, socioeconomics, land use, and other non-roadway variables into consideration.

1

Engineers have long studied relationships between traffic crashes and potential causal factors, traditionally focusing on roadway geometrics. The studies have generally not considered characteristics of demographics, socioeconomices, and land use in the area proximate to crashes. Efforts on a microscopic (intersection or corridor) level have been made to determine crash causality based on socioeconomic and demographic features, but little has been done to expand this to a macroscopic (network or citywide) level.

Many studies have focused on determining causal factors for traffic crashes [1, 2, 3, 4]. Other studies utilize traffic crash data to determine cost effectiveness of improvements [5, 6]. Still others focus on factors to reduce crash frequency, fatalities and injuries, and response time. Few sources mention land use, demographics, or socioeconomics in relation to traffic accidents. Of these, two older sources (1965 and 1969) focus on demographics of persons involved in crashes [7, 8], one mentions land development and traffic influences on road accidents [9], and another analyzes a variety of subjects in addition to land use [10]. No articles found considered demographic, socioeconomic, or land use data in relation to traffic crashes on a macroscopic level.

The evaluation of non-roadway variables may support two related types of safety management efforts. First, it may identify additional causal factors for roadway crashes. Once all such factors have been identified and analyzed, better informed decisions can be made to remediate existing or potential hazardous locations. Identified non-roadway causal factors will enable engineers and planners to design and plan safer roadways and neighborhoods by providing a clearer picture of contributing factors in certain crashes or crash types. Changes in crash numbers would more clearly be linked to actual causes.

Second, short of causality, the identification of empirical relationships between crashes and non-roadway factors may provide better estimates of the impact of future changes in land use, demographics, and socioeconomics. Such empirical relationships would be useful to guide the allocation of emergency response (e.g., ambulance and police) resources necessary to respond to

the potential additional demands presented by new residential and economic developments located in specific locations, and by changing demographic and socioeconomic patterns. However, as few studies have considered the relationship of demographics, socioeconomics, or land use to crashes or crash rates, these variables are not available for design, planning, or analysis.

Recent efforts use Geographic Information Systems (GIS) or non-spatial relational databases to combine crash and other data to assess correlation and causation [11, 12, 13]. GIS's provide excellent tools to analyze location specific crash data. Multiple layers can be viewed and analyzed at once. In addition, GIS's enable development of a methodology to consider non-roadway variables.

Currently, the Center for Transportation Research and Education (CTRE) is developing a GIS-based accident location and analysis system for the state of Iowa that facilitates spatial analyses of crash incidence. Iowa is fortunate 1) to have a comprehensive location –based database covering 10 years of all traffic crashes on all road systems, and 2) to have developed one of the better systems for analyses, Personal Computer-based Accident Location and Analysis System (PC-ALAS). Many approaches are available to analyze crash data in a GIS environment. The variety of data available, both within the traditional approach and with the addition of demographic, socioeconomic, and land use data, creates a complex analytical environment. The complexity of these analyses warrants development of a typology to structure an assessment of the best approach in a given situation.

A topological (i.e., based on feature class) division of crash rates based on feature class includes three types of geographic representations: point, line, and polygon. Points can either represent the location of a single crash or the location of a point where multiple crashes have occurred. Lines can denote a segment or corridor with multiple crashes or a network made up of a series of lines, combining the crashes on each line to develop the crash rate. Polygon representations combine crashes within an area in order to develop an areawide crash rate.

Polygons can be further divided, representing regions using an arbitrary grid or block groups, depending on the data available and the desired analysis.

Utilizing the topological representation of crash rates as the dependent (Y) variable, various independent (X) variables, which also can be represented with varying topology, can be used to determine potential causal relationships. As the analysis of these topological representations can become quite complex, a classification scheme (typology) to structure the analyses is helpful. This paper presents a concept typology to organize the use of GIS, along with statistical techniques, to explore the relationship between crash incidence and underlying demographic, socioeconomic, and land use data.

TYPOLOGY

The typology, as shown in Figure 1, consists of two topological dimensions: dependent variable (crash

crashes (point) overlaid on:

	economics (point)	socioeconomic/ demographics by block group (poly)	land use by block group (poly)
arbitrary grid (poly)	impact of business point locations on areal (grid) crash rate	impact of census tract median income on areal (grid) crash rate	impact of land use zoning on areal (grid) crash rate
block group (poly)	impact of business point locations on areal (census) crash rate	impact of census tract average age range on areal (census) crash rate	impact of land use zoning on areal (census) crash rate
roadway (line)	impact of business point locations on segment based (roadway) crash rate	impact of census tract average vehicles per household on segment based (roadway) crash rate	impact of land use zoning on segment based (roadway) crash rate

vs.

Figure 1: Crash Rate Typology

4

rate) and independent variable (here, demographic, socioeconomic, and land use). Prior to representation with varying topology, the dependent variable must be created from a spatial combination of crash incidence and exposure (traffic levels). In this study, crash locations are represented as points. Three methods are presented here to develop crash rates (point on line and point on polygon, including arbitrary grid and census block), creating three sets of dependent variables for subsequent analyses. In addition, the three sets of dependent variables are statistically related to three independent variables, creating nine or more possible types of analyses.

Each dependent variable/independent variable pair can be utilized to assess the impact of different features of the independent variables on crash rates as shown in Figure 2. For example,

	traffic/ geometrics	demographics/ socioeconomics/ land use	employment
points	ALAS file fields related to roadway crash characteristics	sex, age, DWI, ALAS file	# employees, point locations of employers
line	Base Records (AADT, lane width, VMT)	access points buffer	access points buffer
polygon	VMT	census data, zoning	densities

Figure 2. Causal Factors Matrix

the arbitrary grid/economics combination could be utilized to determine impact of business point locations on an areal (grid) crash rate. Employment densities within grids could be related to crash rates within grids. In addition, given an accident location, all businesses within a grid of an accident location could be determined.

METHODOLOGY

The methodology to develop dependent and independent variables consists of six main steps, as shown in Figure 3. The first three steps are used to develop independent variable data, the

```
┌─────────────────────────────┐
│ 1. What's available in      │
│ TIGER/Census and other      │
│ (e.g., employment data)     │
└─────────────────────────────┘
              │
              ▼
┌─────────────────────────────┐
│ 2. Develop/find polygon     │
│ coverage of blocks and      │
│ block-groups or point       │
│ coverage of businesses/     │
│ other land use              │
└─────────────────────────────┘
              │
              ▼
┌─────────────────────────────┐
│ 3. Join census and TIGER    │
│ blocks                      │
└─────────────────────────────┘
        /              \
       ▼                ▼
┌──────────────┐  ┌──────────────┐
│ 4a. Develop  │  │ 4b. Develop  │
│ crash rates  │  │ crash rates  │
│ for each     │  │ for arbitrary│
│ block        │  │ grid         │
└──────────────┘  └──────────────┘
        \              /
         ▼            ▼
┌─────────────────────────────┐
│ 5. Develop independent      │
│ variables for polygons via  │
│ overlay/intersection        │
└─────────────────────────────┘
              │
              ▼
┌─────────────────────────────┐
│ 6. regression/ANOVA/        │
│ MANOVA/... to determine     │
│ significant causal          │
│ relationships               │
└─────────────────────────────┘
```
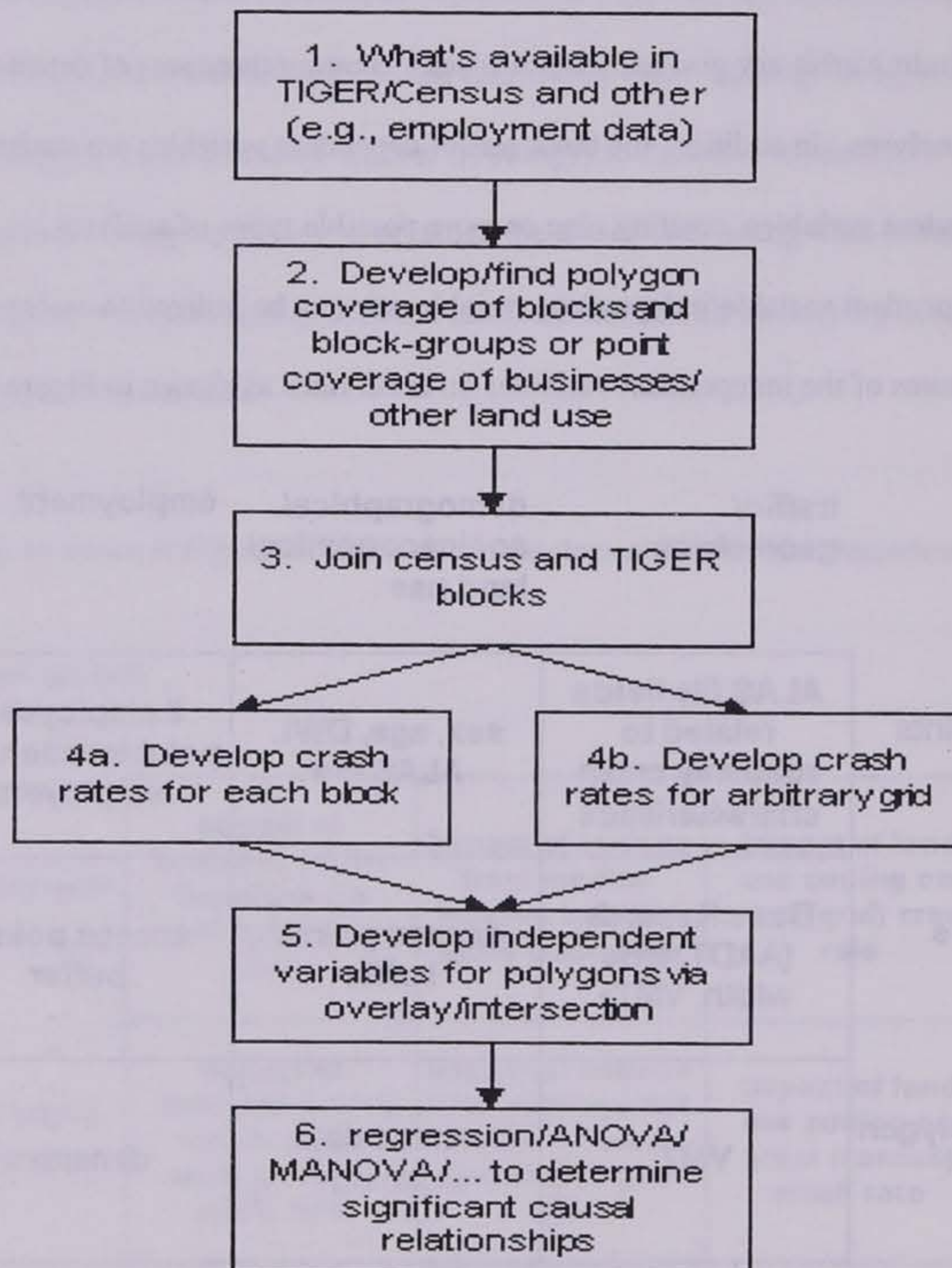
Figure 3. Equation Development Process

fourth to develop dependent variables, the fifth to develop independent variables themselves, and the sixth to apply statistical techniques to determine significant causal relationships. In this paper, the methodology was demonstrated at the block group level.

Step 1

Data available include census data, crash data, infrastructure data (mainly roadway data), and employment data. An enormous amount of data is available, resulting in computational problems for standard statistical packages; therefore, the variable list was narrowed to those viewed as most promising by the authors. Initially, we arbitrarily selected variables that seemed most likely to affect crash rates.

Census data contains over 3,400 data elements that can all be referenced to geographic regions. These elements are divided into several main headings and subheadings. To provide more manageable census data for the purposes of this paper, data under certain headings, unlikely to relate to crash rates, were discarded from consideration. The remaining data elements were contained in 261 main headings and subheadings. From these we arbitrarily selected a portion for subsequent analyses. The selection left us with a large, but much more manageable number of total variables (225 variables under 25 main headings) to consider.

Infrastructure data, obtained from the Iowa Department of Transportation (DOT), include several background GIS coverages such as hydrology, rail lines, secondary roads, primary roads, and municipal roads. The latter three of these were of significant interest for this paper. Included as attributes for the road coverages are AADT and lane length. The AADT and lane length were used to calculate Vehicle Miles Traveled (VMT) for each roadway segment. The VMT, combined with total crashes along each roadway segment, were used to construct the dependent variable, crash rate, for each roadway element.

Crash data, also obtained from the Iowa DOT, includes many data elements related to the crash, the vehicles and drivers, and the injured persons. These data elements are explained in a recently published report detailing current efforts to expand and improve Iowa's accident location and analysis system [14]. For the purposes of this paper, relevant information is the incidence and location of crashes. Combining these data with VMT results in crash rate (crashes/100 million VMT). Future efforts may consider specific crash attributes.

Socioeconomic data contains: business name, address, city, state, zipcode, Standard Industrial Code (SIC), and number of employees. The data were obtained from the Iowa Department of Workforce Development (DWD) and are confidential. The SIC code is the most important element, though number of employees may be of interest. The other variables were used to create a point location map of businesses using the geocode function of a GIS.

Step 2

The second step was to develop or locate polygon coverages of block groups and point coverages of businesses and other land use data. Polygon coverages of block groups, illustrated in Figure 4, were obtained from a commercial product and exported to GIS format. The point

Figure 4. Block Groups

coverages of businesses, displayed in Figure 5, were developed from DWD data. Utilizing the address code of the DWD data and a commercial street address database, point coverages were developed using the geocode function of a desktop GIS.
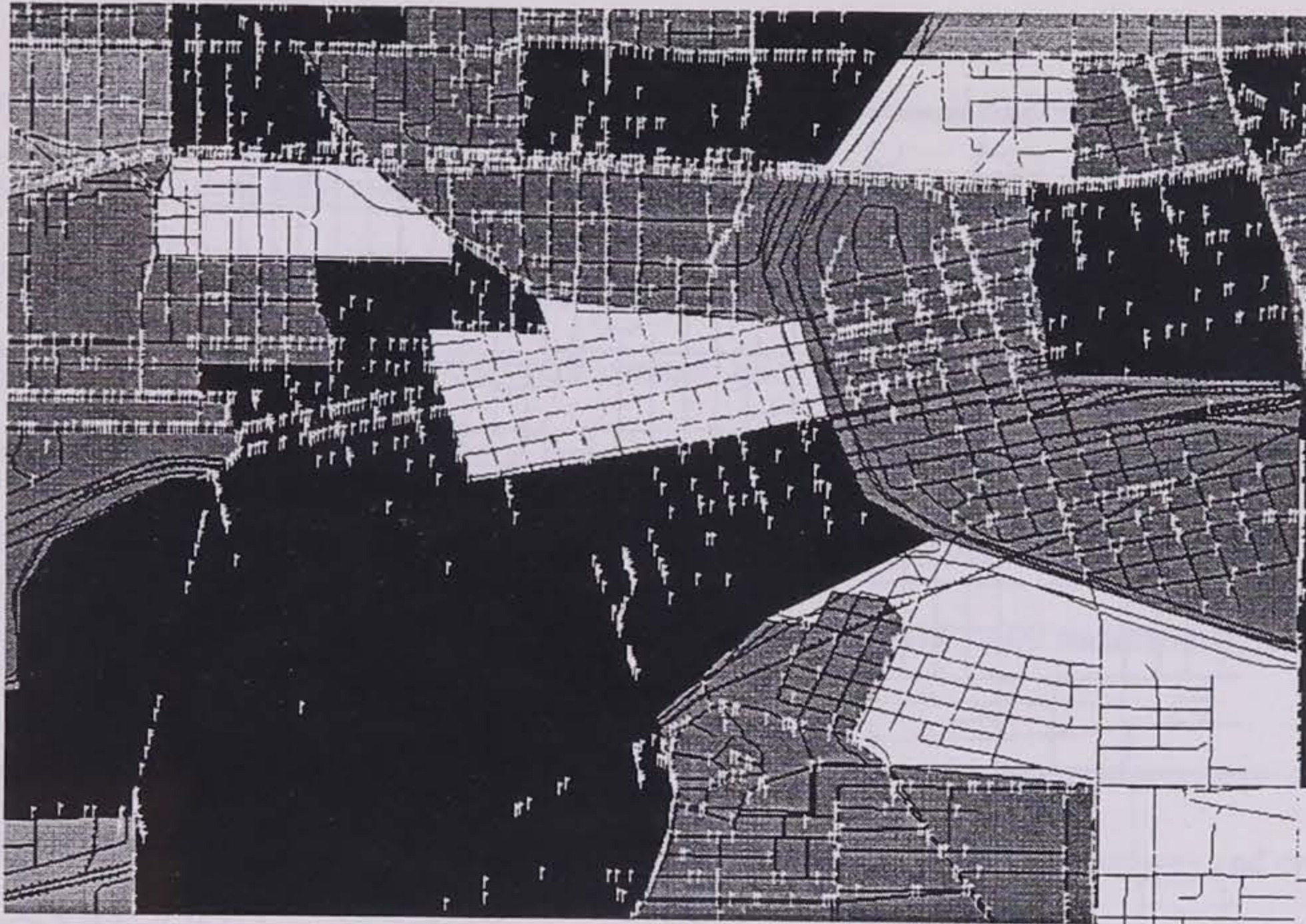
8

Figure 5. Socioeconomic Point Locations

Step 3

The third step was to join census data and Topologically Integrated Geographic Encoding and Referencing (TIGER) blocks (i.e., polygons for block groups). However, the census data and TIGER block join was found to be commercially available; therefore, no work was entailed in this step other than querying for desired census information and exporting it into GIS format.

Step 4

The fourth step was to develop crash rates, the dependent variable, for each independent variable type: block group, arbitrary grid, and linear system. For this paper, only the first, crash rates for block groups, was completed. The latter two independent variable types will be considered in future efforts.

To develop crash rates for block groups, first the Iowa DOT roadway coverages were spatially joined to crash data, as shown in Figure 6. The resultant table was then summarized to produce a table of crashes by using the roadway coverage index fields. The summarization table and roadway coverages were then spatially joined, creating roadway coverages with total crashes along each roadway segment.
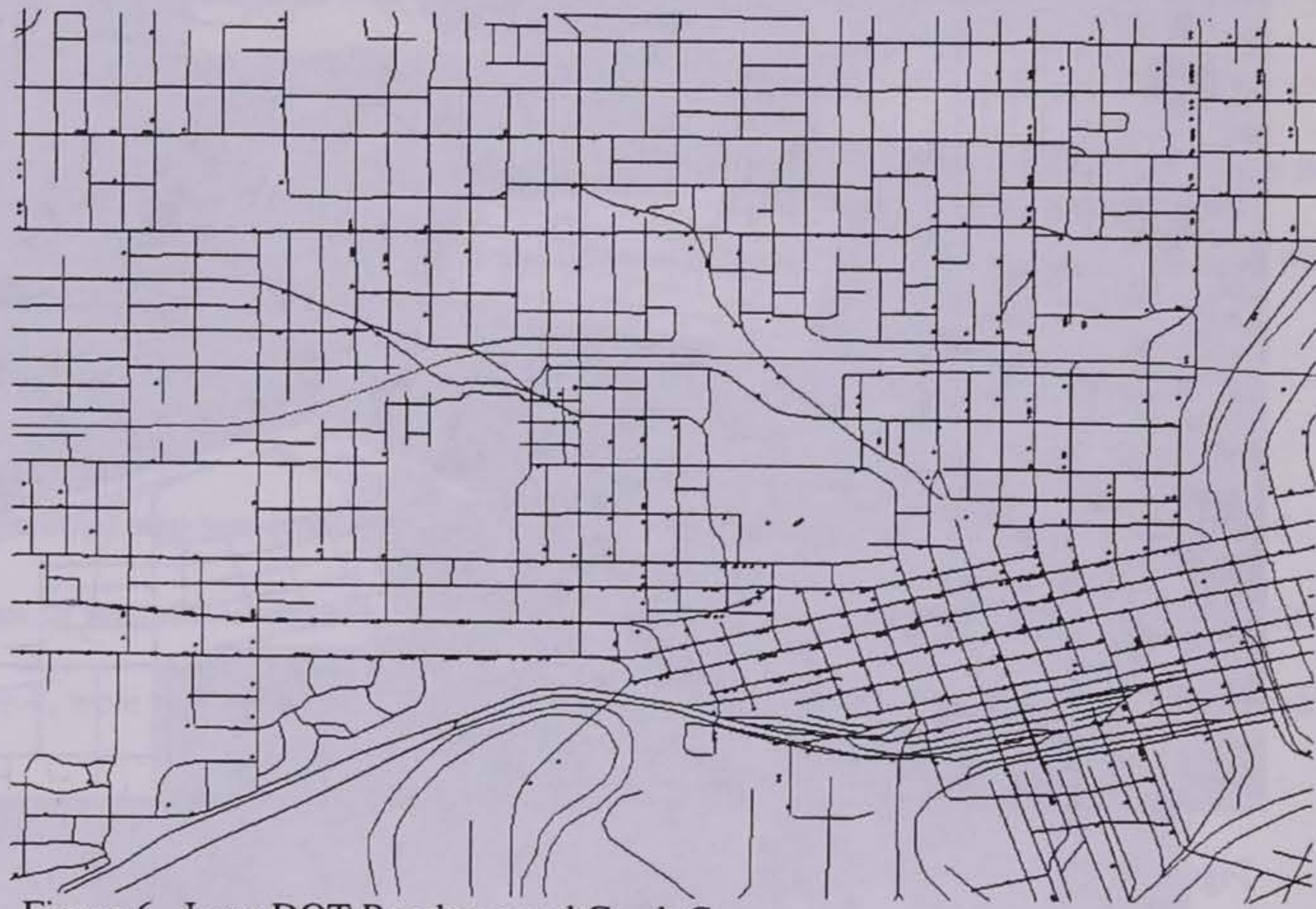
9

Figure 6. Iowa DOT Roadway and Crash Coverages

The VMT for each block group was calculated by first spatially joining each block group to

the road coverages, as shown in Figure 7. The resultant road coverages with the block group
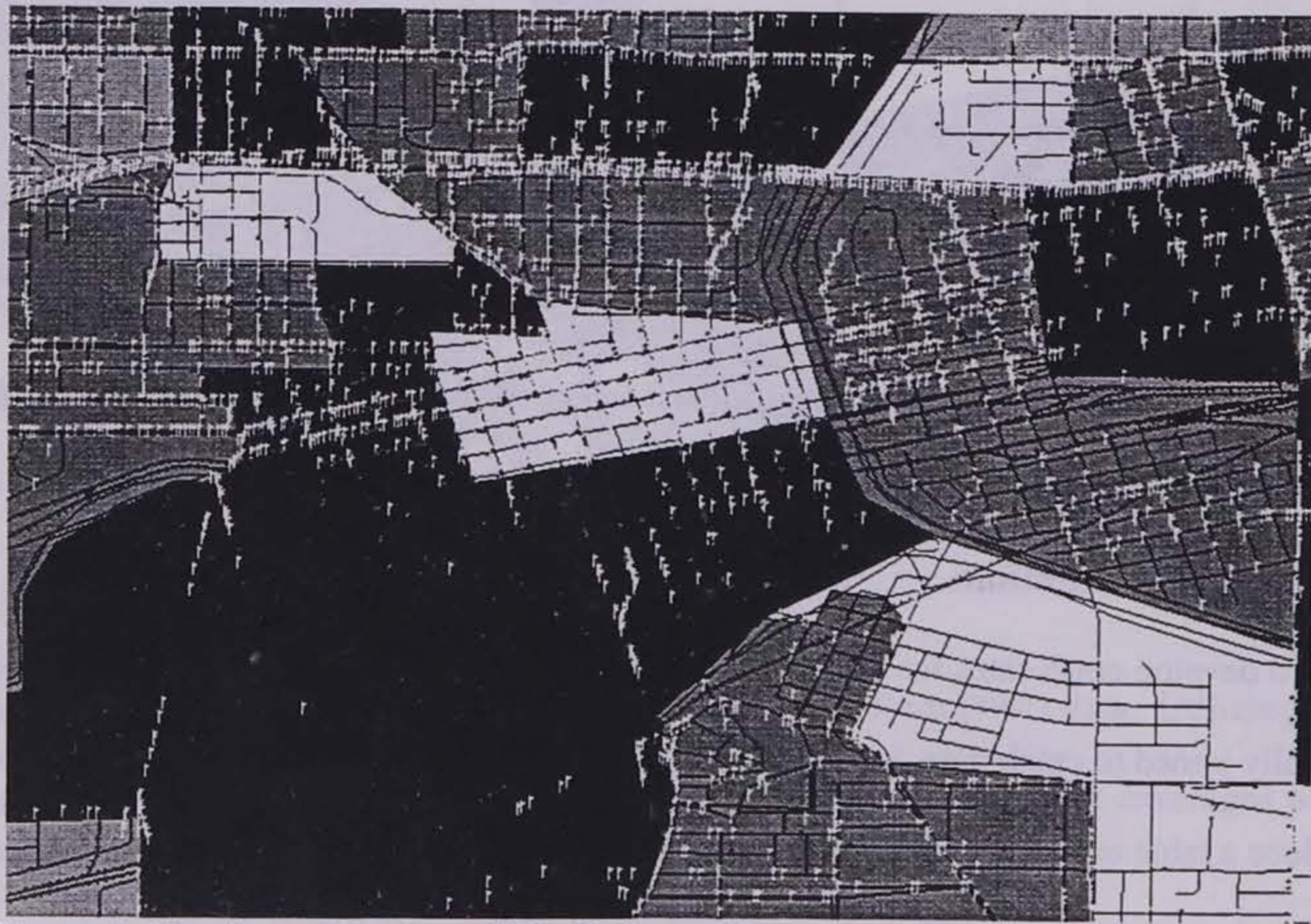

Figure 7. Roadway, Crash, and Block Group Coverages

table was then exported to dBase format and imported into MicroSoft Access. Within Access, the

crashes, average annual daily traffic (AADT), and lane length (meters) were grouped by area

identifier using a summation for each. The grouping results were saved and imported into GIS

and then spatially joined to the block group coverage. Each block group now includes total

number of crashes, total AADT, and total lane length as attributes. Additional fields, VMT and

crash rate, were created and their values calculated for each block group using these formulas:

- VMT = total AADT * 365 days/year * lane length (meters) / 1.609 meters/mile; and
- Crash rate = total crashes/(1000000*VMT).

After generation of the grid, development of crash rates for an arbitrary grid would proceed

similarly. Linear system crash rates would involve the spatial joining of the roadway and crash

data and the subsequent calculation of VMT and crash rate.

Step 5

The fifth step was the development of the independent variables, for polygons via

overlay/intersection. This was accomplished by joining the census data to the crash rate data. An

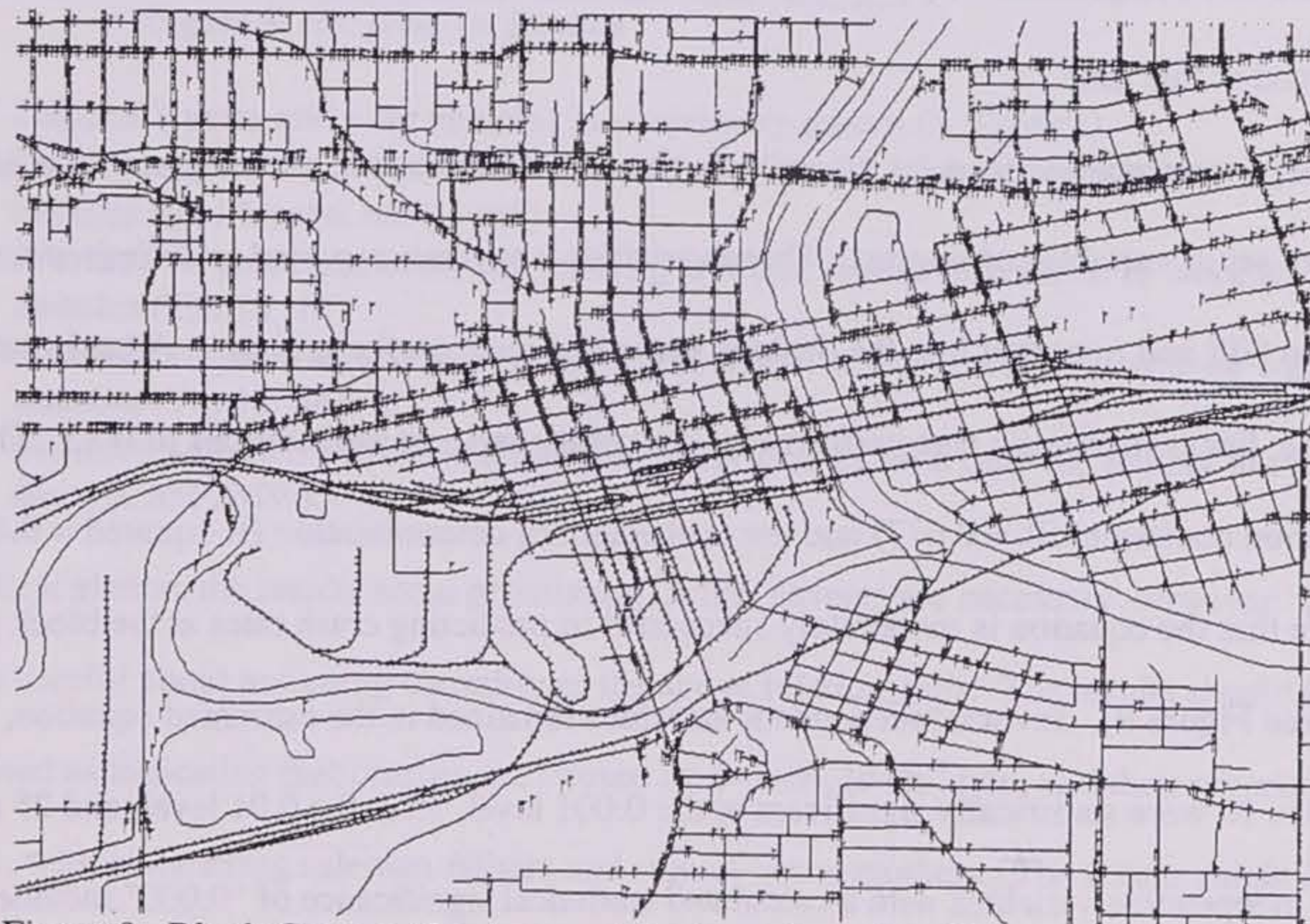overlay of block groups, crashes, and business locations is shown in Figure 8.

Figure 8. Block Groups, Crashes, and Business Location Coverages

Step 6

The sixth step uses the independent and dependent variables developed previously to examine the data for significant causal relationships. Various statistical techniques may be utilized, including linear regression, analysis of variance (ANOVA), multiple regression ANOVA (MANOVA), factor analysis, bivariate regression, time series, and spatial regression. Within the selected GIS environment, few rigorous statistical techniques were available; however, a simple bivariate regression script is available for analyzing data. In addition, exporting the database to a spreadsheet allowed for more involved multiple regression. For this paper, various variables were tested against the block group crash rate for a variety of regions to ascertain whether there were any obvious causal factors. This was done using a desktop statistical software package once the data had been exported in delimited text format from the GIS. Future efforts will involve statistical packages allowing the more robust analyses desired.

ANALYSIS

The initial analysis effort utilized a subset of the available data. Future efforts will analyze the data more comprehensively. However, a variety of factors contributed to the limited analyses performed at this time.

Using a metropolitan region for the analyses, the data fields used in the analyses were pared to an arbitrary set of variables of interest. These variables were then exported to delimited text format from the GIS and imported into the desktop statistical package for analyses. A backward, stepwise, linear regression was performed, using entry and exit probabilities of 0.15. The correlation coefficent (R = 0.677) and the coefficient of determiniation (R-squared = 0.458) indicate that the equation is moderately successful in predicting crash rates at the block group level (see Figure 9). Several independent variables remained in the estimated equation, 27 in all. Of these, 10 were statistically significant at the 0.001 level, 15 at the 0.01 level, and 25 at the 0.05 level. Independent variables with a calculated statistical significance of "0.000" included:

	Coefficient	'P'
S_PrpSch	-12.210	0.000
L_WlkHom	6.533	0.044
OcSales	5.726	0.000
OcFarming	23.837	0.002
InWhoTrd	-8.441	0.001
InBusiness	7.702	0.001
InPerson	-10.363	0.002
InEntert	-9.790	0.024
InPubadm	5.250	0.027
L_SlfEmp	5.028	0.039
Age6	14.813	0.000
Age16	-8.108	0.032
Age35_39	3.006	0.022
Age62_64	6.896	0.001
Age70_74	-5.135	0.003
MC_ChU3	-8.386	0.002
MnW_Ch13	27.187	0.031
DrvWkHom	-7.529	0.030
Tim10_14	-4.668	0.000
Tim35_39	29.098	0.001
Tim40_44	25.684	0.000
Tim60_89	9.317	0.104
Ch5P2FWk	-111596.094	0.104
Ch5P2MWk	2582.544	0.000
Ch17P2FW	-80085.038	0.003
Ch17MaNW	-7775.235	0.014
MedFami	-206287.871	0.031

Figure 9: Regression Results

- Persons 3 years and over enrolled in preprimary school (S_PrpSch)
- Employed persons 16 years and over who are in sales occupations (OcSales)
- Persons aged 6 years old (Age6)
- Workers 16 years and over, not working at home, whose travel time to work was 10-14 minutes (Tim10_14)
- Workers 16 years and over, not working at home, whose travel time to work was 40-44 minutes (Tim14_44)
- Families with two parents and children under 6 years with only the mother in the labor force (Ch5P2MWk)

At first glance, the results seem promising. A few caveats are necessary, however. First, one must be careful about assigning causality to the above relationships. The results should not be interpreted as indicating that crashes are caused by 6-year-old children, and their preprimary aged siblings, with commuting saleman fathers and stay-at-home mothers. The results might indicate, however, that locations with families having these characteristics, may have above-average

block-group-based crash rates (controlling for a limited set of other factors). Second, regression

diagnostics indicated that the above results should be viewed cautiously. In particular, the test for

the impact of outliers indicated that extreme values may be skewing the results. A series of

scatterplots with the dependent variable and selected independent variables indicated that this was

the case. A few block groups with extremely high values greatly affected the results. Normally,

these observations would be discarded, but in crash analysis they are usually the ones of most

interest. Third, although a suprising number of interrelated indepedent variables entered the final

equation, a high degree of multicollinearity, typical with socioeconomic data, can make

regression parameters unstable and substantive interpretation difficult.

To assess the third point, a principal components analysis (PCA) was performed on the 27

independent variables to identify highly correlated groups of variables (minimum eigenvalue =

1.0, varimax rotation). Nine factors resulted from this and are presented in Figure 10. Analysis

	Factor								
	1	2	3	4	5	6	7	8	9
Tim10_14	0.805	-0.167	-0.085	-0.023	0.115	0.184	0.098	0.045	0.04
OcSales	0.757	0.339	0.032	-0.092	0.129	0.081	0.072	-0.003	0.102
Age35_39	0.742	0.028	0.038	0.015	0.328	0.174	0.133	0.109	0.081
lnBusiness	0.674	0.302	0.081	-0.146	0.059	0.058	-0.079	0.007	-0.016
MC_ChU3	0.664	-0.019	0.151	0.099	0.363	0.072	-0.024	0.117	0.314
lnWhoTrd	0.656	-0.195	0.226	0.102	0.211	0.139	0.087	-0.256	0.06
lnPubadm	0.625	-0.228	0.04	0.117	0.176	0.114	0.192	0.061	0.07
lnPerson	0.617	0.257	0.069	-0.266	-0.009	-0.031	0.037	0.055	-0.029
Age16	0.595	0.152	-0.081	0.192	0.106	0.149	-0.007	-0.144	0.036
Ch17MaNW	0.035	0.794	-0.126	0.017	0.154	0.054	0.039	-0.04	-0.027
MedFami	0.177	-0.653	-0.094	-0.119	0.255	0.184	0.099	-0.089	0.091
Crash_Rate	-0.171	-0.079	0.753	-0.145	-0.004	-0.018	0.175	0.061	-0.119
Tim40_44	0.263	0.006	0.703	0.065	0.09	0.049	-0.135	-0.1	0.123
L_WlkHom	-0.125	-0.016	0.048	-0.733	-0.183	-0.108	0.021	0.071	-0.197
DrvWkHom	0.325	-0.166	-0.023	-0.626	0.27	0.212	-0.088	-0.054	0.274
Ch17P2FW	0.093	-0.179	-0.004	0.044	0.761	0.106	0.044	-0.088	-0.084
Ch5P2FWk	0.332	0.084	0.101	0.012	0.567	-0.032	-0.191	0.123	0.219
Age6	0.242	0.388	0.155	0.114	0.553	0.049	0.303	0.12	-0.036
S_PrpSch	0.421	0.135	0.026	-0.024	0.552	0.134	0.304	0.206	0.163
Age70_74	0.238	-0.088	-0.169	0.031	0.055	0.773	0.029	0.063	-0.169
Age62_64	0.174	0.022	0.247	0	0.072	0.755	-0.011	-0.059	0.051
Tim35_39	0.257	-0.009	0.001	-0.001	0.077	-0.029	0.821	-0.096	0.018
Ch5P2MWk	0.113	0.191	0.239	-0.027	0.115	0.193	0.016	0.691	0.276
OcFarming	0.067	0.152	0.29	0.021	0.009	0.211	0.137	-0.69	0.267
lnEntert	0.213	-0.081	-0.033	0.068	0.048	-0.087	0.024	0.015	0.747
MnW_Ch13	0.311	0.128	-0.065	-0.05	0.4	-0.214	-0.369	-0.019	-0.331
Tim60_89	0.297	0.076	0.345	0.231	0.052	0.168	-0.11	0.08	-0.301
L_SlfEmp	0.393	-0.223	-0.006	-0.326	0.403	0.351	-0.024	-0.109	0.253

Figure 10: Factor Analysis Results

of the results requires a bit of interpretation. For instance, variables with high loadings on the

first component include:

- Workers 16 years and over, not working at home, whose travel time to work was 10-14 minutes (Tim10_14);
- Employed persons 16 years and over who are in sales occupations (OcSales);
- Persons aged 35-39; and
- Employed persons 16 years and over who are in public administration industries (InPubadm);

This factor can be interpreted as representing neighborhoods with thirtysomething professional

service industry workers with average commute times. Other components can be similarly

interpreted.

To assess the potential impact of these groups of variables on block-group-based crash rates,

the components can, in turn, be used as independent variables in a regression analysis. The

results were less useful than the original regression, however, since the R (0.276) and R^2 (.076)

were lower (worse for empirical prediction), and the difficult interpretation of the components

that entered the equation makes it difficult to derive any "meaning" from the results that we could

use to establish causal factors. Additionally, only factor 1 (0.054) and factor 6 (0.000), had p-

values of significance. Finally, while it wasn't as useful in this analysis, PCA could still be useful

in future analyses.

CONCLUSIONS

The development of this typology is a promising approach, but mainly for empirical

prediction (e.g., to estimate impact of changes on number of crashes in a given development, city,

or emergency response district). Statistical associations and patterns by using the typology can be

examined for possible "causal" significance, which would then be assessed via more detailed

studies.

Though regression using individual variables gave good results for prediction, the results are

hard to interpet substantively. In addition, use of PCA made the equation worse and didn't aid

interpretation. The next step would be mapping to find block groups with high values for component 1 and component 6.

Some issues with the data made the made the analysis more difficult. Extreme values/outliers make it difficult to get meaningful results from regression. Additionally, these extreme values/outliers skew the analysis. However, these values are more interesting in from a safety perspective.

Additionally, the typology might be developed for two different types of analyses. Examining immediate corridor proximity would facilitate causal analysis and engineering countermeasures. Examining broader areas (e.g., block groups) is better for planning applications such as police and fire response or broader estimates of changes in crash statistics and patterns.

References

1. Zhou, Min and Virginia P. Sisiopiku. "Relationships Between Volume-to-Capacity Ratios and Accident Rates", Transportation Research Record No. 1581, *Safety and Human Performance/Traffic Records, Accident Prediction and Analysis, and Statistical Methods*, Transportation Research Board/National Research Council, National Academy Press, Washington, D.C., 1997, pg. 47-52.
2. Raub, Richard A. "Occurrence of Secondary Crashes on Urban Arterial Roadways", Transportation Research Record No. 1581, *Safety and Human Performance/Traffic Records, Accident Prediction and Analysis, and Statistical Methods*, Transportation Research Board/National Research Council, National Academy Press, Washington, D.C., 1997, pg. 53-58.
3. "Access Management Slows Incidence of Traffic Accidents", Public Works, February 1995, pp. 39-41.
4. Dart, O.K. and L. Mann, "Relationship of Rural Highway Geometry to Accident Rates in Louisiana", Highway Research Record, Volume 312, 1970.
5. *Workshop on Development of the Interactive Highway Safety Design Model Accident Analysis Module*, Publication No. FHWA-RD-96-075, U.S. Department of Transportation/Federal Highway Administration/Research and Development, Turner-Fairbank Highway Research Center, McLean, VA, February 1997, 129p.
6. *Knowledge Acquisition Methods for the IHSDM Diagnostic Review Expert System*, Publication No. FHWA-RD-97-134, U.S. Department of Transportation/Federal Highway Administration/Research and Development, Turner-Fairbank Highway Research Center, McLean, VA, December 1997, 231p.
7. Muench, Loren Oliver. The Relationship of Demographic Variables to Fatal Motor Vehicle Accidents. Master's Thesis, Iowa State University, Ames, Iowa, 1965, 98p.
8. Tack, Leland Richard. Relationship of Demographic Variables to Non-Fatal Motorcycle Accidents, Iowa, 1962-1966. Master's Thesis, Iowa State University, Ames, Iowa, 1969, 65p.
9. Podkowicz, C, "The influence of land development and traffic on road accidents", Transport Quarterly, Vol. 3, No. 2, 1991.
10. Del Mistro, R.F. and R. Fieldwick. The contribution of traffic volume, speed, congestion, road section block length, abutting land use and kerbside activity to accidents on urban arterial roads. National Institute for Transport and Road Research, Pretoria, 1981.
11. Quiroga, Cesar A. and Darcy Bullock. "Geographic Database for Traffic Operations Data", *Journal of Transportation Engineering*, American Society of Civil Engineers, Vol. 122, No. 3, May/June 1996, pg. 226-234.
12. Saccomanno, F.F., K.C. Chong, and S.A. Nassar. "Geographic Information System Platform for Road Accident Risk Modeling", Transportation Research Record No. 1581, *Safety and Human Performance/Traffic Records, Accident Prediction and Analysis, and Statistical Methods*, Transportation Research Board/National Research Council, National Academy Press, Washington, D.C., 1997, pg. 18-26.
13. Pawlovich, Michael D. and Reginald R. Souleyrette. "A GIS-based Accident Location and Analysis System (GIS-ALAS)", *1996 Semisesquicentennial Transportation Conference Proceedings*, Iowa Department of Transportation/Iowa State University/Center for Transportation Research and Education (CTRE), Ames, Iowa, 1996, pg. 29-34.
14. Souleyrette, Strauss, Pawlovich, Estochen. GIS-based Accident Location and Analysis System (GIS-ALAS) Project report: Phase 1, Iowa Department of Transportation/Center for Transportation Research and Education, April 1998.

Bradley Estochen
MS Student - Transportation Engineering
Civil and Construction Engineering
Iowa State University

*An Assessment of
Emergency Vehicle Response Predeployment
Using GIS Identification of
High-Accident Density Locations*

INTRODUCTION

It is well known that EMS response time is critical in traffic crashes involving injury. Emergency medical service planning involves decisions from both strategic and tactical viewpoints. Strategic decisions involve the location and number of vehicles to attain overall system goals. Tactical decisions involve responses to situations that arise given a fixed number of vehicles (1).

Response time is crucial to the survival of many traffic accident victims. In a potentially fatal accident, the time of starting an intravenous drip (IV) is often imperative to the survival of the victim (2). Additional basic life support may also be needed soon after the crash to increase the chance of survival (3). All factors that might increase response time are matter of concern. Some variables related to response time include land variables, such as differences in travel time and terrain between rural and urban settings, and road variables, such as variations in traffic flow related to time of day, weather, and congestion (3).

Various government policies have encouraged the combination of hospital accident and emergency departments into centralized units, responsible for large geographic areas. While this provides an improved quality of medical care, travel time to a crash scene is often compromised for those not near these centralized locations (4). According to Brown, there is a positive association between ambulance delay and the ratio of fatal to serious injuries. This study found an increased mortality rate in counties that had a low population density, further suggesting a link between elevated response time and prognosis (5). Numerous other studies have also demonstrated the relationship between decreases in response time and corresponding decreases in mortality (1).

RURAL AND URBAN RESPONSES

Emergency calls generate different approaches to providing service for individuals in need. This is evident in analyzing the difference in response hierarchy in rural and urban settings. Response characteristics vary by geographic area. Rural areas provide service to a large geographic area with limited resources (6). Optimal strategic location of facilities is a key element in meeting rural emergency response needs (6).

With higher population densities, urban areas may consolidate services from a limited number of locations. Simultaneous requests for service are also more commonplace in urban settings. Therefore, the positioning of such facilities should provide efficient service to a diverse area.

TYPICAL EMS SYSTEM

The typical EMS service response is shown in Figure 1. A communication center operator receives a request for service, usually by phone or two-way radio. The operator makes an initial screening to determine if an ambulance should be dispatched and what particular response code should be used (if needed). Next, the dispatcher assesses the geographical location and the availability of the fleet based upon the particular assignment hierarchy established by the management. It is a generally accepted rule to send the closest unit to the incident. At this point the appropriate crew is assigned to respond. The time elapsed during this phase is referred to as the dispatch delay.

The response unit gathers any necessary equipment that may not be resident on the vehicle and proceeds to the specified location. The interval between the time the response unit receives a call to the time the response vehicle is in motion is called crew generation time (however, some operations include this as part of the dispatch delay).

2

The travel time is the time elapsed from the initial movement of the vehicle until the dispatcher is notified of the arrival. The total system response time is represented by the time interval between the call notification and the arrival on the scene. However, it is common for EMS systems to view response time delay without the dispatch delay, not taking into consideration the factors external to the mobilization process.
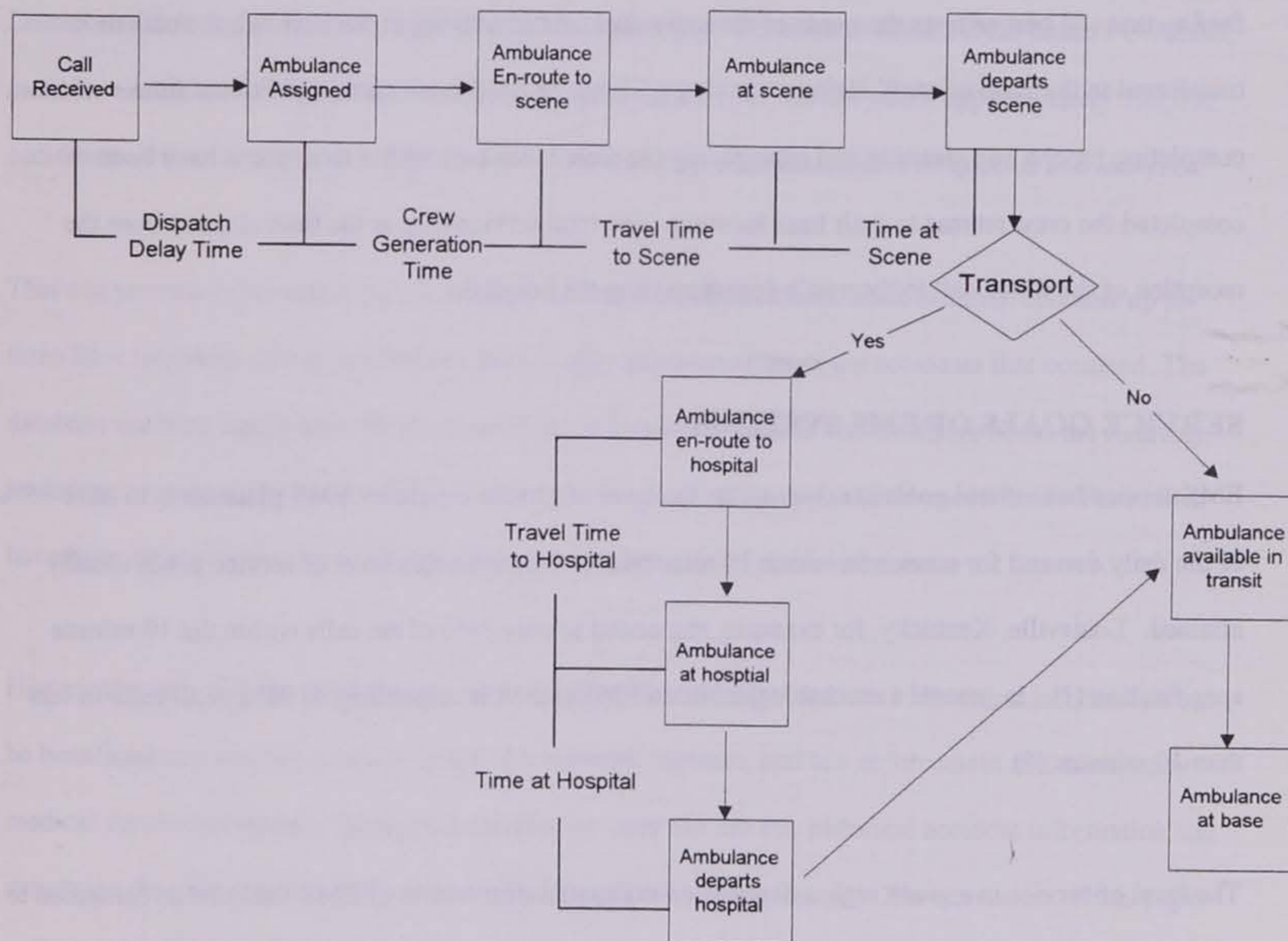

Figure 1. The EMS Process (*1*)

Dispatchers usually decide if an ambulance needs to be deployed. This does not occur in all cases. At times the necessity of an ambulance cannot be determined until notification from police or other responding units arrive at the scene. Often a short time is spent on the scene because the service is not

3

needed or the victim refuses medical attention or transportation. When this occurs the crew departs and

heads back to the base. During the time in transit back to base the unit is available to respond to another

call if needed; however this does not occur often and when it does it is usually in large cities during peak

hours (7).

In cases where medical attention is deemed necessary, the crew determines the appropriate medical

facility that can best address the needs of the individual. After arriving at the hospital, the patient is

transferred to the hospital staff. Before returning to duty, the EMS crew spends additional time

completing reports and cleaning and resupplying the ambulance unit. After these steps have been

completed the crew returns to their base location. The total service time is the time elapsed from the

reception of the initial call to the unit's departure from the hospital.

SERVICE GOALS OF EMS SYSTEMS

EMS service has several goals in urban areas; the level of service sought by EMS planners is to have 95%

of the daily demand for service be within 10 minutes (8). However, this level of service is not usually

attained. Louisville, Kentucky, for example, responded to only 84% of the calls within the 10-minute

specification (1). In general a reachable goal of an EMS station is responding to 90% of all calls in less

than 10 minutes (9).

The level of service in a given region depends on the spatial distribution of EMS facilities as compared to

the spatial pattern of the demand. EMS facilities located near areas with high demand, like crash

densities, while not neglecting other areas can provide lower response times and improved levels of

service and final outcomes. A geographic information system (GIS) can be used to identify existing EMS

service areas, to compare these areas with traffic crash patterns, and to generate strategies to improve

EMS services. The next section uses EMS facility and traffic crash data for the City of Des Moines and

4

Polk County to illustrate the use of GIS in assessing existing EMS response patterns and the potential impacts of alternative locations EMS facilities.

GIS-ALAS

The Iowa Department of Transportation, with the assistance from the Center for Transportation Research and Education at Iowa State University, has developed a Geographic Information System Accident Location and Analysis System (GIS-ALAS). The system, an extension of Iowa's DOS based PC-ALAS, includes the location of all crashes on all roads in the state for the last ten years, approximately 700,000 accidents. It provides spatial displays of accidents and allows the database to be queried and analyzed.

This can provide information on the locations of high-density accidents. Each accident contains up to three files (accident, driver, and injury) that provide information about the accidents that occurred. The database contains injury severity and time of day information. Data is also available about the roadway, including average daily traffic (ADT), lane width, length of each segment, and speed limit. These files have been created allowing a GIS to provide a spatial graphic of crash locations.

Historical trends can provide information on high accident density locations. Historical information can be beneficial to a number of users including engineers, planners, and law enforcement and emergency medical service personnel. Emergency medical services can use this historical accident information and determine the characteristics relevant to vehicle crashes involving injuries. The remainder of this paper will examine high-density locations in Des Moines, Iowa and compare response service areas from static facilities, exploring the potential for pre-dispatching in areas of need for locations that do not have adequate service.

LOCATING HIGH ACCIDENT AREAS

5

In GIS-ALAS, the roadway is represented as a link-node system. There are approximately 226,000 node locations throughout the State. Each accident is located with respect to two nodes, the reference and direction nodes, and the corresponding distance between each of these nodes. This system provides easy representation of accident density by visually displaying the accident locations with respect to the nodes. The database was queried to determine the number of accidents associated with each reference node. The total number of accidents associated with each reference node was calculated and incorporated with the accident database. This allows the number of accidents at each reference node to be visually displayed within the GIS, the larger the dot the increased frequency of accidents. (See Figure 2).
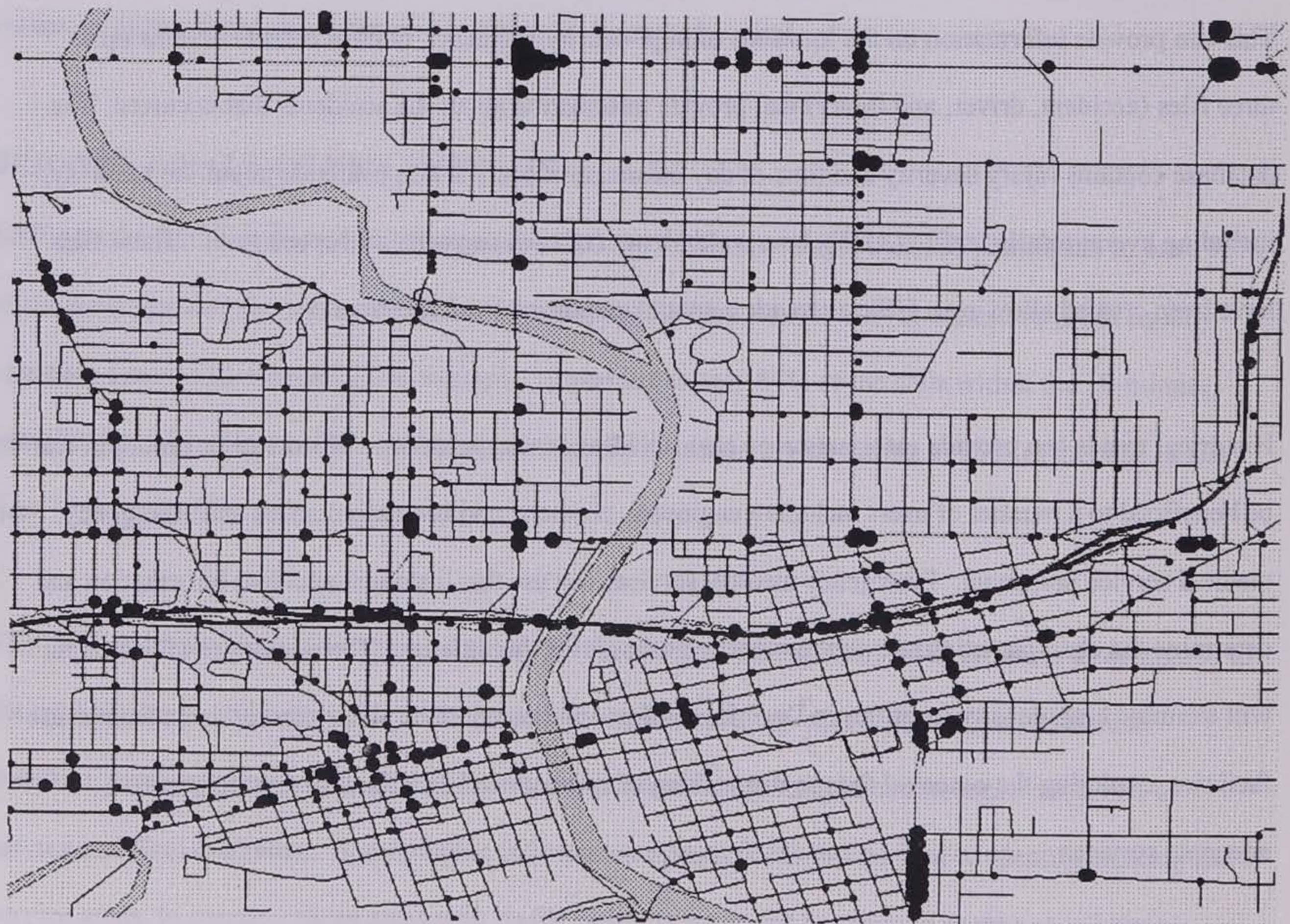
Figure 2. Graphical Representation of Crash Locations

Inspection of the Des Moines metropolitan area identified accident locations based upon five years of crash data (1991-1995). The objective of locating these crashes was to determine if pre-dispatching emergency vehicles would provide benefits to crash victims by reducing EMS response time. The time intervals were used to determine the peak period of crash occurrence for the metropolitan areas. These crashes were then examined based upon time of day. The a.m. peak period for crashes was determined to be from 6:30 – 9:00, while the afternoon peak period was 3:30 –6:30. These intervals had 13% and 26%, respectively, of the total crashes within the metropolitan area for the five years of data provided.

The determination of the high crash locations provides useful information regarding the geographic characteristics of the crashes. However, other information can also be obtained including the number of injuries and fatalities. As stated, at times the necessity of an ambulance unit cannot be determined until an EMS unit is present at the scene (7); therefore accidents that involve non-injuries are also important to EMS providers, as well as the crash victims.

SERVICE AREAS

Using the analytical capabilities of the GIS, the response times from each EMS location can be computed and graphically displayed to determine if service to particular areas is satisfactory. The locations of the EMS facilities were added to the GIS using data from the Iowa Department of Public Health (Figure 3) The roadway files were obtained from the Iowa Department of Transportation Office of Cartography; attribute information was also used to enhance the data set.
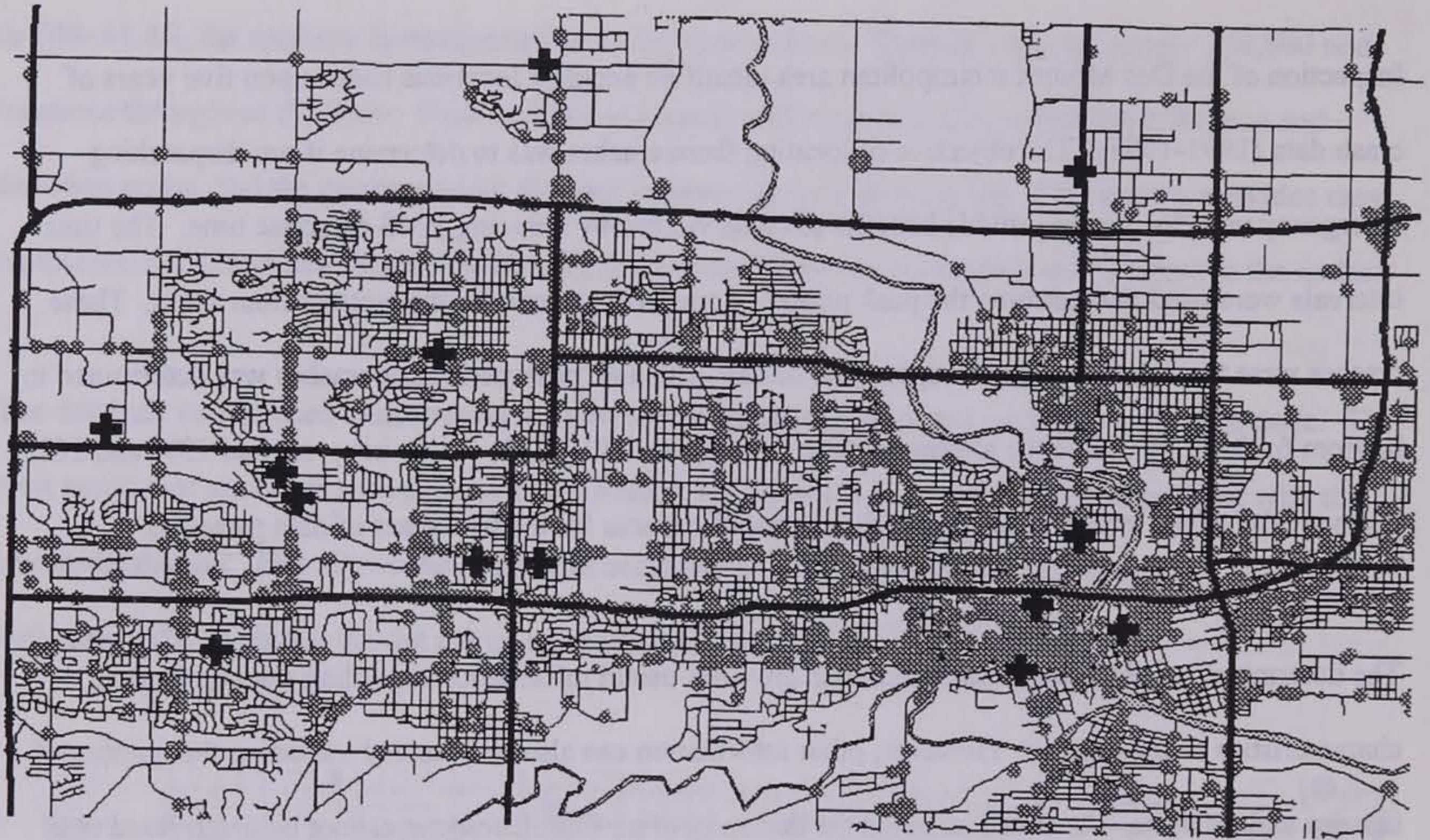
Figure 3. EMS Locations With Respect to Traffic Crashes Within the Des Moines Metro Area.

Segment length and speed limit are used to compute a travel time for road links. This provides each individual segment with a travel time value; however, this value is only an approximation. This value does not take into consideration time delays associated with traffic control and traffic congestion.

RESULTS

Travel time areas from each of the facilities were computed and are displayed in Figure 4. The rings around the facilities indicate the areas, and accidents, that can be reached within 5, 7, and 10 minutes. Several facilities are located in clusters in close proximity to each other, especially in downtown Des Moines and in the western suburbs. Neighborhoods near these clusters are located within overlapping 5-minute service areas of several facilities. In contrast, areas in the county's periphery tend to be in the 10-minute service area or beyond. (The results may be partially affected by data limitations related to the connectivity and characteristics of the road network.) Service area maps like Figure 4 can be used to

8

provide an initial indication of countywide EMS coverage and identification of potentially underserved areas.
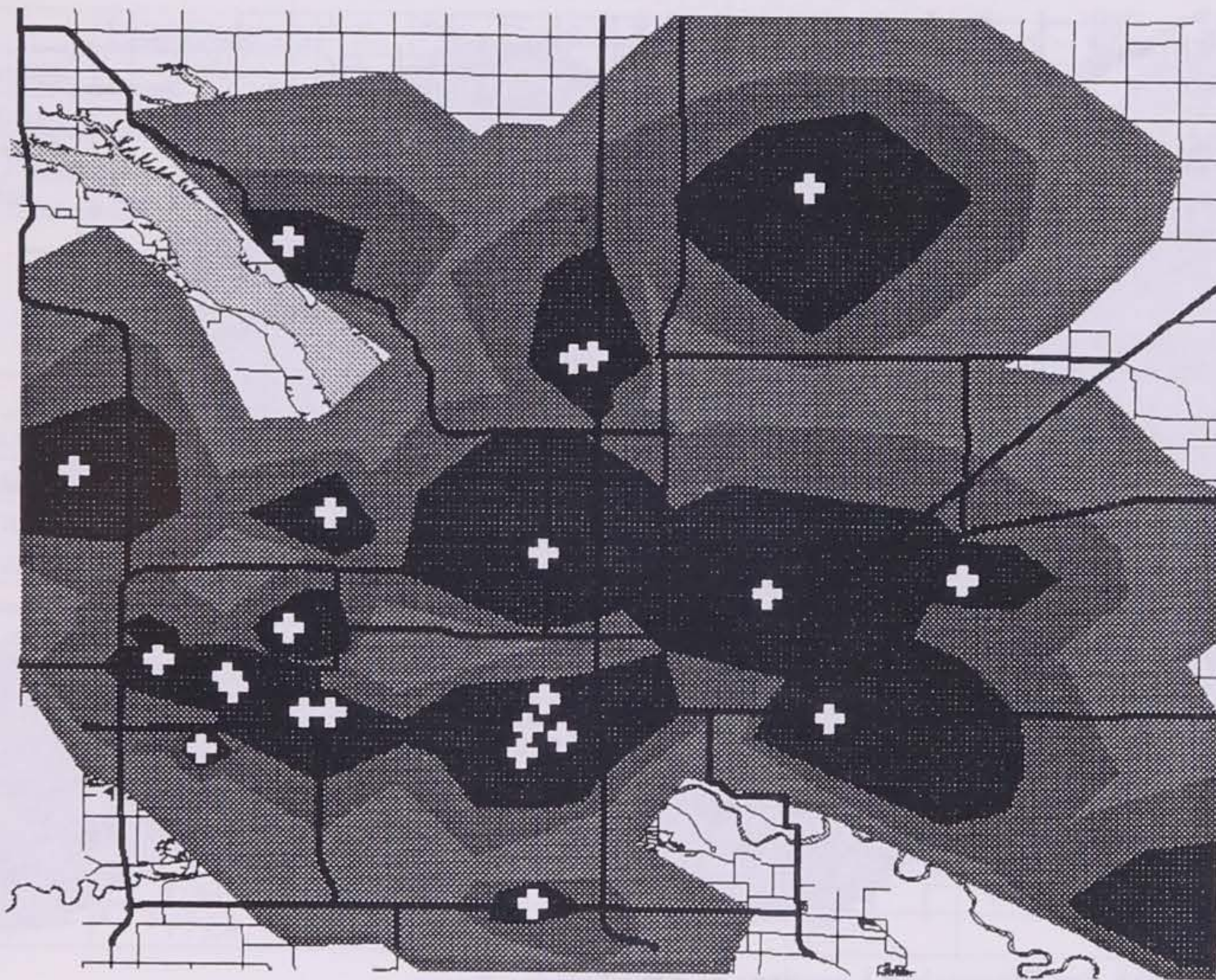
**Figure 4. EMS Travel Ranges (5, 7, and 10 Minutes)**

These response areas were broken further down into one-minute intervals to estimate the number of crashes occurring during each response-time interval. This was then used to determine the average response time for the entire region. The estimated average response time, given the locations of 1991-1995 crashes and EMS facilities, for the a.m. and p.m. peak periods is 4.91 and 4.92 minutes, respectively, for the Des Moines metropolitan area.

The locations of the facilities were moved in GIS to simulate possible changes in EMS activities, such as pre-dispatching vehicles to areas with high crash densities. These areas were based upon historical crash

9

patterns identified using GIS-ALAS. . (The differences in the facility locations can be found in Figure 5.) The resulting changes in service areas and response times were computed and compared to the current situation.
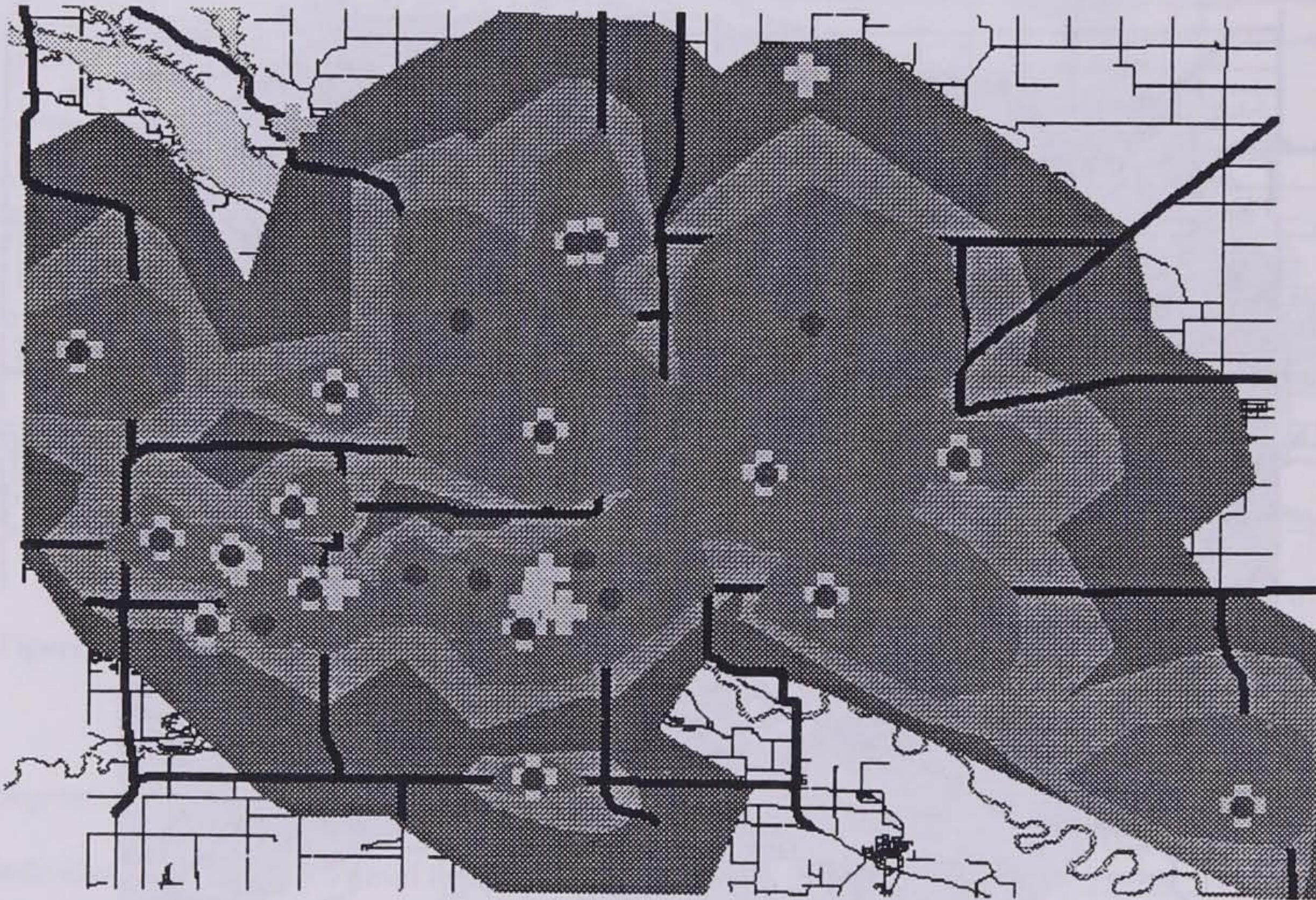
Figure 5. EMS Pre-Dispatched Locations and the Service Areas.

The overall response time for the pre-dispatched vehicles was 0.4 minutes (24 seconds) lower for both the a.m. and p.m. periods. In practice, this difference may be insignificant for most crash outcomes but critical for others. The change in facility location also resulted in an increased percentage of crashes reached within the 5-minute threshold -- 56.4% before the change vs. 63.2% after for a.m. crashes, and 58.7% vs. 65.8% for p.m. crashes, about a 7% improvement for both time periods (see Tables 1-4). This benefit decreases at the 7-minute threshold (about a 2% improvement), and at the 10-minute threshold the percentage of crashes reached is roughly the same for both sets of EMS facility locations. Figures 6

10

further illustrates the shift toward shorter response times. Data for injury crashes and the number injured show similar patterns. (The number of fatalities was too small to provide significant comparisons.)

Table 1. Response During AM Peak Period (Current EMS Locations)

	Total Crashes	%	Fatal Crashes	%	Injury Crashes	%	Number Injured	%
5 Minutes	4356	56.4	4	33.3	1429	55.3	1902	54.9
7 Minutes	6330	81.9	9	75	2076	80.3	2776	80.1
10 Minutes	7320	94.7	11	91.7	2411	93.2	3241	93.5
Total	7729		12		2586		3467	

Table 2. Response During PM Peak Periods (Current EMS Locations)

	Total Crashes	%	Fatal Crashes	%	Injury Crashes	%	Number Injured	%
5 Minutes	9245	58.7	18	50	3186	53.7	5027	57.9
7 Minutes	13124	83.3	24	66.7	4932	83.2	7132	82.2
10 Minutes	15131	96.1	33	91.7	5714	96.4	8329	96
Total	15752		36		5928		8679	

Table 3. Response During AM Peak Periods (With Pre-dispatched Locations)

	Total Crashes	%	Fatal Crashes	%	Injury Crashes	%	Number Injured	%
5 Minutes	4884	63.2	4	33.3	1604	62	2138	61.7
7 Minutes	6482	83.8	8	66.7	2111	81.6	2823	81.4
10 Minutes	7302	94.5	11	91.7	2412	93.3	3243	93.5
Total	7729		12		2586		3467	

Table 4. Response During PM Peak Periods (With Pre-dispatched Locations)

	Total Crashes	%	Fatal Crashes	%	Injury Crashes	%	Number Injured	%
5 Minutes	10360	65.8	22	61.1	3901	65.8	5557	64
7 Minutes	13421	85.2	24	75	5040	85.2	7312	84.2
10 Minutes	15129	96	32	88.9	5712	96.3	8315	95.8
Total	15752		36		5928		8679	

11

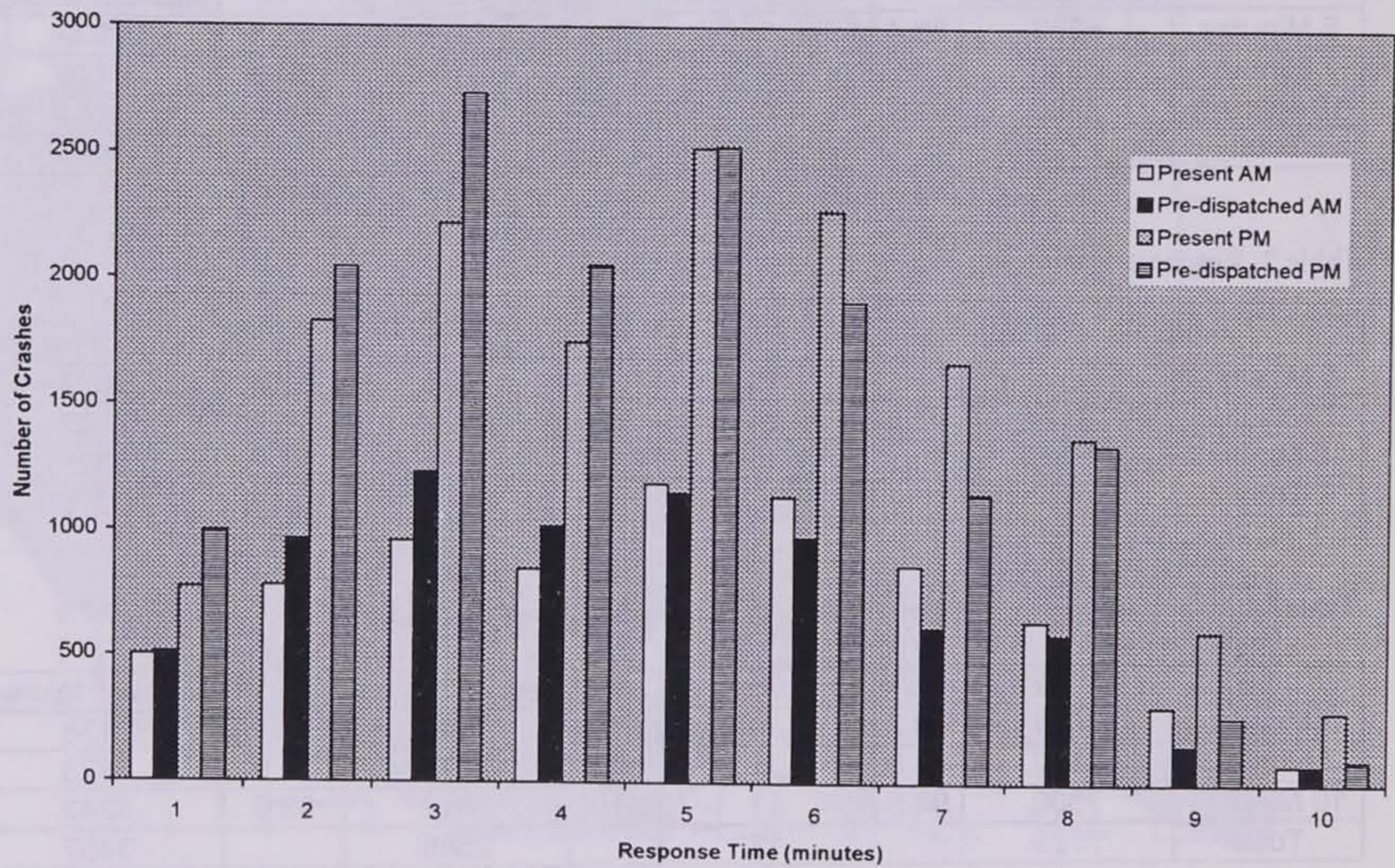**Changes in Response Times With Pre-Dispatched Units**

Figure 6. **Changes in AM Response Times Due to Pre-Dispatching Units**

CONCLUSIONS

The ability of EMS personnel to quickly reach crash sites is a critical determinant of final crash outcome.

Response times are closely linked to the locations of EMS facilities in relation to the locations of crashes.

GIS can be used to assess existing service areas, identify potentially underserved areas, and to evaluate

the implications of potential changes in EMS systems. The case study presented here illustrates that

changing the location of EMS services, such as through the pre-deployment of vehicles, can result in

improved response times. The benefits, in terms of improved outcomes, and costs associated with this

strategy is an issue for future research.

12

REFERENCES

1) Repede, John F., Bernardo, John J., Developing and Validating a Decision Support System for Locating Emergency Vehicles in Louisville, Kentucky, European Journal of Operational Research, June 30, 1994 v 75, n 3.

2) Williams F.L.R., O.LI. Lloyd, J.A. Dunbar, Deaths From Road Traffic Accidents in Scotland: 1979-1988. Does it matter where you live? Public Health, July 1991 p 319-326.

3) Brodsky, Harold. Delay in Ambulance Dispatch to Road Accidents, American Journal of Public Health, June 1992, v 82 n 6 p 873-875.

4) Jones, A.P. Bentham, G. Emergency Medical Service Accessibility and Outcome from Road Traffic Accidents, Public Health, May 1995, p 169-177.

5) Brown, DB. Proxy measures in accident countermeasure evaluation: a study of emergency medical services, Journal of Safety Research 1979, p 11, 37-41.

6) Daberkow, S.G., Location and Cost of Ambulances Serving a Rural Area, Health Services Research, Fall 1977, p 299-311.

7) Goldberg, Jeffery, Dietrich, Robert, Chen, Jen Ming, Mitwasi, M. George, Valenzuela, Terry, and Criss, Elizabeth. Validating and Applying a Model for Locating Emergency Medical Vehicles in Tucson, AZ, European Journal of Operational Research v 49 n 3 Dec 14 1990 p 308-324.

8) Daskin, Mark S, Hierarchical Objective Set Covering Model for Emergency Medical Service Vehicle Deployment, Transportation Science v 15 n 2 May 1981 p 137-152.

9) Scott, D.W., Factor ,LE., Gorry, G.A., Predicting Response Time of an Urban Ambulance System, Health Services Research, Winter 1978 p 404-417.

Clifton Melcher
MS Student - Structural Engineering
Civil and Construction Engineering
Iowa State University

Methods of Shear Testing and
Their Relation to Fiber Composite Dowel Bars

Introduction:

Fiber composites can be used in many diverse applications. They have been used routinely in automobiles, aircraft, offshore structures, piping and many other areas. Recently, they have surfaced as a promising new material in the civil engineering field. Fiber composite materials possess many qualities that include corrosion resistance, light weight, excellent fatigue strength, impact resistance, magnetic transparency, fire-resistance, durability, low-specific gravity, high strength modulus to weight ratio, and the ability to be formed into many different shapes. [1,2,3,4]

Fiber composite materials have been used routinely since the 1960s. Composite materials are very diverse, variable, and have been developed so fast, that reliable information on their properties can be hard to find; therefore, a need for testing exists. [5] Initially, fiber composites were tested following the standard testing procedures for metals. Many of these tests were inadequate to test the non-homogeneous and anisotropic properties of fiber composites. The properties of composite materials are determined through tests conducted on specimens in a laboratory. The determination of their properties is important to efficiently utilize the potential of the composite material. These properties are used for the design of practical structures. This report will narrow its focus to the determination of shear properties.

There are three different types of shear deformations:

1. Transverse shear or interlaminer shear (in the case of laminates) - A shear deformation normal to the plane of a composite material.

2. In-plane shear or horizontal shear - A shear deformation that occurs entirely in the plane of a composite material.

3. Twisting shear –A twisting type of shear deformation on the cross section of a composite material. [6]

In this report, the first two shears, the traverse and in-plane shear, will be addressed.

The shear properties of fiber components depend on numerous characteristics of fiber composites that include:

1. Composition of the material
2. Distribution of fiber and matrix
3. Interaction of the fibers to the matrix
4. Orthropicity and,
5. Fiber and laminate orientation

The composition of composite materials can be classified into two distinct categories: composites particle-reinforced and fiber-reinforced composites. A particle-reinforced composite is composed of nonfibrous reinforcing that does not have a long-dimension. Fiber-reinforced composites, which will be analyzed in this report, are composed of a reinforcing fiber embedded into a matrix. [2] Fibers can be orientated unidirectionally or multidirectionally. Unidirectional composites are composites with fibers oriented in one direction. The two most common directions are 0° and 90°. The fiber direction is specified relative to the longitudinal direction. Hence, a specimen with a 0° orientation is one in which the fibers are parallel to the longitudinal axis and a 90° orientation of a specimen is designated as fibers orientated perpendicular to the longitudinal direction. A

multidirectional composite is a composite with fibers orientated in two or more directions. [2] The orientation of fibers in composites greatly affects the shear properties.

Composite properties, including shear, are strongly influenced by elementary materials, distribution, and interactions. Fiber composites are principally composed of a fiber and a matrix. The fiber are the predominate material and have high static and fatigue strength. [7] They occupy the largest volume fraction and support a majority of the load. The fibers are embedded into the matrix material to form a fibrous composite. The matrix binds the fibers together. It also acts to transfer stresses between fibers, protect against adverse environments, and mechanical abrasions of the surface.

Strong interfacial bonds make composites more rigid and brittle, while a weak bond tends to decrease the stiffness and enhance the toughness. A median between the two strengths is desirable. [5] The matrix can have a major influence on the in-plane and transverse shear properties. Fiber composites may also contain coupling agents, coatings, and fillers. The coupling agents and coatings help the adhesion of the interface of the fiber and matrix. The fillers are used to make the fiber composites more cost efficient and the specimens more stable. [3]

Composite material testing differs from the testing of many other materials, like steel, because the performance of the material depends on the component make-up. Transverse shear is important to structures under bending loads. [3] Transverse shear strength depends on the fiber and matrix interfacial shear strengths. The bond between the fiber and matrix is one of fiber composite's weakest properties, and therefore one of the most important to determine. Increasing the matrix tensile strength and matrix volume fraction can increase the transverse shear strength. A study on transverse shear failure at the University of

Leeds on unidirectional composite epoxy resin concluded that "for fibre volume fractions greater than 0.3, the shear failure is controlled by the adhesion between the fibre and the resin. At fibre volume fractions greater than 0.3 the failure is increasingly dominated by the shear failure of the resin." [8] The In-plane shear is important to structures under torsional loads. [3] A small amount of eccentricity of a load can produce a significant amount of torsion.

Fiber composite properties are direction dependent on three orthogonal planes, which in general, classify them as orthotropic materials. The three planes are the 1-2 plane, 2-3 plane and the 3-1 plane [2]. Where the first subscript denotes the plane and the second subscript denotes the direction (Figure 1). [9] Plane 1 designates the fiber direction, plane 2, the transverse direction, and plane 3, the laminate direction. Where plane 3 can be designated as the z-axis and plane 1 is referenced by the orientation of the ply angle to the x-axis. The longitudinal direction is the direction of plane 1. The transverse direction is the direction perpendicular to the fibers and is any direction in the 2-3 plane. The properties on each of these planes are affected by the orientation of the fibers. The maximum strength and modulus of fiber composites is in the longitudinal direction. When the fibers are perpendicular to the load the fibers are unable to support the load; Thus the matrix must support the majority of the load. [3]

3-axis or z-axis (laminate direction)

2-axis
(transverse direction)

1-axis (fiber direction)   θ   x-axis (laminate reference direction)
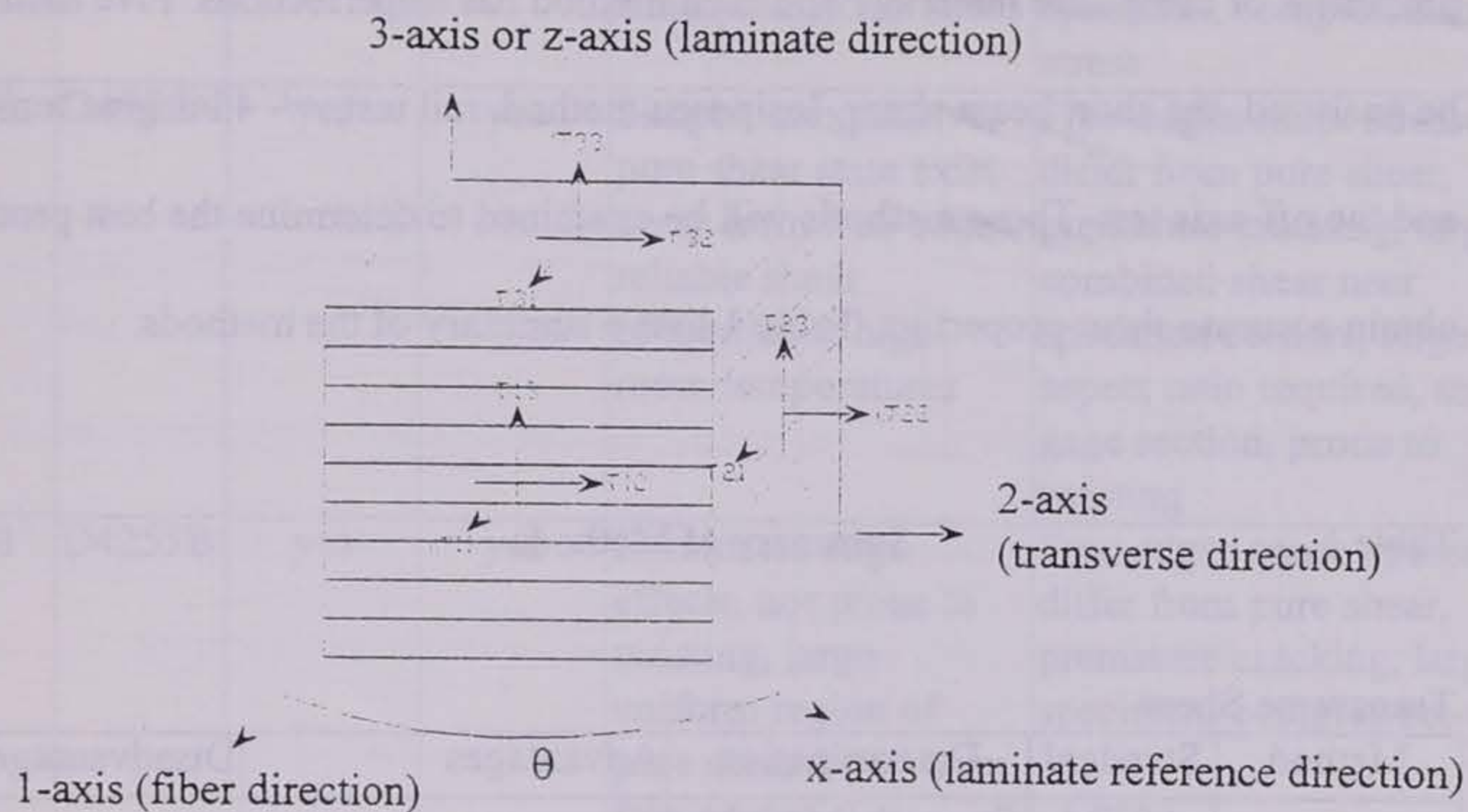
Fig. 1 Composite Material Planes [20]

The orientation of fibers is not to be confused with the orientation of laminates. Laminates can be oriented in many different configurations. Laminates are designated by their angle, in degrees, between the laminate direction and the fiber orientation. Adjacent laminates are described by a slash if their representative angles are different. A laminate list starts from one extremity of the laminate composite and ends at the other extremity. The orientation of laminates can effect shear properties substantially. Laminates in the 1-2 plane determine in-plane shear. Laminates in the 1-3 and 2-3 planes determine interlaminer shear. [2]

Shear is one of the most difficult properties to accurately determine because of the inability to obtain a uniform pure shear stress field. The difficulty of determining pure shear in a specimen increases in composite materials due to the increase of anisotropy and

inhomogeneous of the material. [2] Numerous methods can be used to determine the shear

properties of composite materials and each method has imperfections. Five methods will

be analyzed, the short beam shear, Iosipescu method, rail test, +/- 45 degree tensile test,

and the off-axis test. These methods will be examined to determine the best procedure to

obtain accurate shear properties. Table 1 lists a summary of the methods.

Table 1   Summary of Methods

Transverse Shear

Method	Standard	Determination		Advantages	Disadvantages
	ASTM	Strength	Modulus		
Short Beam	D2344	Yes	no	Simplicity, inexpensive, time saving, easy specimen fabrication	Specimen not subjected to state of pure shear, not capable of determining stress strain curve and shear modulus
Iosipescu	D5379	Yes	yes	Good shear data, test wide range of thickness', test materials in 1-2, 1-3 and 2-3 plane, 90-deg specimen in pure shear state.	0-deg specimen not in pure shear, shear modulus test for 0-deg and 90-deg specimen do not agree, large variations in shear-strain for 0-deg and 90-deg specimens

In-plane shear

Method	Standard	Determination		Advantages	Disadvantages
	ASTM	Strength	Modulus		
Short beam	D4475	Yes	no	Simplicity, inexpensive, time saving, easy specimen fabrication	Specimen not subjected to state of pure shear, not capable of determining stress strain curve and shear modulus
Iosipescu	D5379	yes	yes	Good shear data, test wide range of thickness', test materials in 1-2, 1-3 and 2-3 plane, 90-deg specimen in pure	0-deg specimen not in pure shear, shear modulus test for 0-deg and 90-deg specimen do not agree, large variations in shear-strain for 0-deg and 90-deg specimens

				shear state.	
+/-45 tension	D3518	yes	yes	Good shear data, simply, uniform stress	Limitations imposed on specimen, complex state of stress
Two-rail	D4255A	yes	yes	Simple, inexpensive, pure shear state exist away from free-edges, reliable shear properties at high room temperatures	Free-edges cause stresses to differ from pure shear, premature cracking, large combined shear near specimen corners, large aspect ratio required, small gage section, prone to twisting
Three-Rail	D4255B	yes	yes	Eliminates edge effects, not prone to twisting, large uniform region of pure shear away from free-edges	Free-edges cause stresses to differ from pure shear, premature cracking, large specimen, complex set-up
Leesard modified three-rail	D4255	yes	yes	Good shear data, eliminates premature cracking, consistent data	Large specimen, fixture not rigorously tested, test only conducted on multidirectional laminates, complex installation
off-axis	----	yes	yes	Inexpensive, easy set-up, easy specimen fabrication	End constraint effects, gives low strength and high modulus

Short Beam Shear

The short beam shear method involves loading a specimen under three-point bending. The short beam theory states that "failure by interlaminer shear can theoretically be induced by making the beam short enough so that under load, the shear stress will reach its limiting value before the normal stress does." [10 p.293] The shear stress is independent of specimen length, however the normal stress is dependent on the bending moment and is a linear function of the specimen length. [10] A shear failure can be induced by applying a load to a short beam, thus referred to as the "short beam test". The method

has two separate ASTM standards that are very similar with only minor differences in the

procedures. One standard determines transverse shear and the other determines in-plane

shear. The transverse shear is determined by reorienting the principle material axis of the

specimen.

The short beam shear method (ASTM D2344-84) determines the transverse shear

strength of parallel fiber composites. Two similar but not identical apparatuses are used

depending on the geometry of the specimen. Both apparatuses consist of two supports,

one on each side that allows lateral motion, and a load applied at the midpoint. The flat

laminate apparatus consists of a force that applies pressure on the specimen by means of a

6.35mm diameter cylinder and is supported by two 3.2mm diameter cylinders (Figure 2).

The second type of geometry that can be tested by this ASTM standard is a ring

specimen. The ring specimen apparatus consists of the same loading cylinder as used by

the flat laminate. The ring specimen is supported by two flat supports, which are movable

to fit the correct span length. The ring specimen has a maximum allowable diameter of

6.5mm. The beam must have a sufficiently small span to thickness ratio to insure that a

shear failure occurs. The specimen span length to thickness is 5 for filament

reinforcement having a Young's modulus less than 10×10^9 Pa and 4 for filament

reinforcement with Young's modulus above 10×10^9 Pa. However, a range of various

spans length-to-thicknesses should be tested to determine a correct ratio. The flat

laminate specimen should have an overhang equal to its depth on each side. No overhang

is required for the ring specimen. The specimen should be loaded at a rate of 1.3 mm/min

until failure occurs. The shear strength is calculated using the beam theory equation, eqn.

1. [11]

$$\tau = 3P/4bd \qquad\qquad\qquad \text{(eqn. 1)}$$

Where:

τ = shear strength, N/m^2 (psi)

P_B = load, N (lbf)

b = width of specimen, m (in.) and

d = thickness of specimen, m (in.)
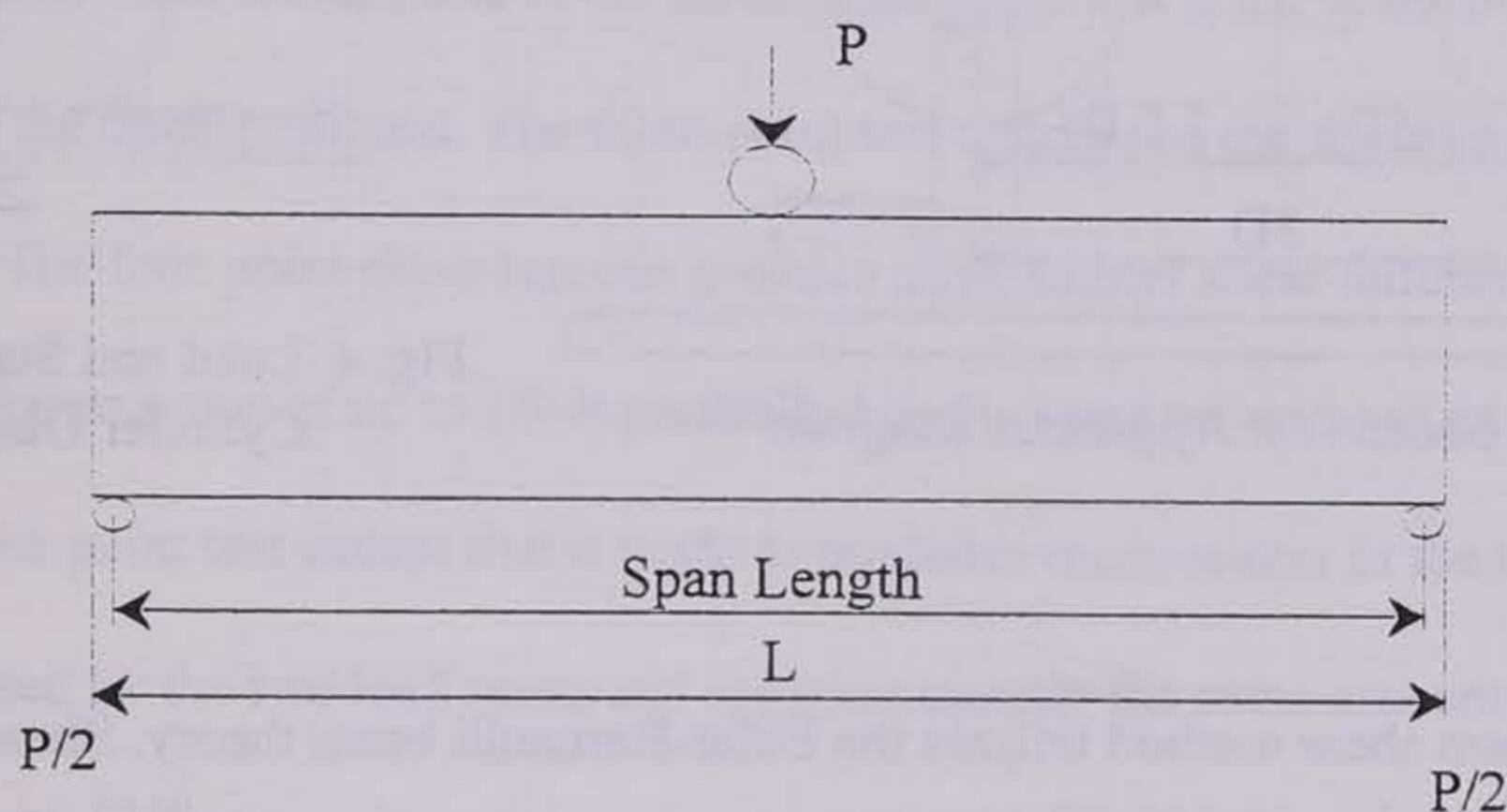
Fig. 2 Horizontal Shear Load Diagram (Flat Laminate) [11]

The short beam shear method (ASTM D4475-85) determines the in-plane shear strength of parallel fiber composite plastic rods. The apparatus used to test the specimen consist of two supports, one on each side that allow lateral motion and a load applied at the midpoint (Figure 3). The loading and support cylinder consists of a thread-spool-like design. A 1.5D cylinder that is a minimum of 1.5D thick and has a radius symmetrically removed of D/2 (Figure 4). The span length can range from 3D to a maximum 6D as required to produce a shear failure. [12]
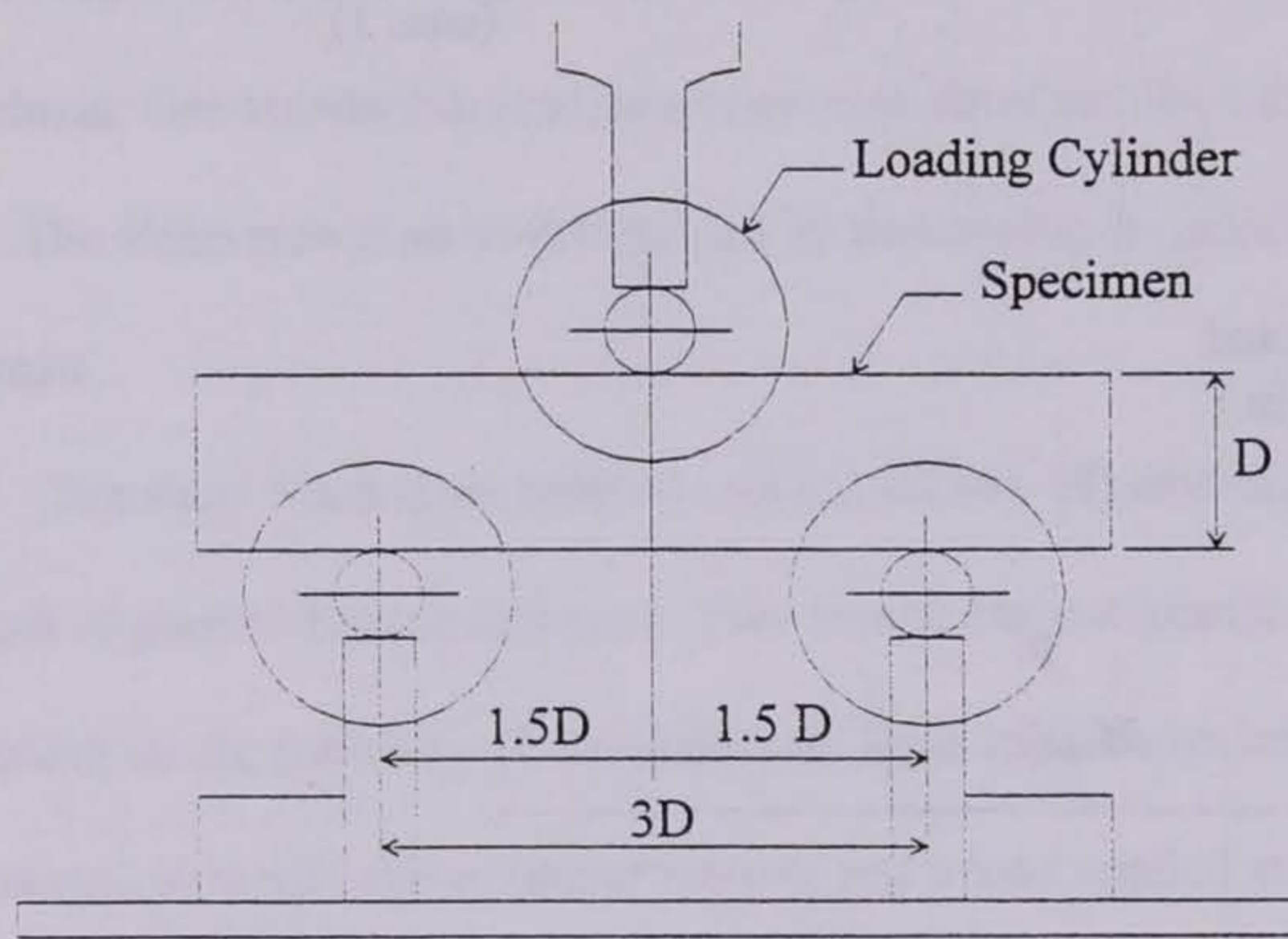
Fig. 3 Horizontal Shear Test Apparatus Diagram [12]
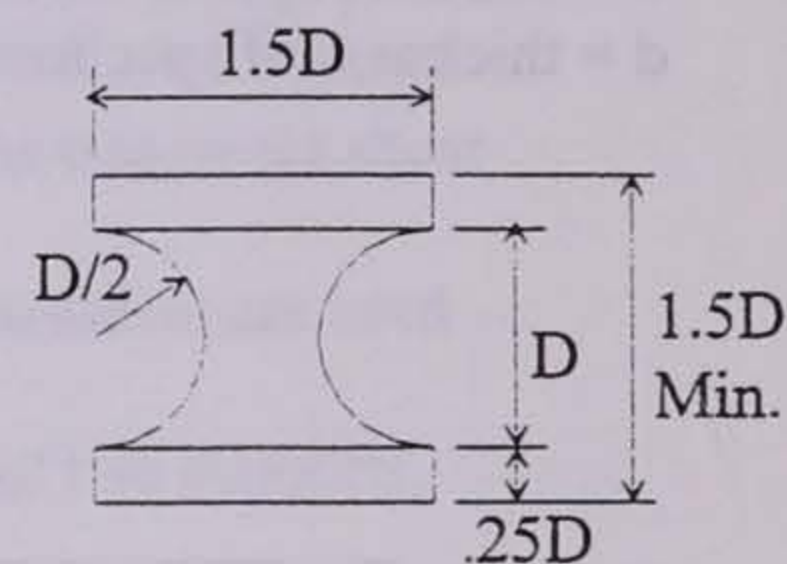
Fig. 4 Load and Support Cylinder Diagram [12]

The short beam shear method utilizes the Euler-Bernenlli beam theory. Shear stresses across the face are parabolically distributed with the maximum occurring at the middle of the beam. Eqn. 2 represents the maximum stress for a test specimen with a circular cross section.

$$\tau = .849P/(d^2) \hspace{4cm} \text{(eqn. 2)}$$

Where:
τ = shear stress, N/m^2 (psi)
P = load, N (lbf) and
d = diameter, m (in)

This equation is only relative to specimens with large span to depth ratios, thus thin specimens will be invalid. As concluded by Xie and Adams [13] "A specimen with a low span to thickness ratio will exhibit a high apparent shear strength." When in actuality the shear strength should be much lower.

The inability of the three-point beam shear test to produce interlaminer shear failure in thin specimens led to the development of the four-point shear test. The four-point shear test does not have an ASTM standard, but the four-point flexural test (ASTM D790) procedures can be followed. The four-point shear utilizes the same principles as the three-point beam shear. According to beam theory, the maximum shear stress in the four-point shear test is same as the three-point shear test if the span-to-thickness is twice that of the three-point test. The three-point test distributes the shear stress over the entire beam. The four-point shear test can produce interlaminer shear failures in specimen span to thickness ratios of up to 16. It generally has the same advantages and disadvantages as the three-point test except that it tends to produces more scatter in the test data. This may be caused by the two load noses not applying exactly the same amount of pressure to the specimen. [13,14]

The simplicity of the short beam shear test makes it a popular method for determining shear strength. Also, the specimen is easy to fabricate and the simplicity of the test makes it relatively inexpensive and timesaving. Numerous samples can be tested in a short period of time. The short beam shear test does have many faults. It does not subject the specimen to a state of pure shear, bending stress is significant. The correct shear strength is obtained only when shear exists and a pure shear break is produced. Many times, a break occurs due to the combination of shear and moment, called a "mixed break". [1] Thus the short-beam shear test validity must be questioned. These mixed breaks must be avoided to obtain more accurate results. In addition, the short beam shear test produces a non-uniform shear stress distribution and is not capable of determining the stress-strain curve and the shear modulus. Which make it an unappealing option for the

determination of design criteria. The short beam shear test is generally recognized for

quality control and specification purposes, not as a method to determine accurate shear

strength. [14]

Iosipescu Shear Test

Nicolas Iosipescu originally created the Iospescu shear method in the 1960s for

the use of measuring the shear strength of metals. [15] Although it was originally

developed for use with metals, it has been widely used for a variety of fiber composites.

Since the 1960s many modifications to the original Iosipescu shear test have been

introduced. The Modified Wyoming test fixture by Walrath and Adams is the most

widely used. [16-19]

The Iosipescu shear method (D5379-93) determines shear property data for

material specifications. The specimen is tested in a v-notched, beam test fixture (Figure

5). The test fixture is antisymmetrical with four-point loading. Each side has adjustable-

grip wedges that clamp on to the specimen. The specimen is rectangular with

symmetrically centered v-notches. The v-notches are cut at a 45° angle parallel to the

specimen. The center of the specimen, location of the v-notches, should be centered over

the load by means of the alignment pin that is equipped on the apparatus. The specimen

halves are compressed at a rate to induce failure within one to ten minutes and monitored.

Shear is measured by two strain gages elements orientated at 45 degrees to the loading

axis in the center of the specimen, away from the notches, and along the load axis. [20] A

third strain gage can be used on the longitudinal axis to estimate the moment produced in

the test section and thus, determine the shear purity. [16,21]
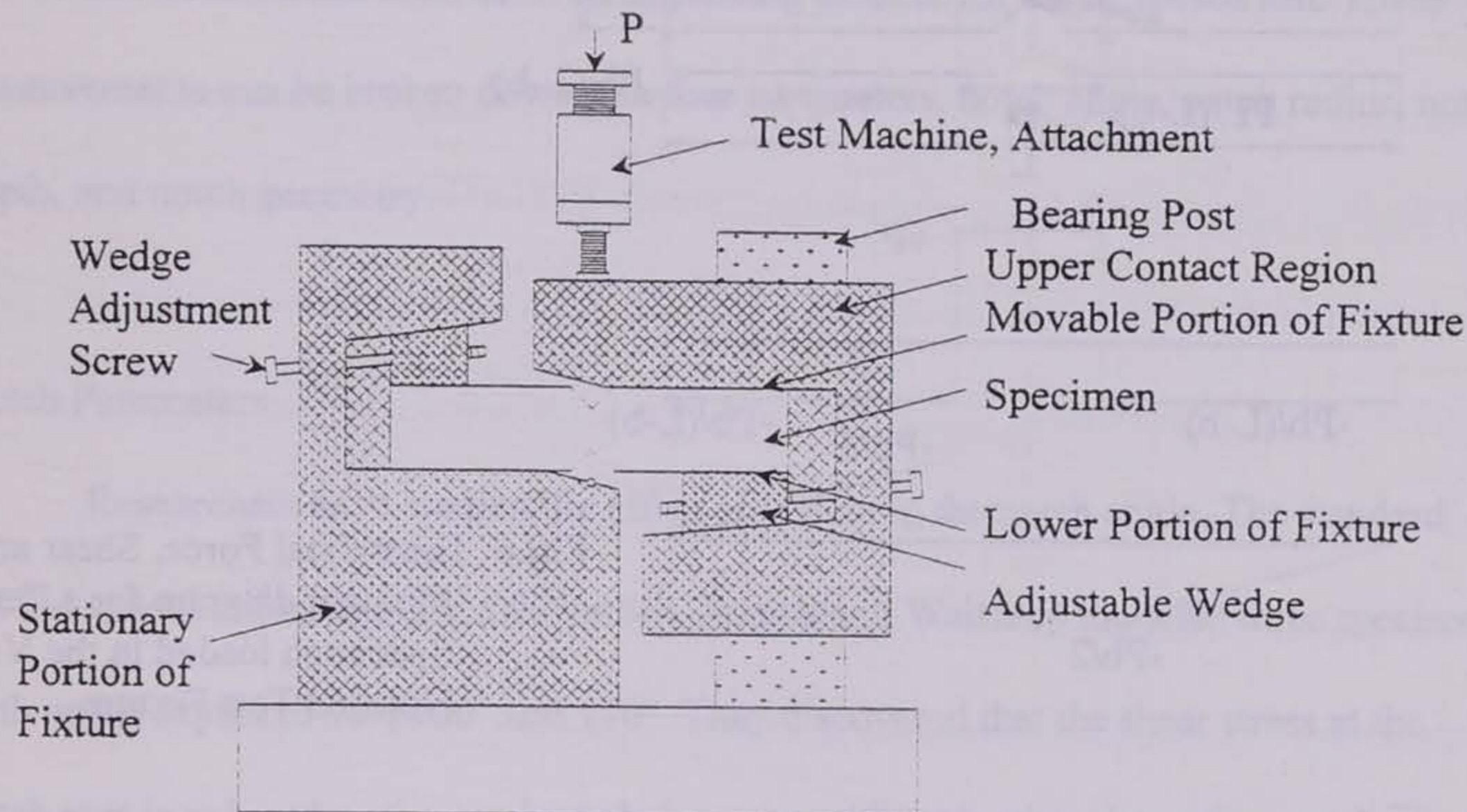
Fig. 5 Modified Wyoming Test Fixture [16]

The Iosipescu shear test is aligned to produce two antisymmetrical forces. These

forces create two counteracting moments that generate a pure shear between the gages,

and produce a zero bending moment at the notch (Figure 6). Thus, in theory, a pure shear

break will be produced. [3,22] Both 0° and 90° fiber orientation can be tested by the

Iosipescu fixture, but in general 0° specimens are tested most often. The 0° specimens are

favored because they produce a better shear stress-strain response than do the 90°

specimens. [16-18]

Pb/(L-b)   PL/(L-b)

D

PL/(L-b)   B

L

+P

-Pb/(L-b)   -Pb/(L-b)

-Pb/2

-Pb/2
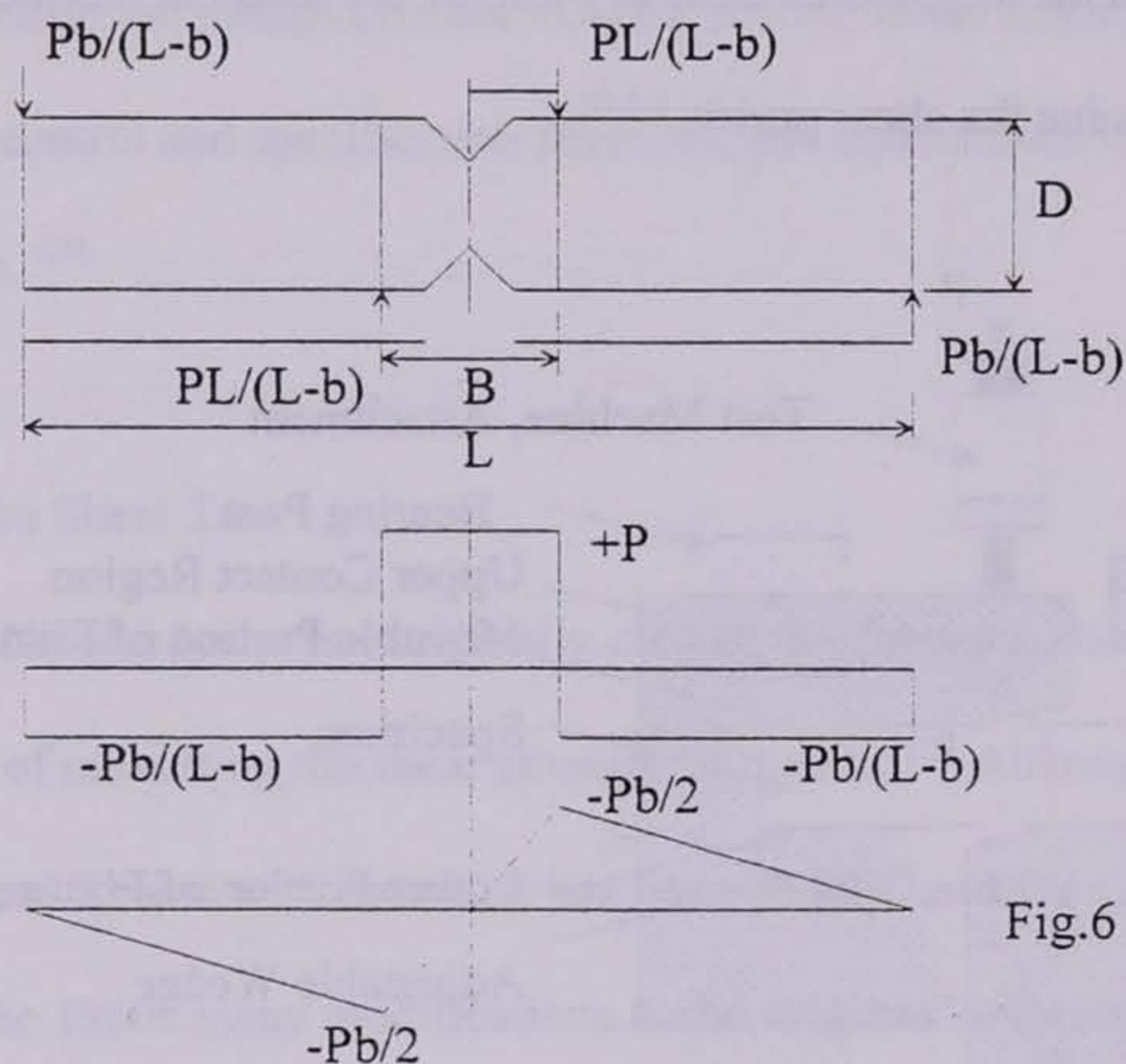
Fig.6 Theoretical Force, Shear and Moment diagram for a Test Specimen loaded in the V-Notched Test Fixture

Iosipescu's original intent of placing a notch in the specimen was three-fold: (1) To weaken the specimen in the desired failure section, (2) to not generate stress concentrations in the test section, and (3) to obtain a uniform shear stress in the test section. The specimen should fail at the location of zero moment in order to obtain a pure shear break. The cross sectional area is reduced by means of two symmetrically centered v-notches to insure failure at the desired zero moment location. To not generate stress concentrations in the test section, a 90° notch aligns the sides of the notches parallel to the normal stresses, thus in theory no stress concentrations will develop. A 90° notch forces the shear-stress distribution to be uniform as opposed to parabolic as in the case of an unnotched specimen. [15,23] However, Iosipescu originally designed this method for the use with metals and some of his ideas do not pertain to composite materials. It has been proven that the shear-stress distribution across the notches is not uniform, and there is a

significant shear stress concentration at the notch tip for composite materials. Correction

factors have been applied to relive some of the affects of the non-uniformity of the test.

[16,19] Much research has been done on improving notches for the Iosipescu test. These

improvements can be broken down into four parameters, notch angle, notch radius, notch

depth, and notch geometry.

Notch Parameters

Researchers have studied the effect of widening the notch angle. The standard

ASTM specification calls for a 90° notch. Adams and Walthrop modeled three specimens

with notch depths of 90°, 100° and 110°. They discovered that the shear stress at the

notch root is reduced as the notch angle increases although others have disagreed. [23]

Chiang concluded as the notch angle is widened from 90° to 120° that the uniformity

decreases. [24]

Tests have shown that introducing a small notch radius significantly reduces the

shear stresses concentrated at the root and the shear-stress distribution becomes more

uniform. Although it also has some adverse effects, increasing the radius tends to move

the failure away from the notch root and towards the nearest load point. [16,23,24] Adams

and Walthrop [23] concluded that a 1.27-mm radius is optimal.

Iosipescu concluded that the optimum notch depth was 20 to 25 percent of the

specimen thickness. Other researchers have resolved that the notch depth does not

significantly affect the results over a practical range of 20 to 30 percent, but a large notch

depth slightly decreases the uniformity of the shear stress distribution. [21,23,24]

The notch geometry can significantly affect the results. Two examples of changes in notch geometry are the flat bottom notch and the u-notch. Adams and Lewis [21] prevented premature cracking which caused sudden drop in the shear stress distribution by using a flat bottom notch. (Figure 7) V-notched specimens have a tendency to have sudden drops in shear stress due to premature cracking. Removing this material successfully eliminated the shear stress drops. Ho [16] conducted tests on a u-notched specimen to try to obtain a more uniform shear stress. (Figure 8) Ho received mixed results with the u-notched specimen. The 0° u-notched specimen exhibited a reduction in shear stress concentrations and a more uniform shear-stress near the notches and in the gage section. However, a [0/90] v-notched specimen shear-stress distribution was more uniform than the u-notched specimen. The 90° u-notched specimen shear stress was higher than the v-notched specimen. [16]
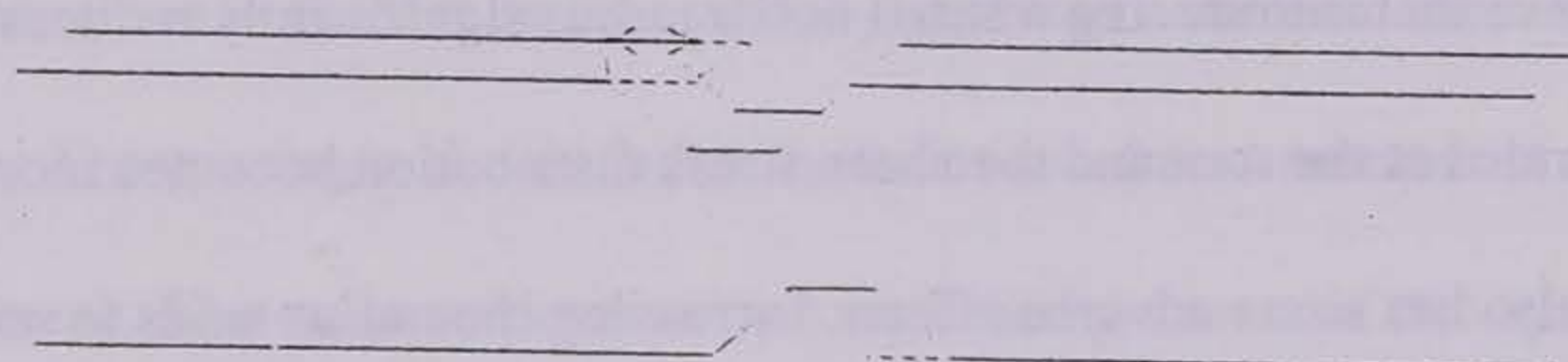
Fig. 7 Flat-Bottom Specimen [21]
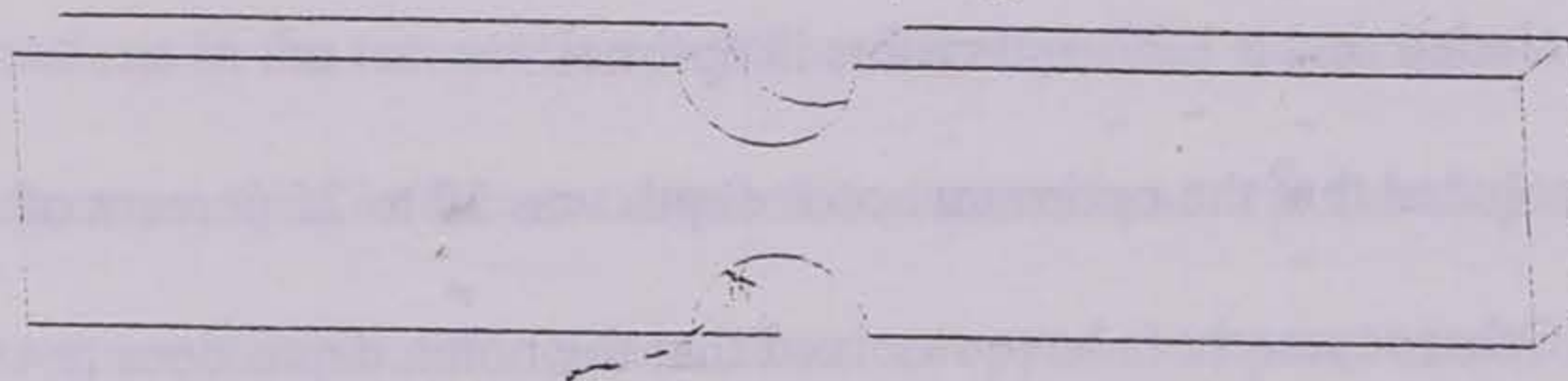
Fig. 8 U-notched Specimen [16]

The ultimate strength is calculated using eqn. 3 [20] and the shear modulus is calculated at each data point using eqn. 4. [20]

$$F_u = P_{max}/A \qquad \text{(eqn. 3)}$$

$$\tau_i = P_i/A \qquad \text{(eqn. 4)}$$

Where:
F_u = ultimate strength, Mpa (psi)
P_{max} = maximum load prior to failure, N (lbf)
τ_i = shear stress at the ith data point, Mpa (psi)
P_i = load at the ith data point, N (lbf) and
A = Cross-sectional area, mm^2 (in^2)

The shear-strain corresponding to the average shear-stress across the specimen is required to determine the shear modulus. Two strain gage rosettes determine the strain. One of the gages measures compression, ε_{+45} gage, while the other gage measures tension, ε_{-45} gage. The strain can be calculated by adding the absolute strain values of gage 1 and 2 at each data point, eqn. 5. [20]

$$\gamma_i = |\varepsilon_{+45}| + |\varepsilon_{-45}| \qquad \text{(eqn. 5)}$$

Where:
γ_i = shear strain at the ith data point, μ_ε
ε_{+45} = +45° normal strain at the ith data point, μ_ε and
ε_{-45} = -45° normal strain at the ith data point, μ_ε

The shear modulus is calculated by determining the average shear stress of τ_i and dividing by the shear strain, eqn. 6.

$$G_{xy} = \tau_{avg}/\gamma_{xy} \qquad \text{(eqn. 6)}$$

The Iosipescu shear method does have many advantages; the Isopescu test has the ability to test a wide range of thicknesses for unidirectional and multidirectional laminate specimens. They have the ability to test material properties in 1-2, 1-3, and 2-3 planes (Figure 9), capability to determine in-plane and traverse shear properties, potential to measure shear strength and shear modulus and a pure shear state for the 90° specimen exists. The Iosipescu shear method also has some disadvantages; if the specimen is in pure shear, the magnitude of ± 45° shear strains should be equal in magnitude and opposite in sign. Iosipescu tests conducted by Ho [16] concluded that the 0° specimens are not in pure shear, but 90° specimens are in a state of pure shear. Thus the validity of 0° specimens is questioned. Although Ho and others have concluded that accurate shear properties can be obtained without a state of pure shear for the Iosipescu 0° specimen. [16,18,21,25] Ho claimed that based on his test with graphite-epoxy laminates, "the proximity of the load point to the test section and the materials orthotropy greatly influence the individual gage readings, however, shear modulus determination is not significantly affected by the lack of pure shear."

Adams and Lewis [21] concurred with Ho's conclusion. They also resolved that the difference in the strain gage readings is caused by a rotation of the principle plane and not a strain-gage misalignment (Figure 10). Two strains ε_x and ε_y cause this rotation. The strain, ε_x, shifts the top of the Mohr's circle into a tensile-strain region and a strain, ε_x shifts the bottom of the Mohr's circle into a compressive strain region. This rotation of the Mohr's circle causes the +45° gage to be larger than the -45° gage. Because of this

rotation, the ± 45° strain gage measurements are not the principle strains. The normal

strains do not affect the shear strain because the +45° increases the same amount as the -

45° decreases relative to pure shear. Adams and Lewis stated that "even though a pure

shear state does not exist (in the gage section) the determination of the shear modulus is

not affected by the normal strain." They also concluded that the high ε_y in the test section

is attributed to a low-transverse stiffness and that the ε_x is caused either by a Poisson

effect or by a misalignment of the specimen. Other disadvantages include a small region

of pure shear, shear modulus test for the 0° and 90° specimen do not produce the same

results, and large variation in shear stress strain for 0° and 90° specimens occur. [21]
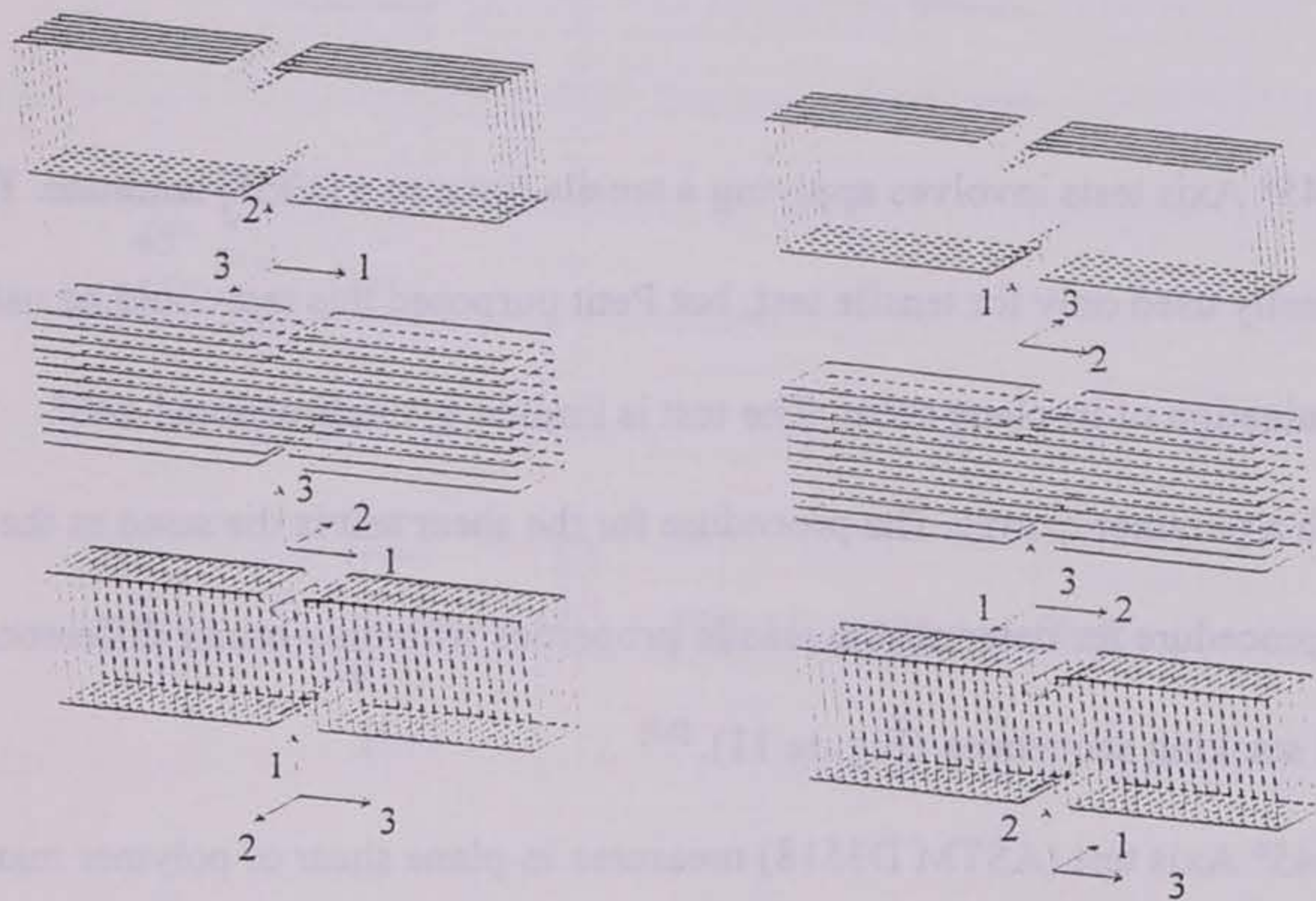
Fig. 9 3-D Orientation of Material

ε_{+45} ε_{-45}

$\varepsilon_x, -\gamma_{xy}$

ε

2θ
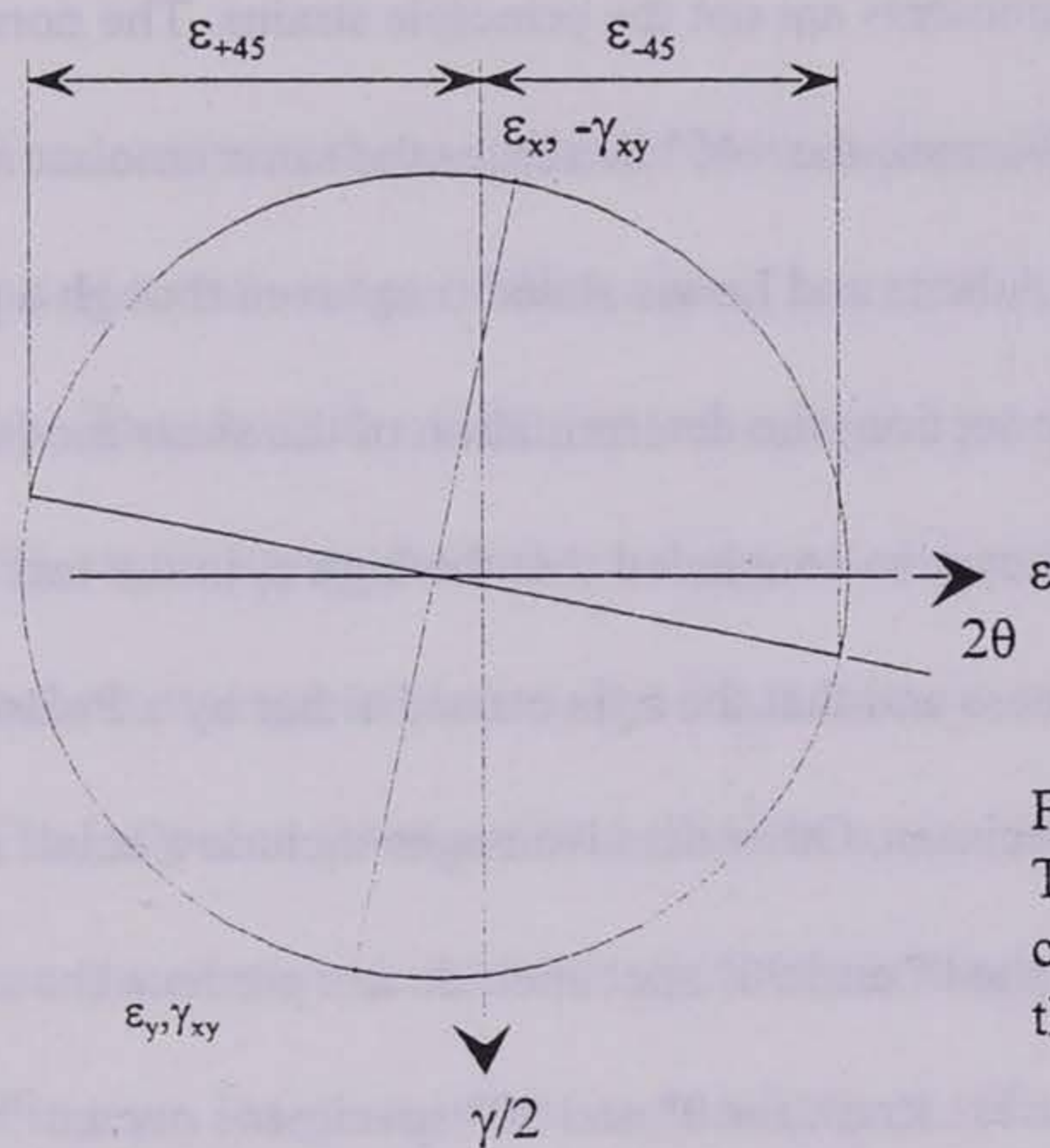
Fig. 10 Mohr's Circle
The shifting of circle
causes ε+45 to be large
than the ε-45. [21]

$\varepsilon_y, \gamma_{xy}$

$\gamma/2$

± 45° Axis Test

The ±45° Axis tests involves applying a tensile force to a [±45°] laminate. The

test was originally used only for tensile test, but Petit purposed this test could be used for

limited determination of in-plane shear. The test is limited to unidirectional ±45°

laminates with a polymer matrix. The procedure for the shear test is the same as the

ASTM 3039 procedure for determining tensile properties with only minor differences in

thickness and stacking sequences (Figure 11). [2,3]

The ±45° Axis test (ASTM D3518) measures in-plane shear of polymer matrix

composite. The fiber composite must have a thin, constant, rectangular shape. Its ends are

placed into grips and a controlled tension load is applied. To prevent premature failures,

end tabs are bonded to the specimen or attached by the pressure of the grip. The specimen

is monitored by normal strain gage in the longitudinal and transverse directions. It should

be loaded at a constant strain to induce failure within one to ten minutes. The maximum

in-plane shear can be calculated using laminate plate theory eqn. 7. [26,27]

$$\tau_{12}{}^m = P^m/(2A) \qquad \text{(eqn. 7)}$$

Where:

$\tau_{12}{}^m$ = Maximum in-plane shear stress, Mpa (psi)
P^m = Maximum load at or below 5 % shear strain, N (lbf) and
A = Cross-sectional area, mm² (in²)

The shear strain is calculated by eqn. 8

$$\gamma_{12} = \varepsilon_x - \varepsilon_y \qquad \text{(eqn. 8)}$$

Where:

γ_{12} = shear strain, μ_ε
ε_x, ε_y = axial and transverse strains respectively, μ_ε
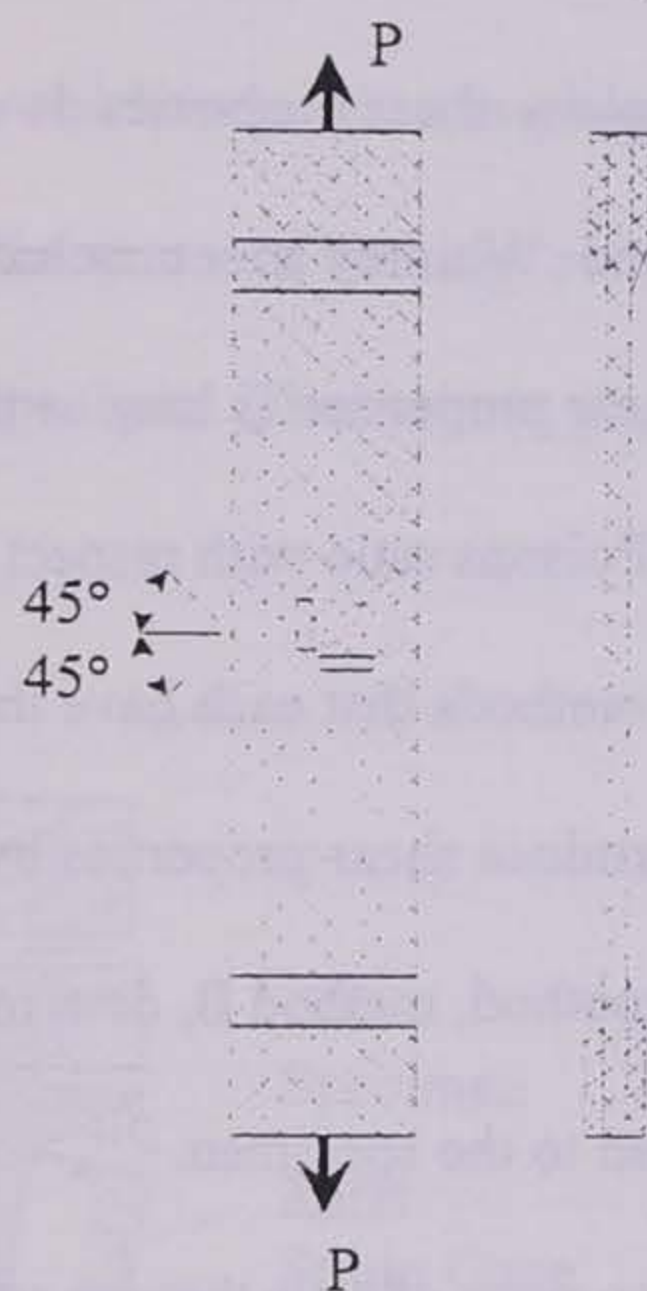
Fig. 11 ± 45° Axis Test

Pagano and Halipin studied the effects of end constraints. They determined that

the ends of the specimens tend to pull out from under the grips. They also determined that

the two, main problems associated with the end constraints are the rigid gripping and the

prevention of rotation. Pidera and Herakovich used a special fixture designed to

eliminate these end-constraint problems and only constrained the centerline of the specimen from rotation. They determined that the data was much better and more reproducible than the original fixture. [28]

The advantages of using this test include: simplicity of the test, uniform stress, and the shear stress is simply measured by two strain gages. The most significant disadvantages of the +/- 45° axis test are the limitations that the test imposes on the specimen, and the complex stress state in the specimen. [29,30]

Rail Test

The rail test (ASTM D4255) determines in-plane shear properties. It was first used to determine in-plane shear by Henessey in 1965. Whintey later concluded that the rail test was a valid test for determining in-plane shear properties as long as the length to width ratio, L/W, was greater than ten and that the Poisons ratio with respect to the edge was less than one. [5] The rail test has two different methods that each have their own separate fixtures. The first method, method A, determines shear-properties by applying an edgewise shear-load on the specimen. The second method, method B, determines shear properties by applying a tension or compression load to the specimen. [31]

The rail test method A fixture consists of two pairs of rails that are attached to the test specimen by bolts (Figure 12). The specimen's long sides are clamped between the two rails. (ASTM D4255) A tensile force is applied to the rails in opposing directions, which cause a relative displacement of the rails parallel to each other. This relative displacement causes an in-plane shear load on the specimen. A strain gage is mounted on

the center of the specimen at a 45° to the longitudinal axis that is used to determine the

shear modulus. [31] A 0° strain gage may also be used to determine the purity of the shear.
[32]

     The rail test method B fixture consists of three pairs of rails that are attached to

the specimen by bolts (Figure 13). The outer rails are attached to the test machine at the

top and bottom, while the middle rail slides through the top of the base fixture. The

specimen is centered into the rail shear fixture and clamped securely on opposing edges.

Method B can be loaded in either tension or compression. If a tension load is desired

then the base fixture must be attached to the test machine. The load is applied to the

middle rail, which induces an in-plane shear on the specimen. Two strain gages are

attached to the center of both test sections and orientated at a 45° angle to the longitudinal

axis of the specimen. These strain gages measure the shear modulus. [3,31]
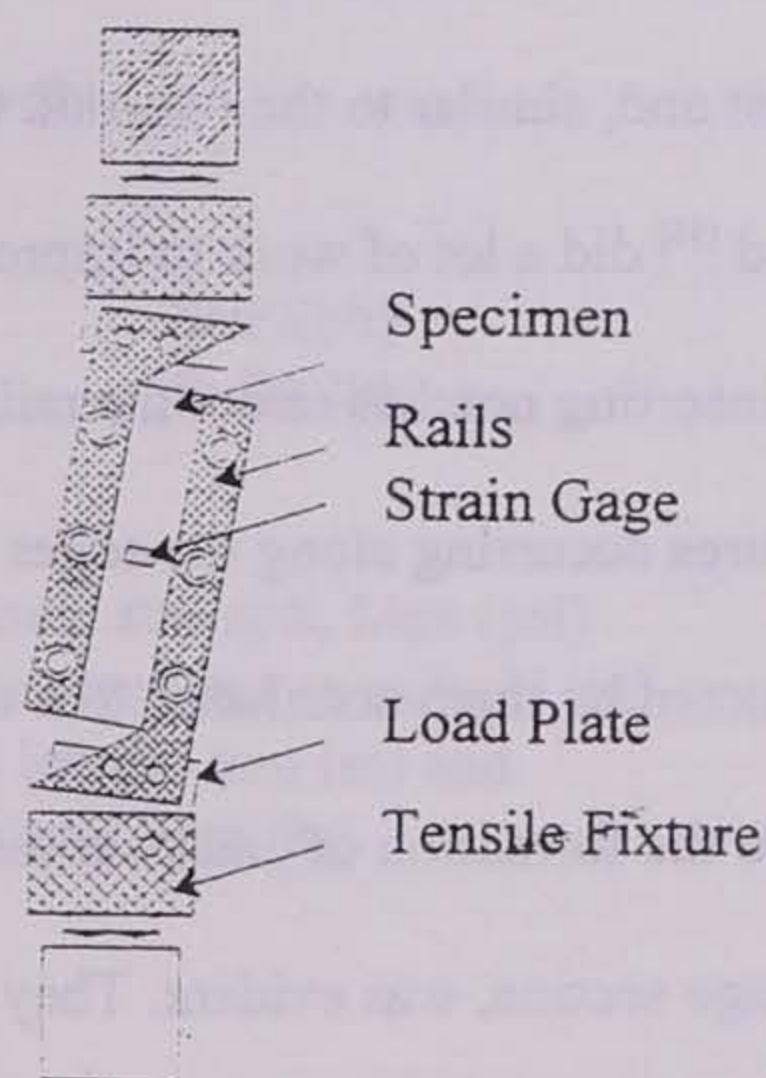
Fig. 12 Two-Rail Test Fixture [31]   Fig. 13 Three-Rail Test Fixture [31]
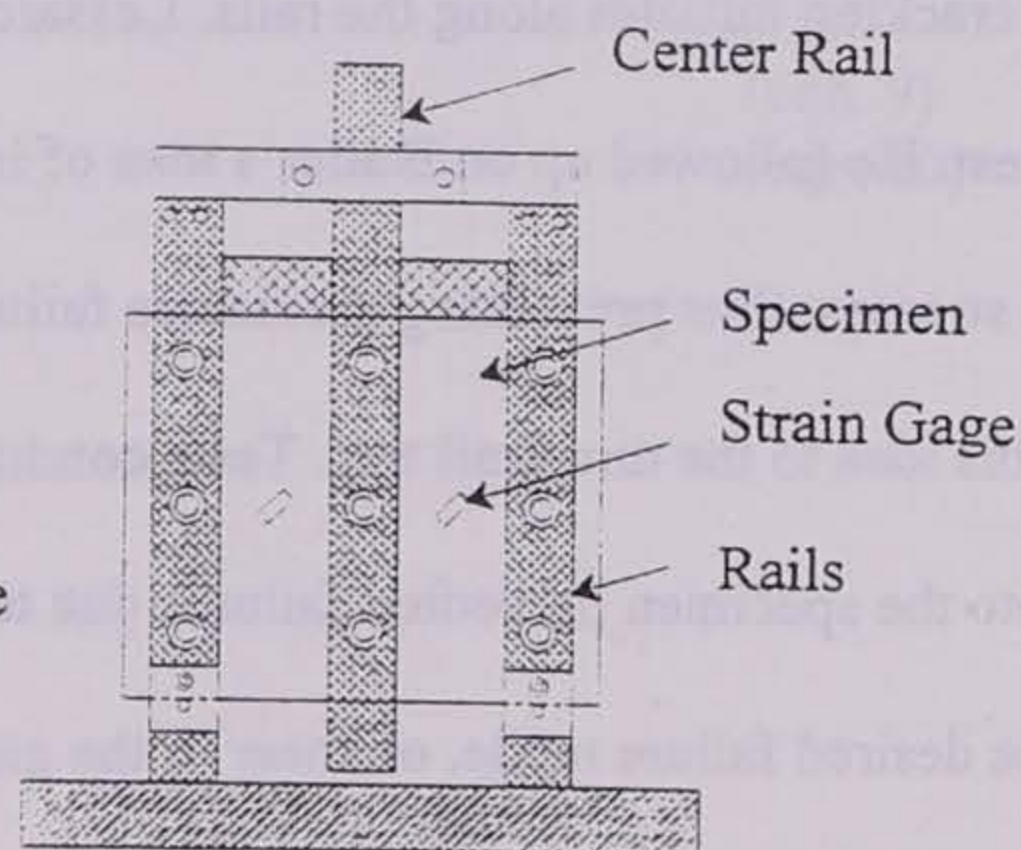
The two-rail test is frequently used because it is simple and inexpensive. It also has the advantages that a state of pure shear exists away from free edges and at high room temperatures it has the ability to determine reliable shear properties. The two-rail test also has many disadvantages; the free edges cause stresses to differ from pure shear which initiate premature cracking and failures at the rail edges. This premature cracking tends to give falsely low shear properties. Also, the steel rails induce large, combined shear near the specimen corners, uniform shear stress near the free-ends can only be obtained when the aspect ratio is large (aspect ratio > 10), narrow gage section violates St. Vernant's principle, and the two-rail test is prone to twisting. [32,33]

Many researchers prefer the three-rail test to the two-rail test because it is not prone to twisting. It also has the advantages over the two-rail test due to its elimination of edge effects, and a large uniform region of pure shear is created away from the free edges. The three-rail test does have some disadvantages; it requires a large specimen, it is more complex and difficult to install than the two-rail test and, similar to the two-rail, test premature cracking initiates along the rails. Lessard [33] did a lot of work to improve the three-rail test. He followed up on Butler's idea of inserting notches under the rails to reduce the stresses, thus preventing premature failures occurring along the edges by applying this idea to the three-rail test. Tests conducted by them concluded that the notch inserted into the specimen prevented failures due to the formation of cracks at the rails. Instead, the desired failure mode, of shear in the gage section, was evident. They also modified the three-rail test fixture and eventually came up with an entirely new fixture. The primary difference of the new fixture is that the middle rail is guided at the top and

bottom of the fixture to eliminate out-of-plane bending. It is also built much sturdier than

the original fixture with strengthened connections, a solid block and pin at the bottom

connection, reinforced top joint, and oilite bronze lining on the contact surfaces. [33]

The new fixture alleviated many weaknesses of the ASTM D4255 three-rail

fixture. Vast improvements in the shear properties were obtained with the new fixture and

the notched specimen was comparable to the original fixture without notches. A test

conducted with the new fixture and the notched specimen showed a 40% increase in shear

strength. The results were also very consistent, allowing for repetition and low scattering

of test. The new fixture does have some disadvantages: it requires a large specimen, the

fixture is new and not satisfactorily tested, the fixture is complex and hard to install

though less so than the original three-rail test fixture. Also, test data may not be valid for

unidirectional composites. The tests were conducted on multidirectional laminates [0/90],

no tests were conducted on unidirectional laminates. [33]

The shear strength of the two-rail and three-rail test is calculated with eqn. 9 and eqn. 10

respectively.

$$S=P/(bh) \qquad \text{(eqn. 9)}$$
$$S=P/(2bh) \qquad \text{(eqn. 10)}$$

Where:
S = ultimate strength, Mpa (psi)
P = maximum load on rails, N (in)
b = total length, mm (in) and
h = thickness, mm (in)

Off-Axis Test

The off-axis test developed by Chamis and Sinclair is not an ASTM standard but can be useful in determining both in-plane shear properties. It is a unidirectional, tensile test with the fibers oriented at a specified alignment from the loading direction. An off-axis test induces three stresses on a specimen: in-plane shear stress, transverse stress, and longitudinal stress. Chamis concluded that, at failure, the in-plane shear stress is the only critical stress, thus making it a valid in-plane shear test. [2,3,34]

The ASTM 3039 test procedure is used as a guide. The specimen is tested by applying a tensile load to a specimen with the fibers orientated 10° from the loading direction. The 10° angle is used to minimize the effect of the longitudinal and transverse stresses. Its ends are placed into grips and a controlled tension load is applied. To prevent premature failures the specimens are reinforced with end tabs. The end tabs are bonded to the specimen or connected by pressure of the grip. The specimen is monitored by normal strain gage in the longitudinal and transverse directions. It is loaded at a constant strain to induce failure within one to ten minutes. The in-plane shear stress is at its maximum at approximately 10° load orientation. The fibers should be aligned as close to 10° as possible, but tests have shown the fracture shear-strain is insensitive to small errors in the angle, i.e. ± 1°. [34] (Figure 14)
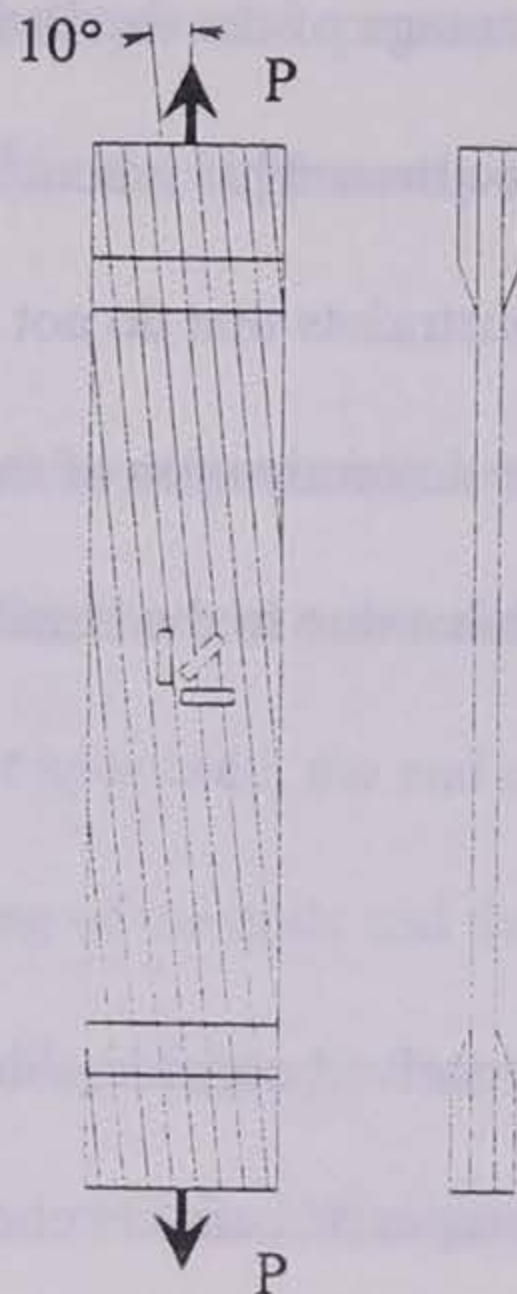
10° P

Fig. 14 Off-Axis test

P

The shear and strain are determined by resolving the applied stress and strain to the

coordinate system aligned with the fibers using eqn. 11 and eqn. 12. respectively. [3]

$$\tau_{12} = 1/2 \, \sigma_{xx} (\sin 2\theta) \qquad \text{(eqn. 11)}$$

Where:

τ_{12} = Shear stress
P = Maximum load prior to failure, N (lbf)
A = Cross sectional area, mm^2 (in^2)
θ = Orientation of the fibers with respect to the loading direction, radians (degrees)

if $\theta = 10°$ then eqn. 11 becomes $\tau_{12} = .171\sigma_{xx}$

$$\gamma_{12} = .5977\varepsilon_{g1} + 1.0794\varepsilon_{g2} - 1.2817\varepsilon_{g3} \qquad \text{(eqn. 12)}$$

Where:

γ_{12} = shear strain, μ_ε
$\varepsilon_{g1}, \varepsilon_{g2}, \varepsilon_{g3}$ = normal strains for gage 1,2,3 respectively, μ_ε

The off-axis test has the advantages that it is inexpensive, easy to set up, easy to

fabricate specimens, and simple to reduce data. The disadvantages of the test far outweigh

the advantages. The biggest disadvantage of the test is that a highly inhomogeneous state of deformation is induced in the specimen. This inhomogeneous state of deformation is caused by the rigid gripping end constraints that do not allow for rotation. These end-constraint effects influence accurate determination of the shear strength. The off-axis test tends to give low strength and modulus due to the tensile shear coupling. [34]

Dowel Bar Testing

Fiber-composite bars have received considerable attention recently in the reinforcement in concrete. Fiber-composite bars are composed of very fine glass fiber strands and are bonded by a thermosetting matrix. The fiber-composite bars consists of 55% E-glass and 45% thermosetting resin. The tensile strength of the fiber-composite bars are very high with some in excess of 100 ksi, but the shear strength in these bars is not as good. The shear strength of these bars needs to be accurately measured to make full use of these bars.

The short-beam shear test method is well suited for testing of fiber composite dowel bars. No revisions of the test methods would need to be made to accommodate the cylindrical shape of the dowel bars. The same test apparatus used for the plastic rods could be used to test the dowel bars (Figure 3 p.6). Although this test is simple and would work well with dowel bars, its numerous disadvantages make it an undesirable test for the determination of design criteria and is not recommended for shear testing to determine design criteria of dowel bars.

The rail test, especially using the modified rail test fixture, has many advantages, which make it a promising method for the determination of shear properties. However, in

both the two-rail and three-rail methods, the specimen can not be easily modified to test cylindrical shaped dowel bars. This test is generally suited to test flat rectangular shaped materials.

The ± 45 axis test is, in many respects is a lot like the 10° off-axis test. To fit the cylindrical-shape of the dowel bars, the end constraints would need to be modified. To ensure a uniform stress in the test specimen, the end constraints would need to be designed to prevent rigid clamping of the ends and the specimen would need to be prevented from rotating. The loading of the specimen at the specified orientation would also cause a problem. This method calls for the alignment of the material in the direction of the load and with the fibers orientated in the specified direction. Although composite dowel bar fibers are in the longitudinal direction, the specimens would need to be tilted to the proper orientation. This method has the potential to be an effective method for measuring the shear properties of fiber composite dowel bars, but the modifications to the testing procedures would require a great deal of experimental testing.

The Iosipescu test is generally used with flat, rectangular-shaped fiber composites. The test specimen would need to be modified to work with the Iosipescu test apparatus. A radial v-notch cut circumferentally at the center of the specimen would work well with the Iosipescu method. The v-notch would weaken the specimen and ensure a failure in the desired zero moment location. The circumferentally cut v-notch would also be a relatively easy cut to make. Due to the attractive features of the Iosipescu test, the relatively simple procedure, and the simple modifications that would need to be changed

to accompany the cylindrical shape of the dowel bars, this test would be the best to use

for evaluating the shear strength of fiber composite dowel bars.

Finite Element Analysis of Iosipescu Dowel Bar Specimen

A finite element analysis was performed using ANSYS 5.3 to determine the

uniformity of a fiber composite dowel bar subjected to an Iosipescu test in the modified

Wyoming test fixture. The fiber composite dowel bar was divided into several smaller

elements, with each element containing eight nodes. An eight-noded brick element, solid

45, was used to model the test specimen. Solid 45 is a three-dimensional brick element.

Eight nodes and the orthotropic material properties define the element. Solid 45 has three

degrees of freedom at each node, translation in the x, y, and z directions.

Two models of the fiber-composite dowel bars were hand generated. First a

course model of the entire fiber-composite dowel bar was created. Next, a submodel of

the test section was generated with a more dense mesh. The course model consisted of a

specimen with a length of three inches and a one-inch diameter. The notch was circularly

inscribed in the specimen at 90° with a depth of 20% of the specimen diameter (Figure

16). The entire specimen was modeled due to asymmetry of the loading (Figure 15). The

constraints were modeled anti-symmetrically with the left side of the specimen, the

stationary portion of the fixture was restrained against vertical motion and the right side,

the movable portion of the test fixture, was given a downward lateral deflection of 1/20 of

an inch. The specimen was restrained against horizontal motion at the upper right corner.

The course model contained 868 nodes and 630 elements. The course model was

generated using a layering pattern across the entire specimen. The model consisted of 30
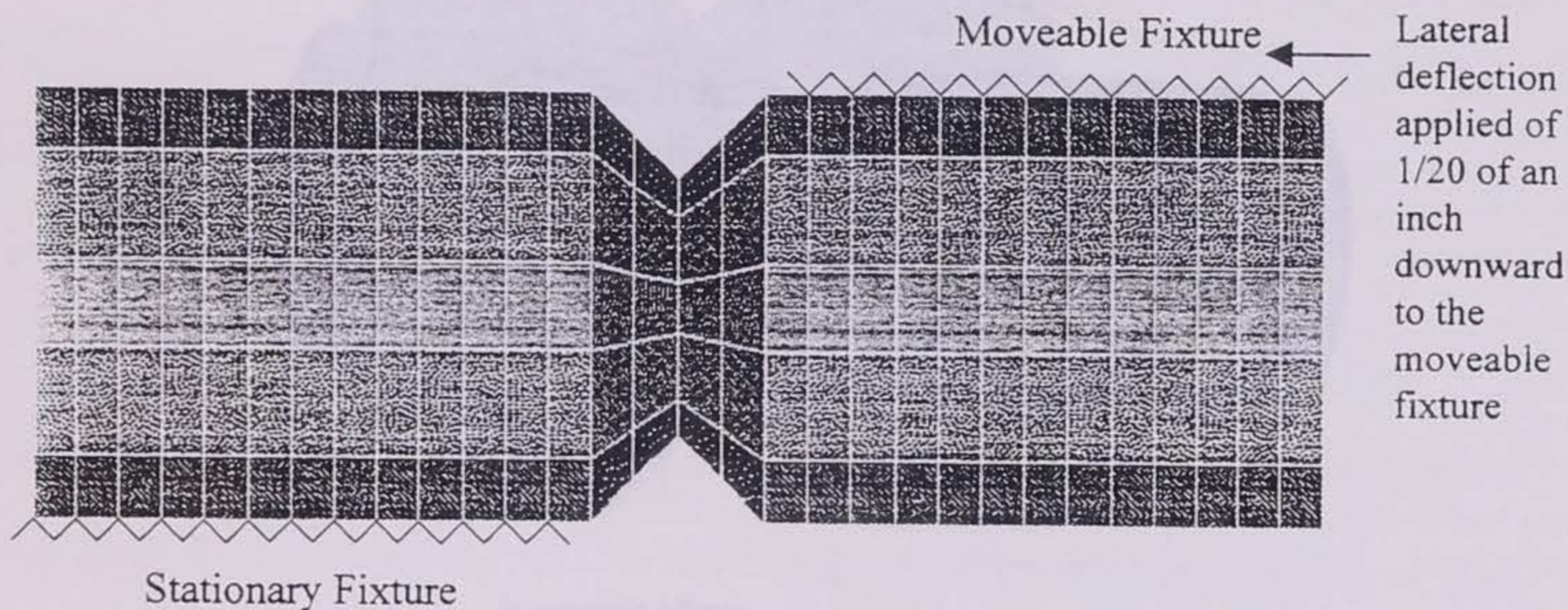
layers, 1/10 of an inch thick with 28 nodes in each layer.


Fig. 15 End Constraints of Course Model

The notch is of primary interest in the model. To provide a better model of the

notch region, a submodel was created. The model was one inch in length, contained 2929

nodes and 2352 elements. The notch and 0.3 inches on each side of the notch were

modeled to include the end constraints in the submodel (Figure 17). The submodel was

layered with 101 nodes in each layer. The notch was modeled densely, with layers 1/40 of

inch thick. The rest of the submodel contained layers with a thickness of 1/20 of an inch.
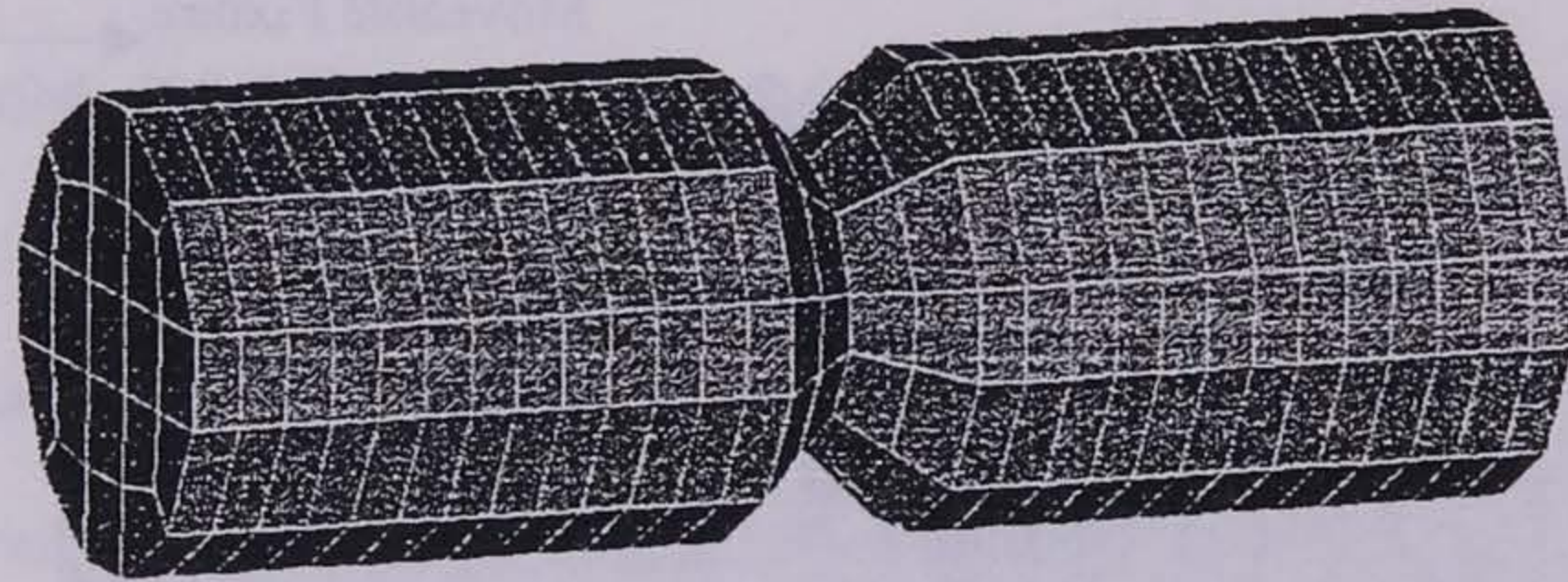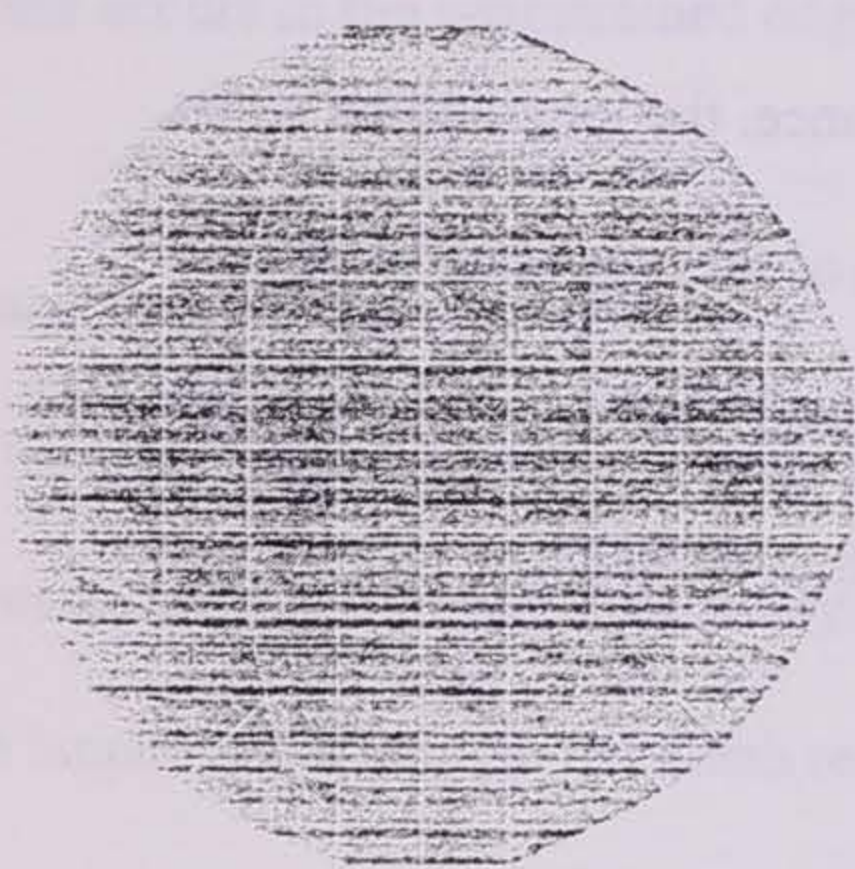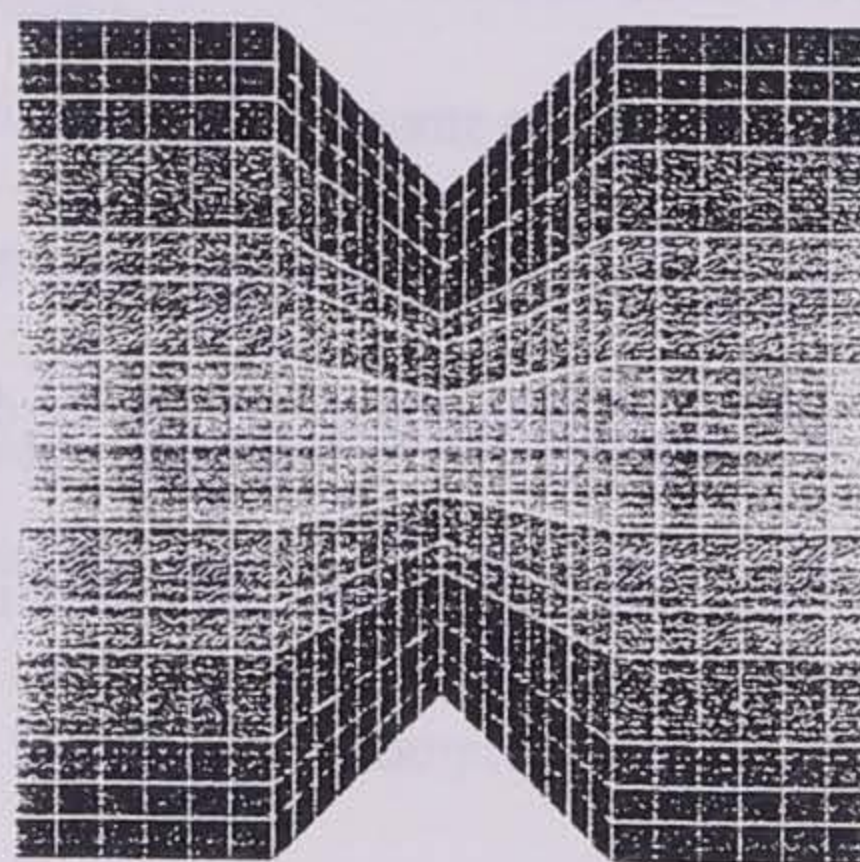
Isometric View
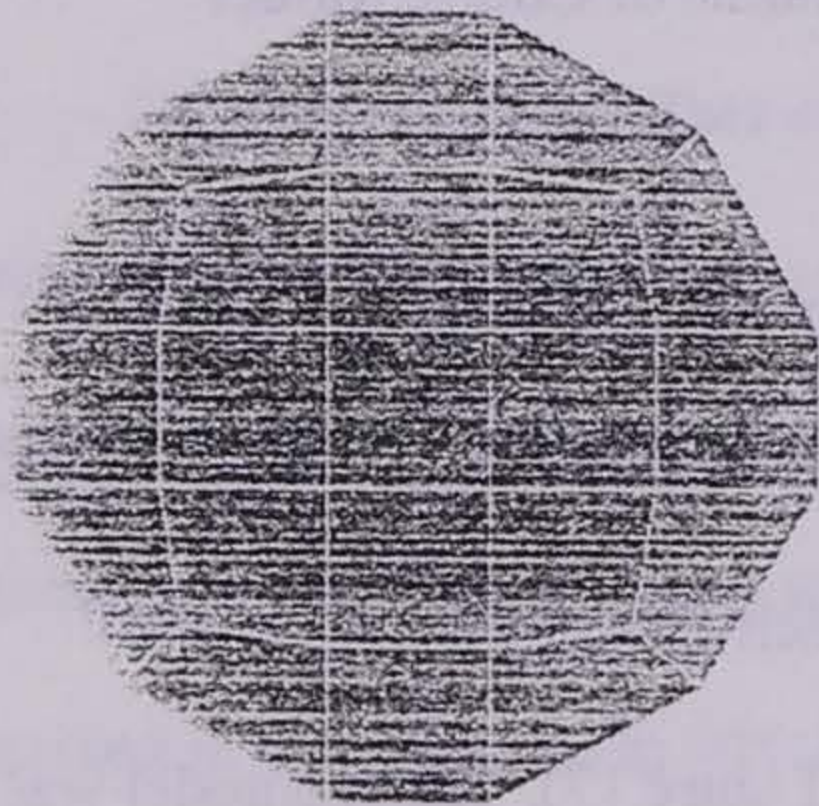
Side View
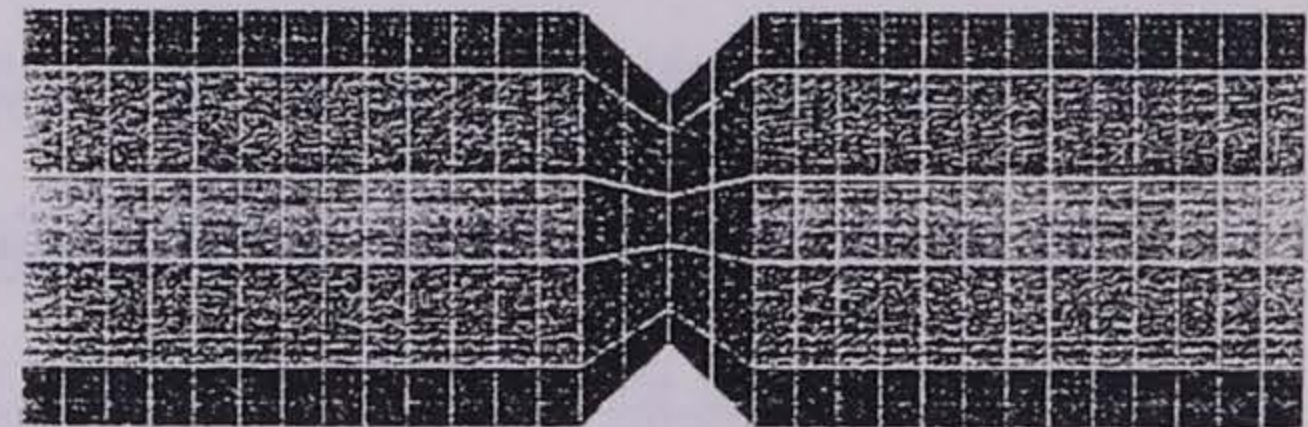
Front View

Fig. 16 Course Finite Element Model
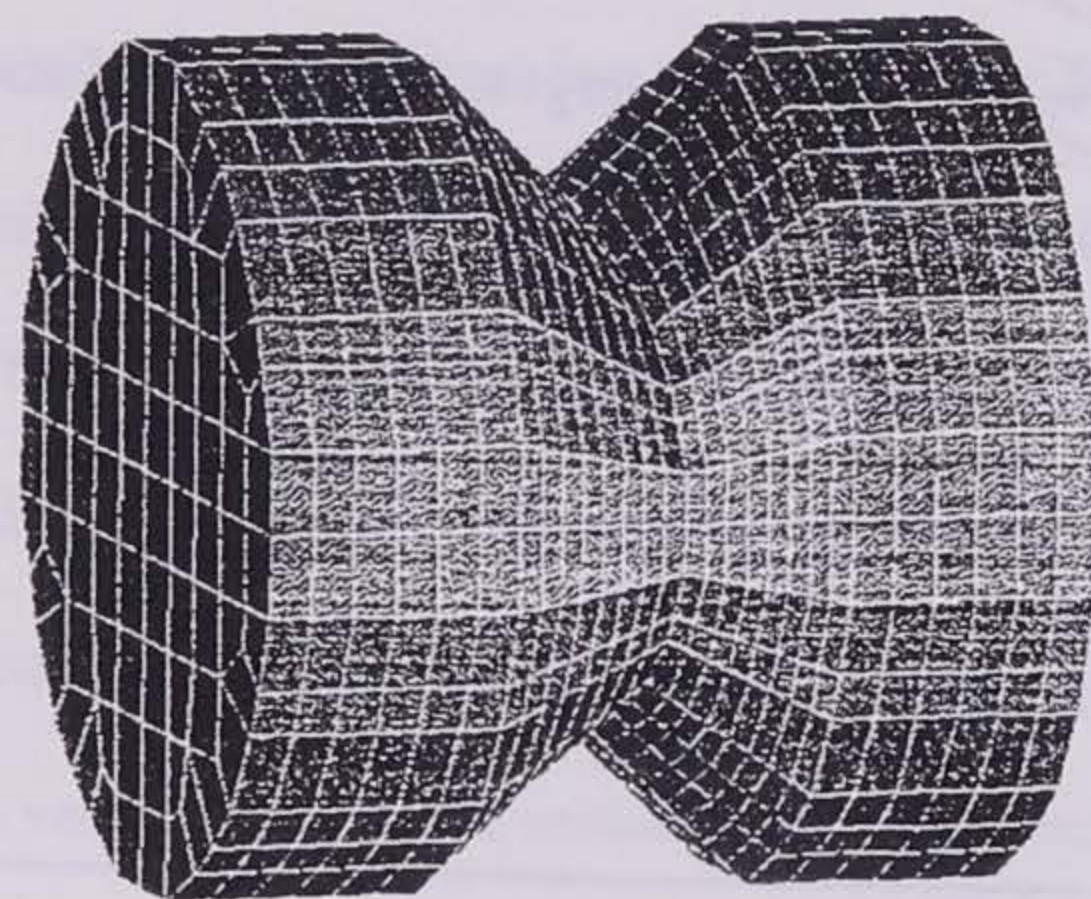
Isometric View

Side View   Front View

Fig. 17 Submodel of the Notch Region

The nodes were placed to create as many rectangles as possible with only slightly

irregular shapes near the surface of the dowel bar. No triangular shapes were used to

create the course and sub meshes. The largest and smallest elements in the course model

were .40 x10^{-3} in^4 and .23 x 10^{-3} in^4 respectively. The largest and smallest elements in the

submodel were 6.45 x 10^{-4} in^4 and 9.40 x 10^{-5} in^4 respectively. The isotropic materials

used are listed in table 2.

Table 2   Material properties for fiber composite dowel bar [35]

Ex	Ey	Ez	Gxy
6.2 x 10^6 psi	1.55 x 10^6 psi	1.55 x 10^6 psi	.476 x 10^6 psi

Due to the three-dimensional model, the average stresses across the thickness (z-

axis) were calculated. Three stresses are of significant importance, the longitudinal stress,

the transverse stress, and the shear stress. Two graphs of each of these stresses were

plotted, stress vs. length (x-axis) and stress vs. depth (y-axis) and a hand-generated stress

contour plot was constructed using the result output generated by ANSYS.

Longitudinal Stress

The average longitudinal stress plotted along the length of the specimen (Figure

18) shows that a minimal stress concentration is generated in the notch region. But a

significant stress occurs at the location of the two end constraints closest to the notch. A

maximum longitudinal stress in the notch region is 17,219 psi in compression and 13,035

psi in tension. The longitudinal stresses that occurred at the closest end constraints are

approximately 90,418 psi in compression, which is about 5.25 times the maximum stress in the notch region.

Figure 19 is a plot of the average stress along the depth of the dowel bar in the notch region. This graph shows that there is a uniform longitudinal stress along the center length of the specimen and that the uniformity decreases towards the top and bottom of the specimen. The stress also tends to be more irregular towards the top and bottom with areas of concentrated higher and lower stresses across the entire notch.

The average longitudinal stress contour plot (Figure 20) reiterates that the longitudinal stress is very uniform in the midsection of the specimen and that very large stress concentrations occur at the end constraints nearest the notch. This graph also shows that the stresses are asymmetrical about the notch axis and that the maximum tension stress occurs in the unrestrained edges of the specimen.

Transverse Stress

The largest transverse stress occurs at the end constraint closest to the notch. The stresses are much higher than at any other location in the specimen. Figure 21 shows that the largest stress seen in the notch region is about 14,183 psi in compression and 10,816 psi in tension. Which, in comparison to the to 115,780 psi stress at the end constraint, is quite small and is only 12.25% of the stress at the end constraint.

Figure 22 shows that the transverse stresses in the midsection are very uniform. It also shows that the stresses along the notch axis are very uniform with the maximum and minimum stresses having s difference of only 2776 psi. However, a large stress concentration occurs 0.025 inches to the left and right of the notch axis and the stresses

are much less uniform with the maximum and minimum having a difference of 24,999 psi. Moving further from the notch axis, the stresses tend to become more uniform.

The transverse stress contour plot (Figure 23) shows that the major stress occurs near the end constraints and they effect approximately 1/3 of the depth of the specimen from the end constraint. Outside the area of the two end constraints nearest the notch, the stresses in the specimen are uniform, and the stresses are asymmetrical along the notch axis.

Shear Stress

The stress vs. length graph (Figure 24) shows that the shear stress maximum does not occur at the two closest end constraints to the notch, but a short distance from the end constraint towards the notch. The maximum shear stress at this location is 30,817 psi. The notch region shear stresses are not as uniform as the other longitudinal and transverse stresses, especially along the notch axis. The maximum stress in the notch region is 19,435 in compression, (located at the notch tip) and 7085.9 in tension. The notch has a stress of about 63% of the stress in between the end constraint and the notch.

Figure 25 shows that the center region, 0.1 inches up from the center to about 0.2 inches downward from the center, has fairly uniform stresses, but the stress uniformity decreases toward the top and bottom of the specimen.

The shear stress contour plot (Figure 26) shows that the stress concentrations occur near the end constraints or in the notch region. The rest of the specimen has a fairly uniform stress and the stresses are asymmetrical along the notch axis.

Conclusion

The applicable shear test methods for testing fiber composite dowel bars are the short-beam shear test and the Iosipescu shear test. The Iosipescu shear test has many advantages over the short-beam shear test, making it the best option for testing of dowel bars. The finite element results show that the stress concentrations induced by the notch are minimal. The largest stress concentrations occur at the closest end constraints to the notch. If the end constraints are moved further from the notch, this may improve the reliability that the shear break will occur at the desired notch location.
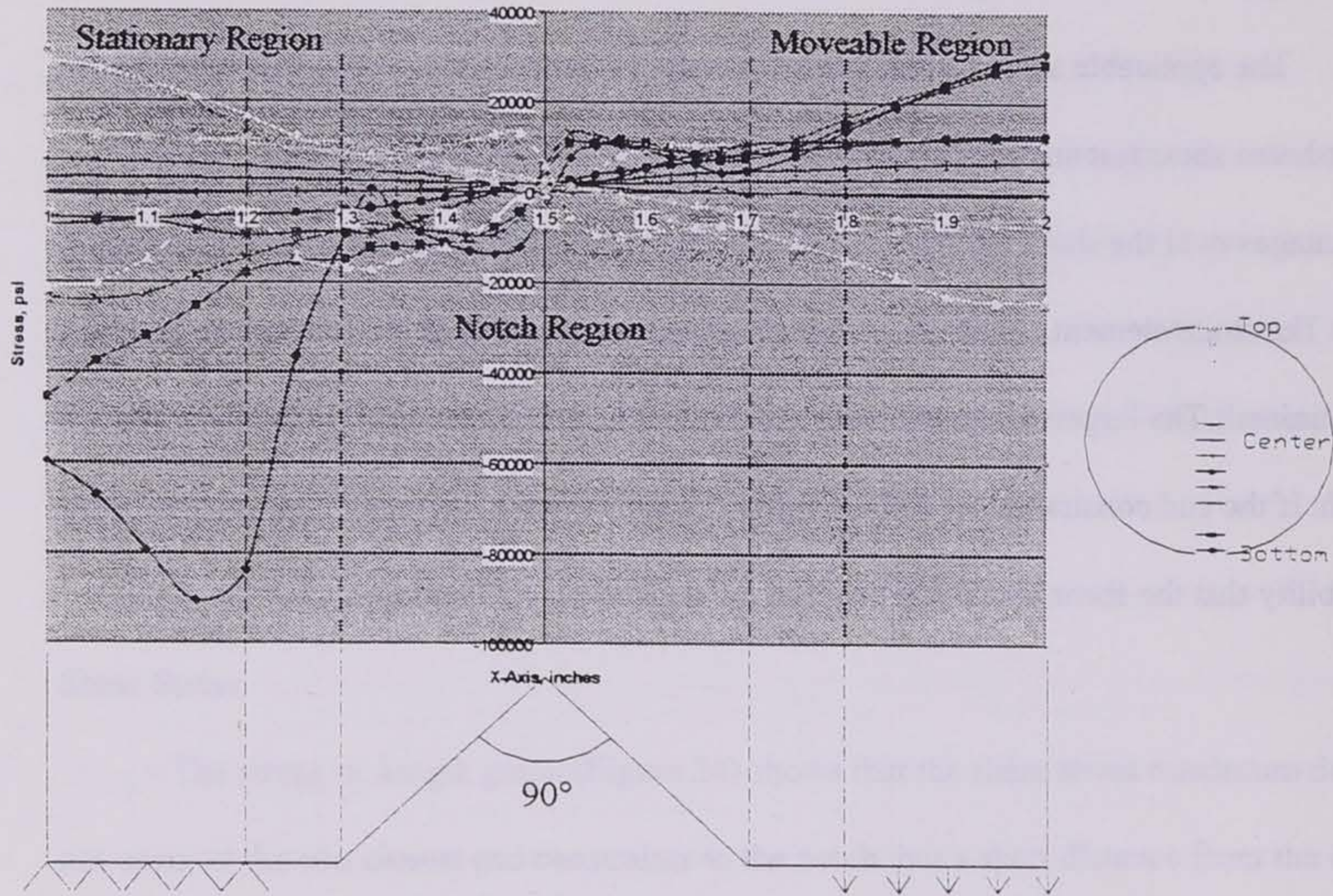
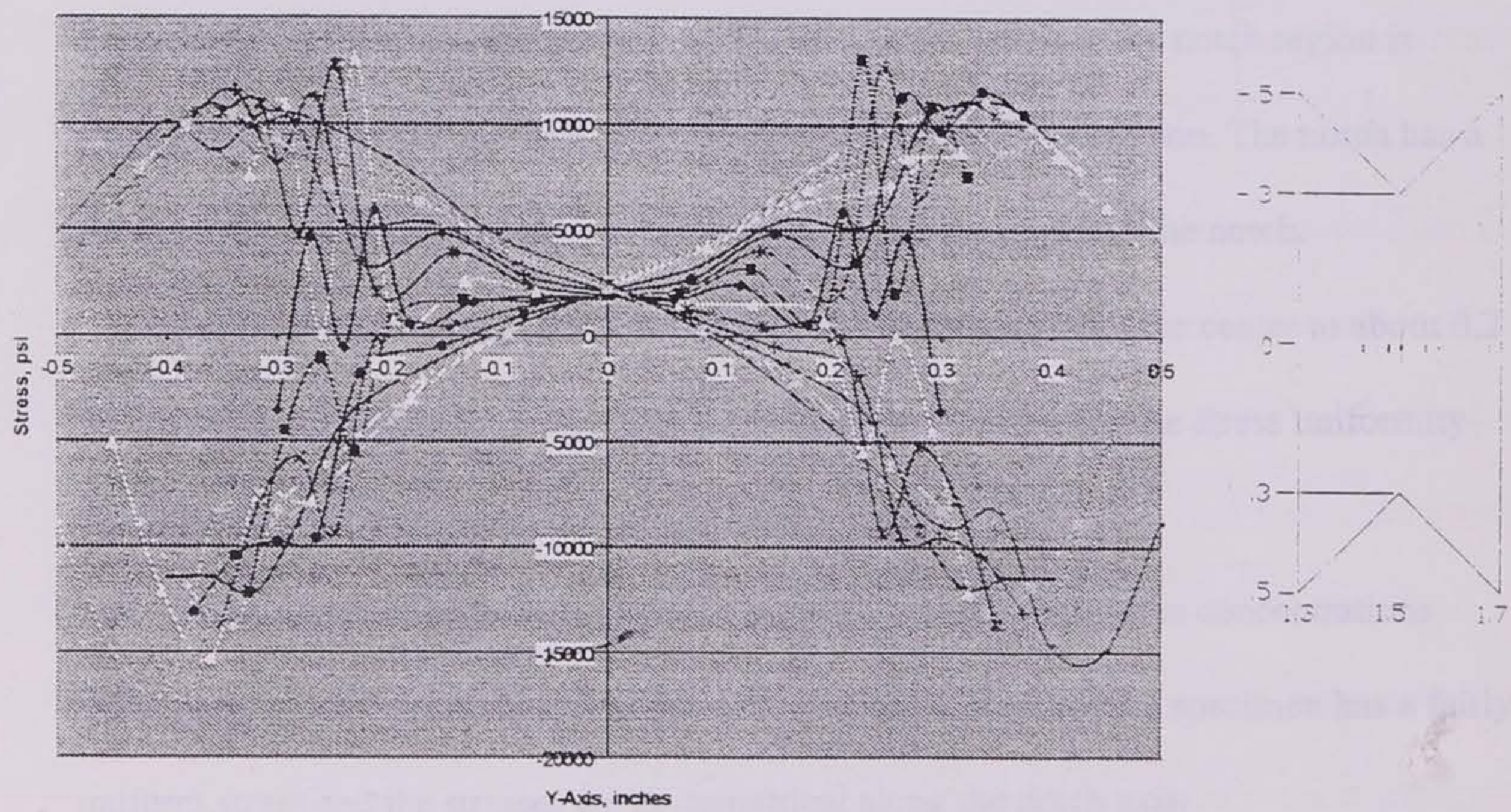Fig. 18 Average Longitudinal Stress plotted along the Dowel Bar Length, σ_x

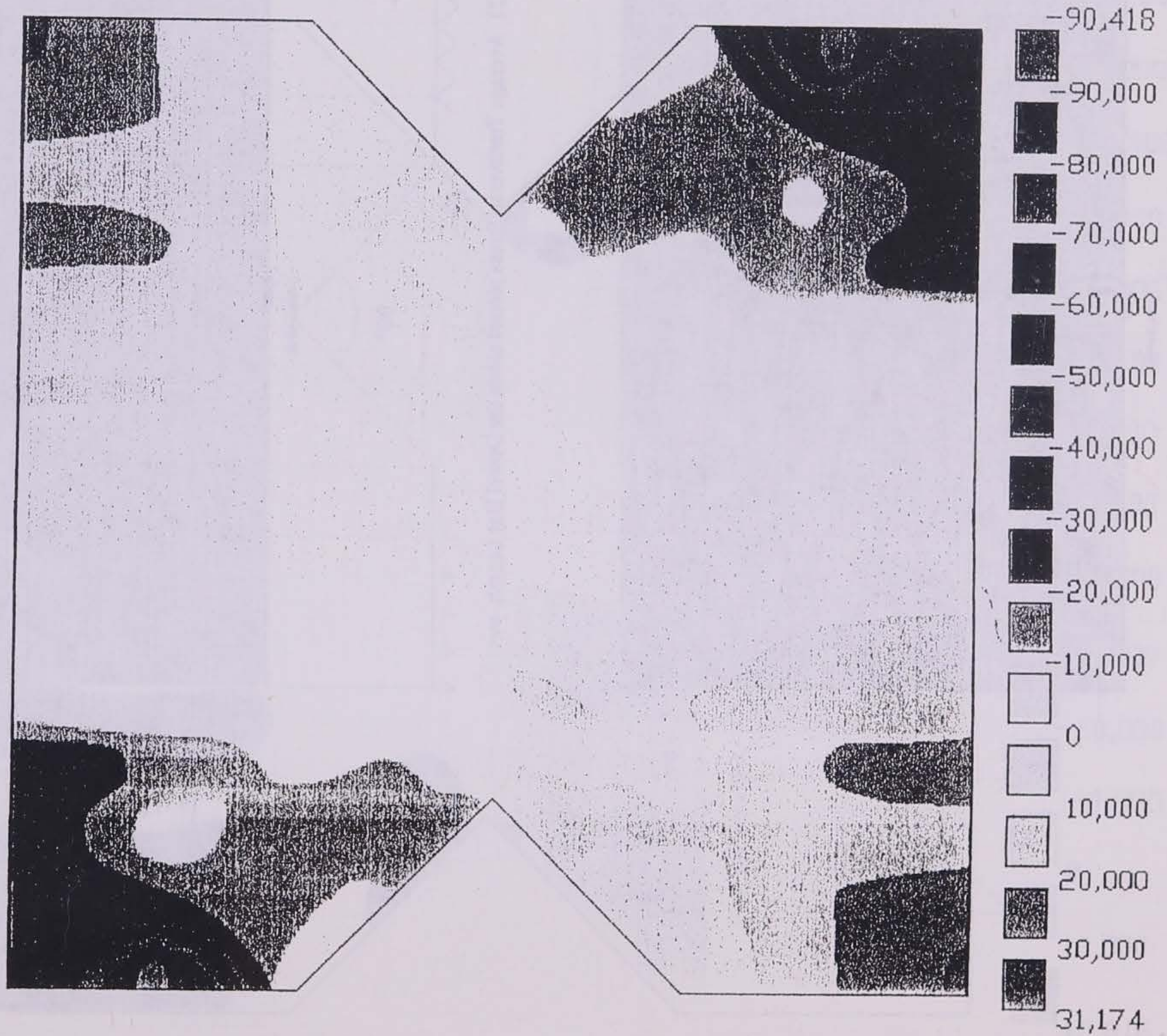Fig. 19 Average Longitudinal Stress plotted along the Depth of the Dowel Bar, σ_x

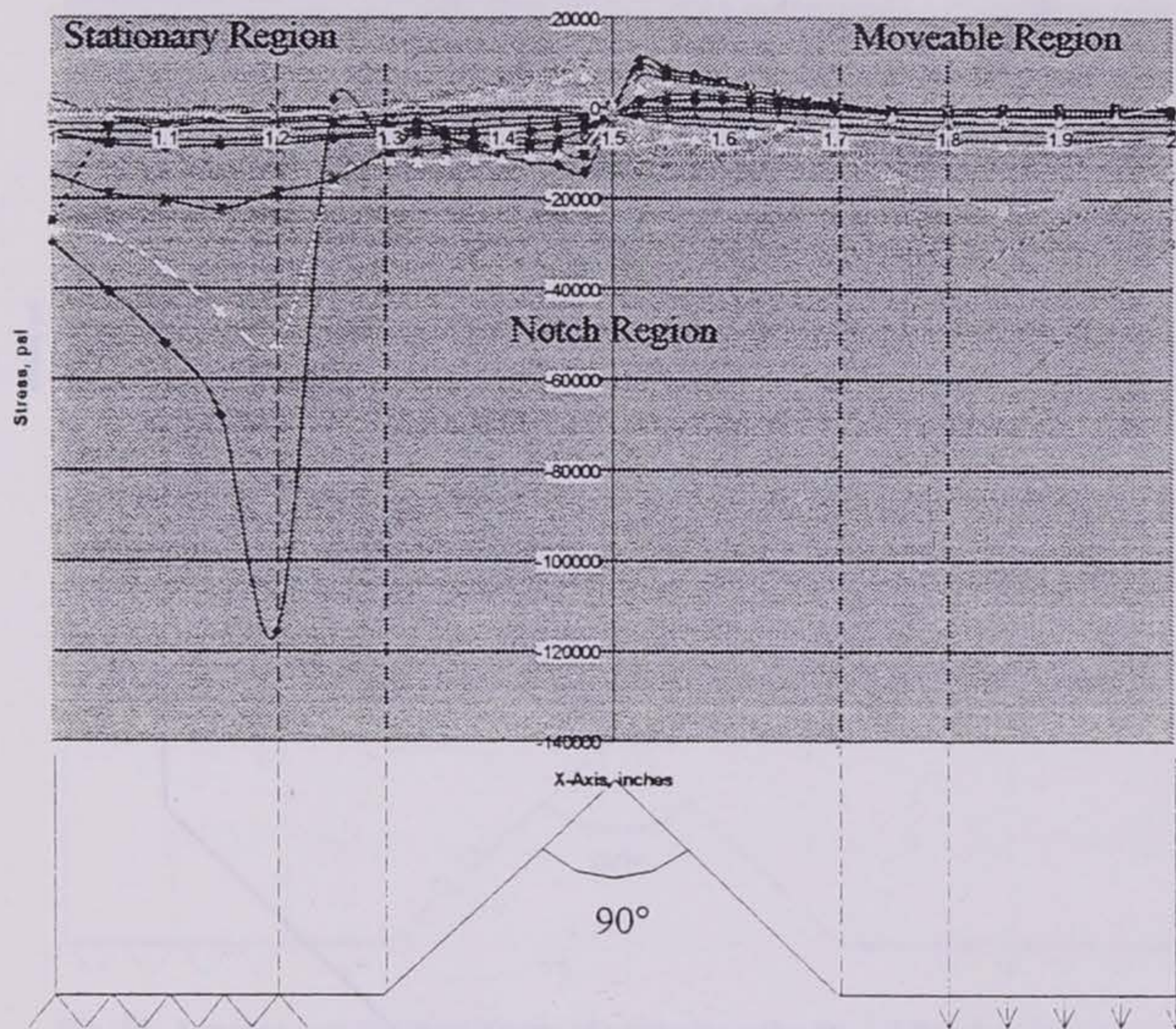|	
	-90,418
	-90,000
	-80,000
	-70,000
	-60,000
	-50,000
	-40,000
	-30,000
	-20,000
	-10,000
	0
	10,000
	20,000
	30,000
	31,174

Fig. 20 Average Longitudinal Stress, σ_x

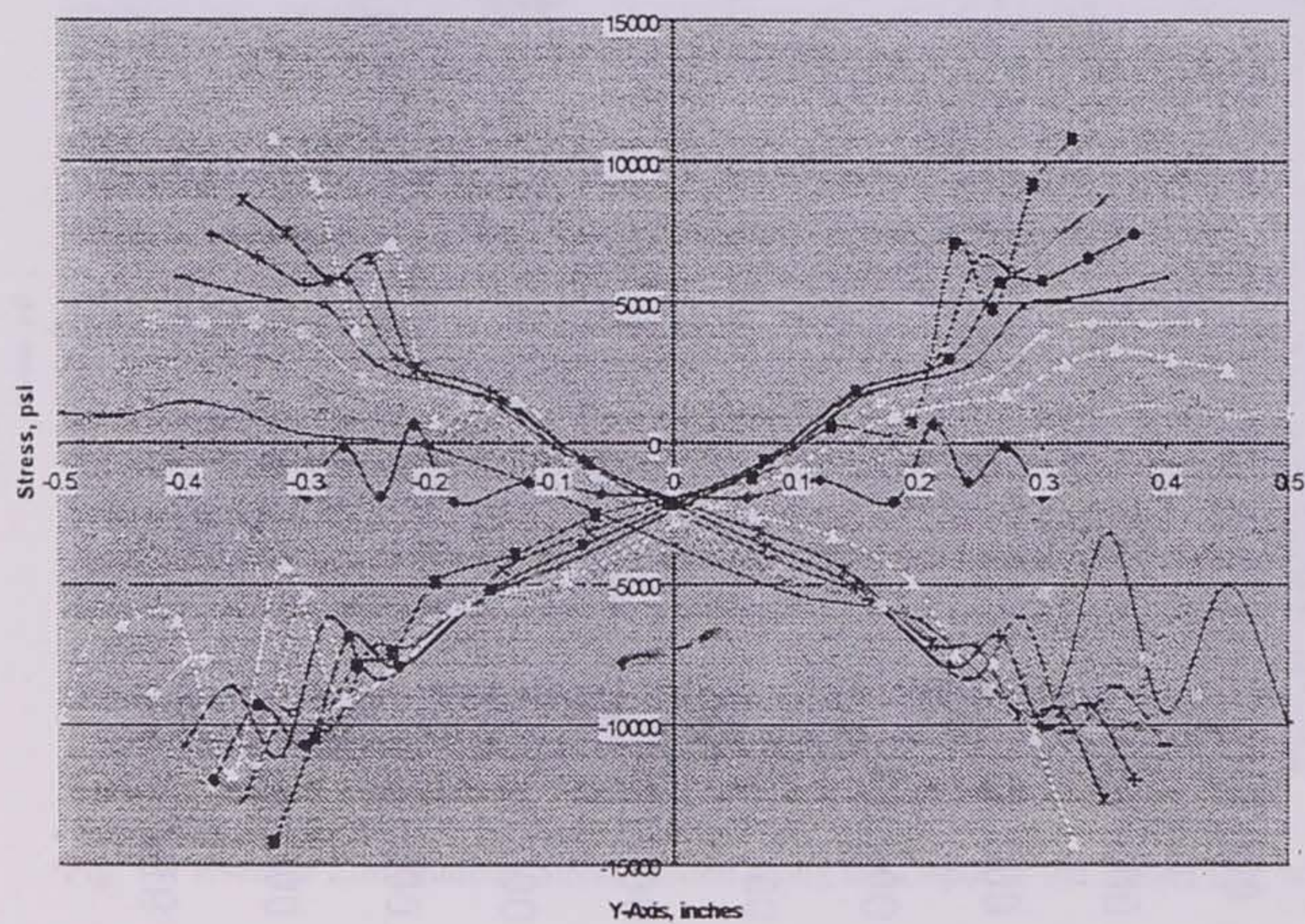Fig. 21 Average Transverse Stress plotted along the Dowel Bar Length, σy

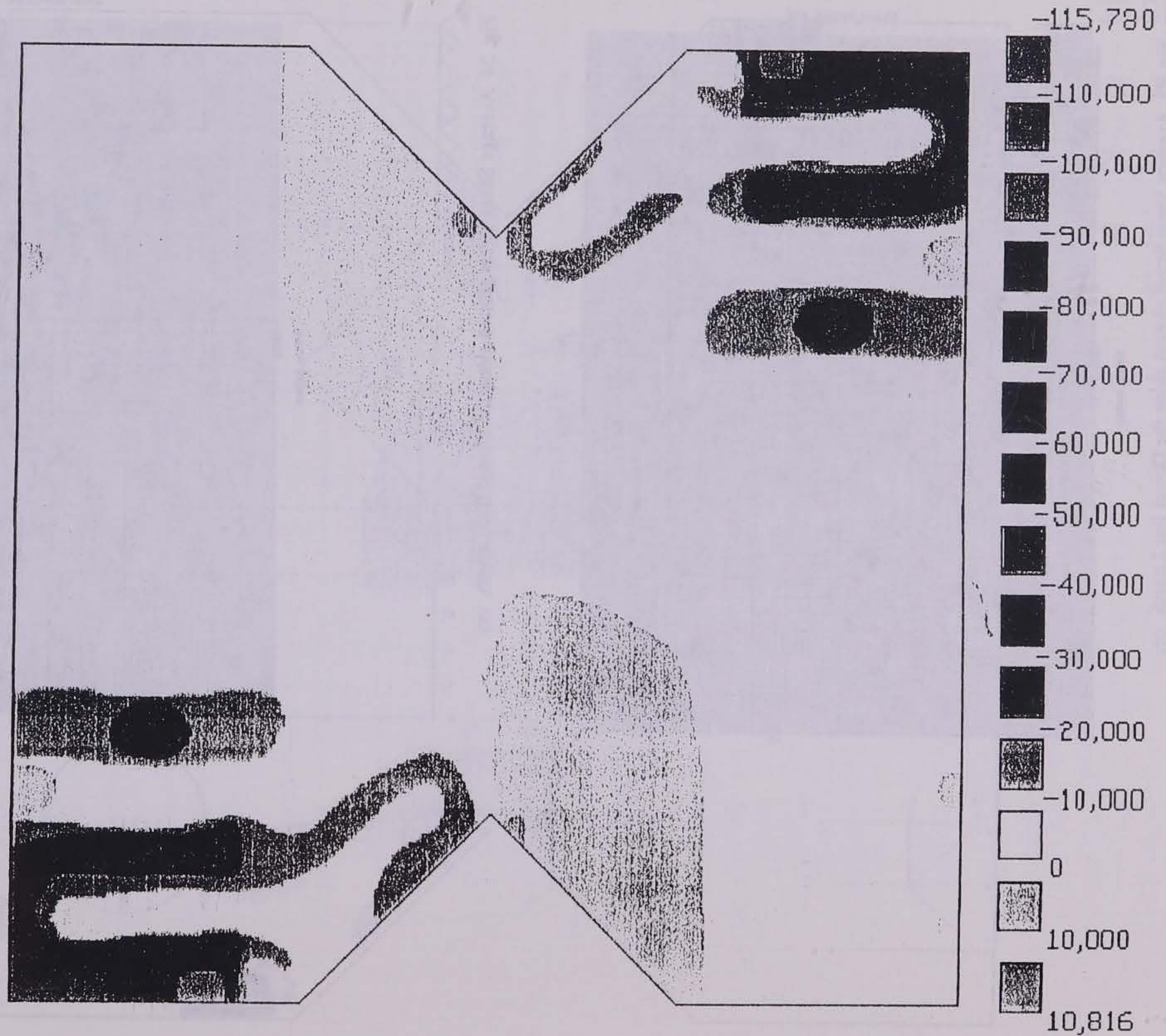Fig. 22 Average Transverse Stress plotted along the Depth of the Dowel, σy
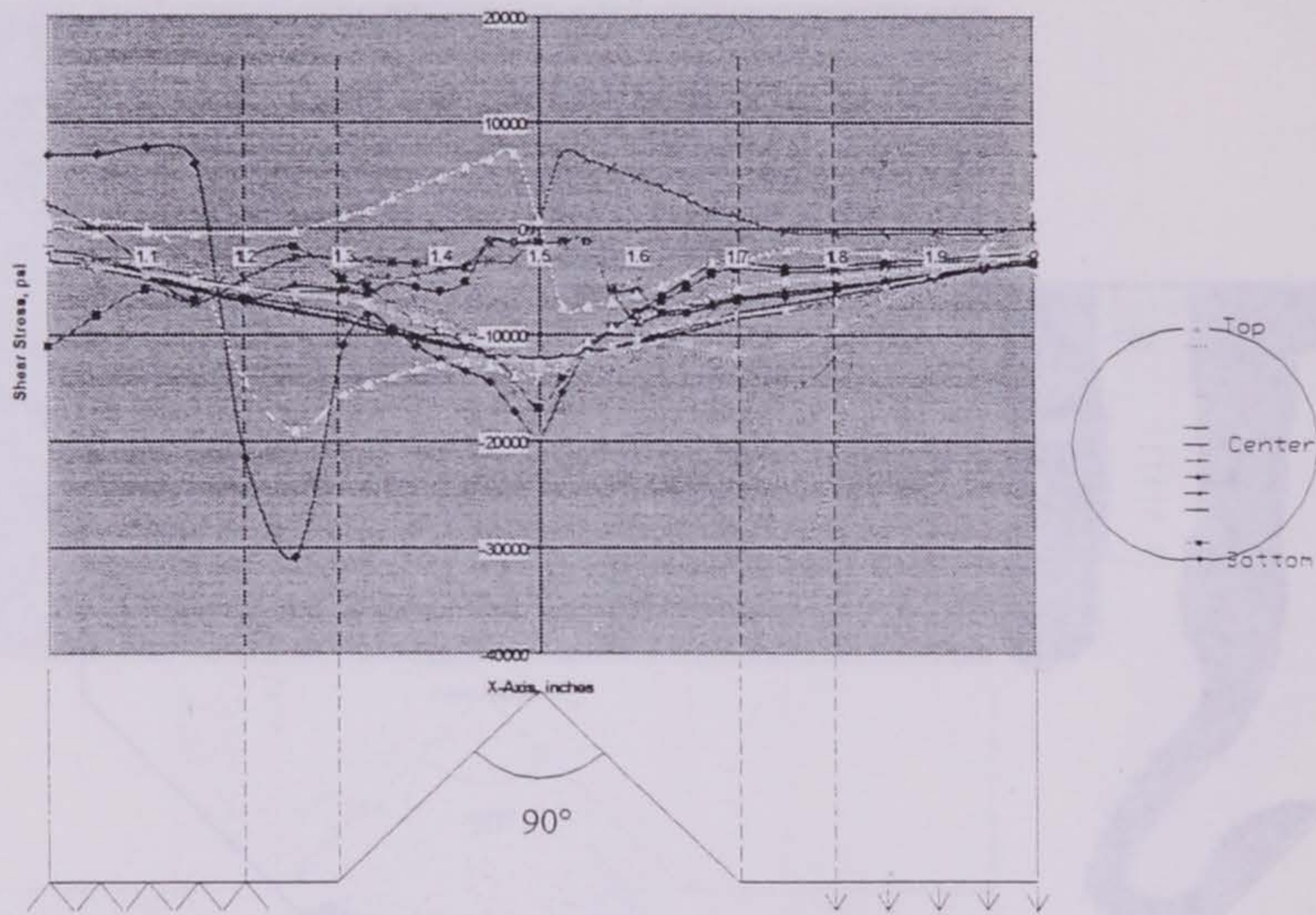
Fig 23 Average Transverse Stress, σ_y

41

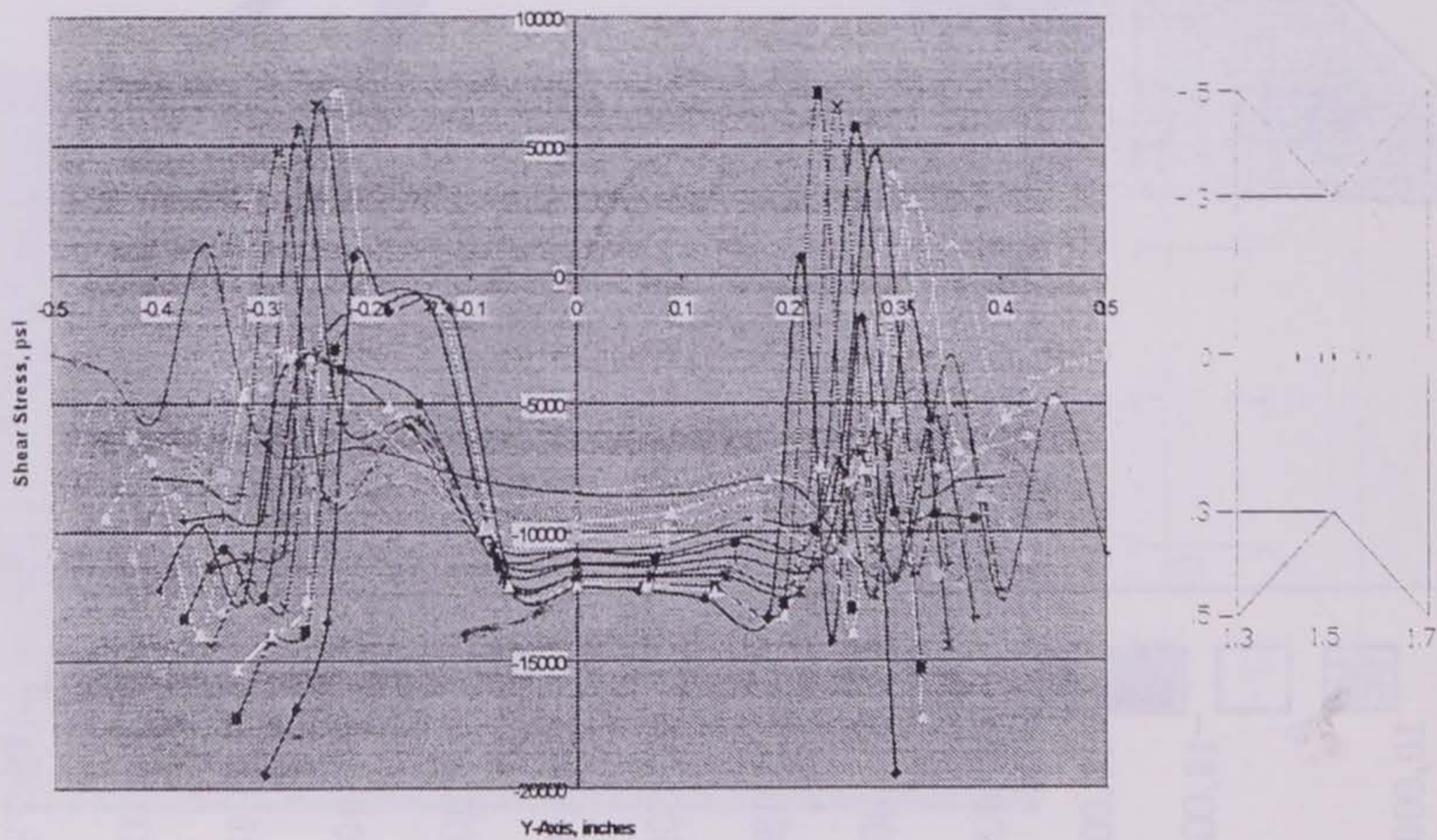Fig. 24 Average Shear Stress plotted along the Dowel Bar Length, τxy

Fig. 25 Average Shear Stress plotted along the Dowel Bar Length, τxy

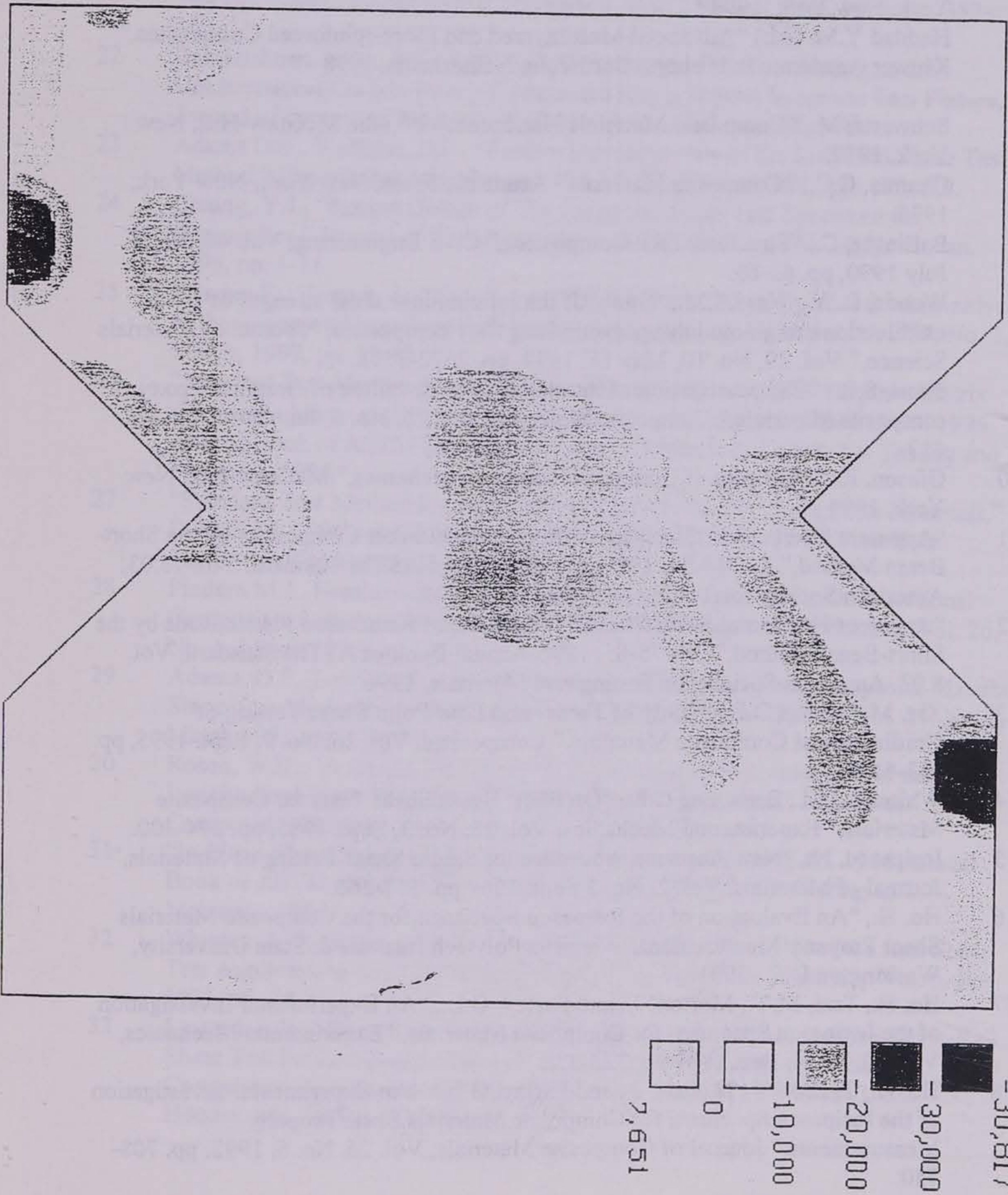Fig. 26 Average Shear Stress, σ_{xy}

7,651
0
-10,000
-20,000
-30,000
-30,817

REFERENCES:

1   Marshall, I. H. "Composite Structures" Volume 6, Elsevier Applied Science, New York, New York, 1991

2   Agarwal, B. D., Broutman L. J. "Analysis and Performance of Fiber Composites" 2nd edn. John Wiley, 1990

3   Mallick P.K. (ed.) "Fiber-Reinforced Composites" 2nd edn. Marcel Dekker, New York, New York, 1993

4   Haddad Y.M. (ed.) "Advanced Multilayered and Fibre-reinforced Composites," Kluwer Academic Publishers, Dordrecht, Netherlands, 1998

5   Schwartz, M., "Composite Materials Handbook," 2nd edn. McGraw-Hill, New York, 1992.

6   Chamis, C.C., "Composite Materials" Academic Press, New York, New York, 1975

7   Ballinger, C., "Structural FRP Composites," Civil Engineering, Vol. 60, No. 7, July 1990, pp. 63-65.

8   Woods, D.W., Ward, I.M., "Study of the interlaminar shear strength of unidirectional high-modulus polyethylene fibre composites, "Journal of Materials Science," Vol. 29, No. 10, May 15, 1994, pp. 2572-2578.

9   Short, S.R., "Characterization of interlaminer shear failure of Graphite/Epoxy composite Materials," Composite Materials, Vol. 26, No. 6, June 1995, pp. 431-449.

10   Gibson, R. "Principles of Composite Material mechanics," McGraw-Hill, New York, 1994.

11   "Apparent Interlaminer Shear Strength of Parallel Fiber Composites by the Short-Beam Method," D2344-84, 1996 Annual Book of ASTM Standard, Vol. 15.03, American Society for Testing and Materials, 1996.

12   "Apparent Horizontal Shear Strength of Pultruded Reinforced Plastic Rods by the Short-Beam Method," D4475-85, 1996 Annual Book of ASTM Standard, Vol. 8.03, American Society for Testing and Materials, 1996.

13   Xie, M., Adams D.F., "Study of Three- and Four Point Shear Testing of Unidirectional Composite Materials," Composites, Vol. 26, No. 9, Sept. 1995, pp. 653-659

14   Whitney, J.M., Browning C.E., "On Short Beam Shear Tests for Composite Materials," Experimental Mechanics, Vol. 25, No. 3, Sept. 1985, pp. 294-300.

15   Iosipescu, N., "New Accurate Procedure for Single Shear Testing of Materials," Journal of Materials, Vol. 2, No. 3 Sept. 1967 pp. 537-566.

16   Ho, H., "An Evaluation of the Iosipescu Specimen for the Composite Materials Shear Property Measurement," Virginia Polytech Institute & State University, Washington D.C., 1991

17   Ho, H., Tsai, M.Y., Morton, J., and Farley, G.L., "An Experimental Investigation of the Iosipescu Specimen for Composite Materials," Experimental Mechanics, Vol. 30, No. 4, Dec. 1991 pp. 328-336

18   Ho, H., Tsai, M.Y., Morton, J., and Farley, G.L., "An Experimental Investigation of the Iosipescu Specimen for Composite Materials Shear Property Measurements," Journal of Composite Materials, Vol. 26, No. 5, 1992, pp. 708-750.

19   Pierron, F., Vautrin, A., and Harris, B., "The Iosipescu In-plane Shear Test: Validation on Iostropic Material," Engineering Mechanics, Vol. 35 No. 2, June 1995, pp. 130-136.

20   "Shear Properties of Composite Materials by the V-notched Beam Method," D5379-93, 1996 Annual Book of ASTM Standard, Vol. 15.03, American Society for Testing and Materials, 1996.

21   Adams, D.F., Lewis E.Q., "Experimental Strain Analysis of the Iosipescu Shear Test Specimen," Experimental Mechanics, Vol. 30, No. 4, Dec. 1995, pp. 352-360.

22   Balakrishnan, M.V., Bansal, B., and Kumosa, M., "Biaxial Testing of the Unidirectional Carbon-Epoxy Composites Using Biaxial Iosipescu Test Fixture," Journal of composite materials, Vol. 31, No. 5, 1997, pp. 486-508.

23   Adams D.F., Waltrath, D.E., "Further Developments of the Iosipescu Shear Test Method," Experimental Mechanics, Vol. 27 No. 2, June 1987, pp. 113-119.

24   Chiang, Y.J., "Robost Design of The Iosipescu Shear Test Specimen for Composites," Journal of Testing and Evaluation, JTEVA, Vol. 24, No. 1, Jan. 1996, pp. 1-11.

25   Pierron, F., Vautrin, A., "Discussion of the Article, "Experimental Strain Analysis of the Iosipescu Shear Test Specimen," Experimental Mechanics, Vol. 37, No. 1, March, 1997, pp. 11-12.

26   "Standard Test Method for the In-plane Shear Response of the Polymer Matrix Composite Materials by the Tensile Test of +/- 45° laminate," D3518-94, 1996 Annual Book of ASTM Standard, Vol. 15.03, American Society for Testing and Materials, 1996.

27   "Standard Test Method for Tensile Properties of Polymer Composite Materials," D 3039-95, 1996 Annual Book of ASTM Standards, Vol. 15.03, American Society for Testing and Materials, 1996.

28   Pindera M.J., Herakovich, C.T., "Shear Characterization of the Unidirectional Composites with the Off-Axis Tension Test," Experimental Mechanics, Vol. 26, No. 1, March 1986, pp.103-112

29   Adams, D.F., Lewis E.Q., "Experimental Assessment of Four Composite Material Shear Test Methods," Journal of Testing and Evaluation, JTEVA, Vol. 25, No. 2, March 1997, pp. 174-181.

30   Rosen, W.B., "A simple Procedure for Experimental Determination of the Longitudinal Shear Modulus of Unidirectional Composites," Journal of Composite Materials, Vol. 6, Oct. 1972, pp. 552-555.

31   "In-Plane Shear Properties of Composite Laminates," D4255-83, 1996 Annual Book of ASTM Standard, Vol. 15.03, American Society for Testing and Materials, 1996.

32   Whitney, J.M., Stansbarger, D.L., and Howell H.B., "Analysis of the Rail Shear Test Applications and Limitations," Journal of Composite Materials, Vol. 5, Jan. 1971, pp. 24-35.

33   Lessard, L.B., Eilers, O.P., and Shokrieh, M.M., "Modification of the Three-Rail Shear Test for Composite Materials Under Static and Fatigue Loading," Composite Materials Testing and Design, Vol. 13, ASTM STP 1242, S. J. Hooper, ed., ASTM, 1997, pp. 217-233.

34   Chamis, C.C., Sinclair, J.H., "Ten-deg. Off-axis Test for Shear Properties in Fiber Composites," Experimental Mechanics, Vol. 17, No. 9, Sept. 1977, pp. 339-346.

35   Porter, M.L., Hughes, B.W., Barnes, B.A., and Viswanath, K.P., "Non-Corrosive Tie Reinforcing and Dowel Bars for Highway Pavement Slabs," Iowa Department of Transportation, Nov. 1994.

Others:

*   "In-Plane Shear Strength of Pultruded Glass Reinforced Plastic Rod," D3914-84, 1996 Annual Book of ASTM Standard, Vol. 8.02, American Society for Testing and Materials, 1996.

*   "Flexural Properties of Fiber Reinforced Pultruded Plastic Rods," D4476-85, 1996 Annual Book of ASTM Standard, Vol. 8.03, American Society for Testing and Materials, 1996.

*   Bazant, Z.P., Daniel, I.M., and Li, Z., "Size Effect and Fracture Characteristics of Composite Laminates," Journal of Engineering Materials and Technology, July 1996, Vol. 118, No. 3, pp. 317-324.

*   Ho, H., Morton, J., and Farley, G.L., "Non-Linear Analysis of the Iosipescu Specimen for the Composite Materials," Composite Science and Technology, May 1994, Vol. 50, pp. 355-365

*   Neumeister, J.M., Palsson, A.C., "Inclined Double Notch Shear Test for the Improved Interlaminar Shear Strength Measurements," Journal of Composites Technology & Research, Vol. 2, No. 2, April 1998, pp. 100-107.

*   Tsai, C.L., Danial, I.M., "Determination of In-plane and Out-of-plane Shear Moduli of Composite Materials," Experimental Mechanics, Vol. 30, No. 3, Sept. 1990, pp. 295-299.

*   Sullivan, J.L., Kao, B.G, and Van Oene, H., "Shear Properties and a Stress Analysis Obtained from Vinyl-ester Iosipescu Specimens," Experimental Mechanics, Vol. 24, No. 3, Sept. 1984, pp. 223-231

*   Pindera, M.J., Ifju, P. and Post, D. "Iosipescu Shear Characterization of Polymeric and metal Matrix Composites," Experimental Mechanics. Vol. 30, No. 1, Mar. 1990, pp. 101-108.

*   Camponeschi, T.C., Jr. (ed.), "Composite Materials Testing and Design," Vol. 11, ASTM, 1993